Magee N

SERIAL NO. SSC-44

COPY NO. 25

PROGRESS REPORT

ON

THE EFFECTS OF WIDTH AND THICKNESS ON STRENGTH, ENERGY ABSORPTION AND TRANSITION TEMPERATURE FOR INTERNALLY NOTCHED FLAT STEEL PLATES

BY

SAMUEL T. CARPENTER, WENDELL P. ROOP, A. W. ZELL, E. KASTEN

SWARTHMORE COLLEGE
Under Bureau of Ships Contract NObs-45521
(Index No. NS011-043)

Transmitted through
NATIONAL RESEARCH COUNCIL'S

COMMITTEE ON SHIP STEEL
Advisory to

SHIP STRUCTURE COMMITTEE
under

Bureau of Ships, Navy Department
Contract NObs-50148
(Index No. NS731-036)

Division of Engineering and Industrial Research
National Research Council
Washington, D. C.
November 15, 1951

NATIONAL RESEARCH COUNCIL

2101 CONSTITUTION AVENUE, WASHINGTON 25, D. C.

COMMITTEE ON SHIP STEEL

OF THE

DIVISION OF ENGINEERING AND INDUSTRIAL RESEARCH

November 15, 1951

Chief, Bureau of Ships
Code 343
Navy Department
Washington 25, D. C.

Dear Sir:

Attached is Report Serial No. SSC-44 entitled "The Effects of Width and Thickness on Strength, Energy Absorption and Transition Temperature for Internally Notched Flat Steel Plates." This report has been submitted by the contractor as a Progress Report of the work done on Research Project SR-118 under Contract NObs-45521, Index No. NS011-043 between the Bureau of Ships, Navy Department and Swarthmore College.

The report has been reviewed and acceptance recommended by representatives of the Committee on Ship Steel, Division of Engineering and Industrial Research, NRC, in accordance with the terms of the contract between the Bureau of Ships, Navy Department and the National Academy of Sciences.

Very truly yours,

Peter E. Kyle

Peter E. Kyle, Chairman
Committee on Ship Steel

Advisory to the SHIP STRUCTURE COMMITTEE, *a committee representing the combined research activities of the member agencies - Bureau of Ships, Dept. of Navy; Military Sea Transportation Service, Dept. of Navy; United States Coast Guard, Treasury Dept.; Maritime Administration, Dept. of Commerce, American Bureau of Shipping.*

PREFACE

The Navy Department through the Bureau of Ships is distributing this report for the SHIP STRUCTURE COMMITTEE to those agencies and individuals who were actively associated with the research work. This report represents results of part of the research program conducted under the Ship Structure Committee's directive to "investigate the design and methods of construction of welded steel merchant vessels".

The distribution of this report is as follows:

Copy No. 1 - Chief, Bureau of Ships, Navy Department
Copy No. 2 - W. W. Rubey, National Research Council

Ship Structure Committee

Copy No. 3 - Rear Admiral K. K. Cowart, USCG - Chairman
Copy No. 4 - Rear Admiral R. L. Hicks, USN, (Ret.), Maritime Administration
Copy No. 5 - Rear Admiral E. W. Sylvester, USN, Bureau of Ships
Copy No. 6 - Captain W. N. Mansfield, USNR, Military Sea Trans. Serv.
Copy No. 7 - D. P. Brown, American Bureau of Shipping

Ship Structure Subcommittee

Copy No. 8 - Capt. E.A. Wright, USN, Bureau of Ships - Chairman
Copy No. 9 - Comdr. E.A. Grantham, USN, Military Sea Transportation Serv.
Copy No. 10 - Comdr. D. B. Henderson, USCG, U.S. Coast Guard Headquarters
Copy No. 11 - Lt. Comdr. M.N.P. Hinkamp, USN, Bureau of Ships
Copy No. 12 - Lt. Comdr. E.L. Perry, USCG, U.S. Coast Guard Headquarters
Copy No. 13 - W.G. Frederick, Maritime Administration
Copy No. 14 - Hubert Kempel, Military Sea Transportation Service
Copy No. 15 - John Crowley, Office of Naval Research
Copy No. 16 - M. J. Letich, American Bureau of Shipping
Copy No. 17 - L. C. Host, American Bureau of Shipping
Copy No. 18 - E.M. MacCutcheon, Jr., Bureau of Ships
Copy No. 19 - V. L. Russo, Maritime Administration
Copy No. 20 - Finn Jonassen, Liaison Representative, NRC
Copy No. 21 - E. H. Davidson, Liaison Representative, AISI
Copy No. 22 - W. P. Gerhart, Liaison Representative, AISI
Copy No. 23 - Wm. Spraragen, Liaison Representative, WRC
Copy No. 24 - Charles Hoch, Military Sea Transportation Serv., Alt. Member
Copy No. 25 - W.E. Magee, U.S. Coast Guard, Alternate Member
Copy No. 26 - J.B. Robertson, Jr., U.S. Coast Guard, Alternate Member
Copy No. 27 - John Vasta, Bureau of Ships, Alternate Member
Copy No. 28 - J. E. Walker, Bureau of Ships, Alternate Member
Copy No. 29 - Edward Wenk, David Taylor Model Basin, Alternate Member

Committee on Ship Steel

Copy No. 30 - P. E. Kyle - Chairman
Copy No. 31 - C. H. Herty, Jr., - Vice Chairman
Copy No. 32 - Wm. M. Baldwin, Jr.
Copy No. 33 - C. S. Barrett

Committee on Ship Steel (Continued)

Copy No. 34 - R. M. Brick
Copy No. 35 - S. L. Hoyt
Copy No. 15 - John Crowley
Copy No. 36 - M. W. Lightner
Copy No. 37 - R. F. Mehl
Copy No. 38 - T. S. Washburn
Copy No. 20 - Finn Jonassen - Technical Director
Copy No. 39 - A. Muller - Consultant

Members of Project Advisory Committees SR-98, SR-99, SR-100, SR-108, SR-109, SR-110 and SR-111 (not listed elsewhere)

Copy No. 40 - R. H. Aborn
Copy No. 41 - E. A. Anderson
Copy No. 42 - L. C. Bibber
Copy No. 43 - Morris Cohen
Copy No. 44 - W. C. Ellis
Copy No. 45 - M. Gensamer
Copy No. 46 - M. F. Hawkes
Copy No. 47 - W. F. Hess
Copy No. 48 - W. R. Hibbard, Jr.
Copy No. 49 - C. E. Jackson
Copy No. 50 - J. R. Low, Jr.
Copy No. 51 - H. W. Pierce
Copy No. 52 - W. A. Reich
Copy No. 53 - C. E. Sims
Copy No. 54 - R. D. Stout
Copy No. 55 - J. G. Thompson
Copy No. 56 - B. G. Johnston, Welding Research Council, Liaison
Copy No. 57 - W. H. Wooding, Philadelphia Naval Shipyard

Committee on Residual Stresses

Copy No. 58 - J. T. Norton - Chairman
Copy No. 32 - Wm. M. Baldwin, Jr.
Copy No. 59 - Paul Ffield
Copy No. 60 - LeVan Griffis
Copy No. 61 - K. Heindlhofer
Copy No. 62 - Daniel Rosenthal
Copy No. 20 - Finn Jonassen - Technical Director

U. S. NAVY

Copy No. 63 - Capt. R. H. Lambert, USN, Philadelphia Naval Shipyard
Copy No. 64 - Capt. C. M. Tooke, USN, Long Beach Naval Shipyard, Calif.
Copy No. 65 - Comdr. H. G. Bowen, USN, Code Re-3, Bureau of Ordnance
Copy No. 66 - Comdr. R.S. Mandelkorn, USN, Armed Forces Special Weapons Proj.
Copy No. 67 - A. Amirikian, Bureau of Yards and Docks
Copy No. 68 - A. G. Bissell, Bureau of Ships

U. S. Navy (Continued)

Copy No. 69 - J. W. Jenkins, Bureau of Ships
Copy No. 70 - Carl Hartbower, Naval Research Laboratory
Copy No. 71 - R. H. Raring, Naval Research Laboratory
Copy No. 72 - Noah Kahn, New York Naval Shipyard
Copy No. 73 - O. T. Marzke, Naval Research Laboratory
Copy No. 74 - W. E. McKenzie, Metallurgical Branch, Naval Gun Factory
Copy No. 75 - J. E. McCambridge, Industrial Testing Lab., Phila. Naval Shipyard
Copy No. 76 - N. E. Promisel, Bureau of Aeronautics
Copy No. 77 - Naval Research Laboratory
Copy No. 78 - Naval Research Laboratory, Mechanical Section
Copy No. 79 - Naval Research Laboratory, Metallurgical Section
Copy No. 80 - Post Graduate School, U. S. Naval Academy
Copies No. 81 and 82 - U. S. Naval Engineering Experiment Station
Copy No. 83 - New York Naval Shipyard, Material Laboratory
Copy No. 84 - Industrial Testing Laboratory
Copy No. 85 - Philadelphia Naval Shipyard
Copy No. 86 - San Francisco Naval Shipyard
Copy No. 87 - David Taylor Model Basin, Attn: Library
Copies No. 88 and 89 - Technical Library, Bureau of Ships, Code 364

U. S. Coast Guard

Copy No. 90 - Capt. R. B. Lank, Jr., USCG
Copy No. 91 - Capt. H. C. Moore, USCG
Copy No. 92 - Capt. G. A. Tyler, USCG
Copy No. 93 - Testing and Development Division
Copy No. 94 - U. S. Coast Guard Academy, New London

U. S. Maritime Administration

Copy No. 95 - Vice Adm. E. L. Cochrane, USN (Ret.)
Copy No. 96 - E. E. Martinsky

Representatives of American Iron and Steel Institute
Committee on Manufacturing Problems

Copy No. 97 - C. M. Parker, Secretary, General Technical Committee, AISI
Copy No. 42 - L. C. Bibber, U. S. Steel Co.
Copy No. 31 - C. H. Herty, Jr., Bethlehem Steel Co.
Copy No. 98 - E. C. Smith, Republic Steel Corp.

Welding Research Council

Copy No. 99 - C. A. Adams
Copy No. 100 - Harry Boardman
Copy No. 101 - LaMotte Grover
Copy No. 23 - Wm. Spraragen

Copy No. 102 - C. R. Soderberg, Chairman, Div. of Engr. & Ind. Res., NRC
Copy No. 37 - R. F. Mehl, Chairman, Committee on Ship Steel
Copy No. 20 - Finn Jonassen, Technical Director, Committee on Ship Steel
Copy No. 103 - S.T. Carpenter, Investigator, Research Project SR-98
Copy No. 104 - W. P. Roop, Investigator, Research Project SR-98
Copy No. 105 - A. W. Zell, Investigator, Research Project SR-98
Copy No. 106 - E. Kasten, Investigator, Research Project SR-98
Copy No. 32 - Wm. M. Baldwin, Jr., Investigator, Res. Projects SR-99, 111
Copy No. 107 - L. J. Ebert, Investigator, Research Project SR-99
Copy No. 108 - L. J. Klingler, Investigator, Research Project SR-99
Copy No. 109 - C. B. Voldrich, Investigator, Research Project SR-100
Copy No. 110 - P. J. Rieppel, Investigator, Research Project SR-100
Copy No. 111 - M. L. Williams, Investigator, Research Project SR-106
Copy No. 37 - R. F. Mehl, Investigator, Research Project SR-108
Copy No. 34 - R. M. Brick, Investigator, Research Project SR-109
Copy No. 112 - C. H. Lorig, Investigator, Research Project SR-110
Copy No. 113 - E. W. Suppiger, Investigator, Research Project SR-113
Copy No. 114 - E. R. Ward, Investigator, Research Project SR-113
Copy No. 115 - Carlo Riparbelli, Investigator, Research Project SR-113
Copy No. 116 - J. F. Wallace, Investigator, Research Project SR-114
Copy No. 19 - V. L. Russo, Investigator, Research Project SR-117
Copy No. 117 - R. A. Hechtman, Investigator, Research Project SR-119
Copy No. 118 - G. S. Mikhalapov, Investigator, Research Project SR-120
Copy No. 119 - Clarence Altenburger, Great Lakes Steel Company
Copy No. 120 - T. N. Armstrong, International Nickel Co., Inc.
Copy No. 121 - A. B. Bagsar, Sun Oil Company
Copy No. 122 - British Shipbuilding Research Association, Attn: J.C. Asher
Copy No. 123 - D. S. Clark, California Institute of Technology
Copy No. 124 - Paul De Garmo, University of California
Copy No. 125 - J. E. Doran, University of California
Copy No. 126 - George Ellinger, National Bureau of Standards
Copy No. 127 - A. E. Flanigan, University of California
Copy No. 128 - O. J. Horger, Timken Roller Bearing Company
Copy No. 129 - H. Kennedy, University of California
Copy No. 130 - E. P. Klier, University of Maryland
Copy No. 131 - J. E. McNutt, Carnegie Institute, Pittsburgh
Copy No. 132 - Robert C. Madden, Kaiser Steel Company
Copy No. 133 - N. M. Newmark, University of Illinois
Copy No. 134 - E. Orowan, Massachusetts Institute of Technology
Copies No. 135 - 159 - E.G. Hill, British Joint Services Mission (Navy Staff)
Copy No. 160 - E. R. Parker, University of California
Copy No. 161 - W. G. Perry, RN, British Joint Services Mission (Navy Staff)
Copy No. 162 - L. J. Rohl, U. S. Steel Company
Copy No. 163 - H. A. Schade, University of California
Copy No. 164 - Saylor Snyder, U. S. Steel Company
Copy No. 165 - Standard Oil Company of California, Attn: K. V. King

Copy No. 166 - Webb Institute of Naval Architecture
Copy No. 167 - Georges Welter, Ecole Polytechnique, Montreal
Copy No. 168 - Carl A. Zapffe, Carl A. Zapffe Laboratories
Copy No. 169 - Division of Metallurgy, National Bureau of Standards
Copy No. 170 - Transportation Corps Board, Brooklyn, New York
Copies No. 171 through 175 - Library of Congress via Bureau of Ships, Code
Copy No. 176 - NACA, Attn: Materials Research Coordination, Navy Dept.
Copy No. 177 - File Copy, Committee on Ship Steel
Copies No. 178 through 182 - Bureau of Ships
Copy No. 183 -
Copy No. 184 -
Copy No. 185 -
Copy No. 186 -
Copy No. 187 -
Copy No. 188 -
Copy No. 189 -
Copy No. 190 -
Copy No. 191 -
Copy No. 192 -
Copy No. 193 -
Copy No. 194 -
Copy No. 195 -
Copy No. 196 -
Copy No. 197 -
Copy No. 198 -
Copy No. 199 -
Copy No. 200 -
Copy No. 201 -
Copy No. 202 -
Copy No. 203 -
Copy No. 204 -
Copy No. 205 -
Copy No. 206 -
Copy No. 207 -
Copy No. 208 -
Copy No. 209 -
Copy No. 210 -
Copy No. 211 -
Copy No. 212 -
Copy No. 213 -
Copy No. 214 -
Copy No. 215 -
Copy No. 216 -
Copy No. 217 -
Copy No. 218 -
Copy No. 219 -
Copy No. 220 -
Copy No. 221 -
Copy No. 222 -
Copy No. 223 -
Copy No. 224 -
Copy No. 225 -

TABLE OF CONTENTS

LIST OF TABLES

List of Tables (Cont'd)

APPENDIX I

Basic data

LIST OF FIGURES

LIST OF FIGURES (Cont'd)

LIST OF FIGURES (Cont'd)

Appendix II

Graphical Summaries of Basic Data

List of Figures (Cont'd)

APPENDIX III

Load-Elongation Curves

List of Figures (Cont'd)

APPENDIX III

* Figs. 48 and 50 are omitted.

ABSTRACT

This report contains the results of tensile tests made on geometrically similar steel specimens. Tests were made in a systematic manner with Aspect Ratios (width divided by thickness) varying from 4 to 20. Each specimen was internally notched with a central transverse notch having a length equal to 1/4 of the width of the specimen. The ends of the notches terminated with a drilled hole. The diameter of the drilled holes was made proportional to plate thickness. Steel plates ranging in "as rolled thicknesses", from 1/2 inch to $1\frac{1}{2}$ inch were investigated from two heats of steel.

The results of the tests are classified on the basis of strength, energy absorption, and transition temperature.

It was found from this investigation that dimensional similarity of specimens does not assure geometrical similarity of plastic strain patterns. Therefore, the geometrical and metallurgical effects of thickness on transition temperature could not be segregated on the basis of geometrically similar specimens in this investigation.

PROGRESS REPORT

NAVY BUSHIPS CONTRACT NObs-45521
(Index No. NS011-043)

PROJECT SR-98

The Effects of Width and Thickness on Strength, Energy Absorption and Transition Temperature for Internally Notched Flat Steel Plates

Prepared by

Samuel T. Carpenter, Wendell P. Roop, A. W. Zell, E. Kasten

SWARTHMORE COLLEGE
DIVISION OF ENGINEERING
SWARTHMORE, PA.

PROGRESS REPORT

NAVY BUSHIPS CONTRACT NObs-45521

PROJECT SR-98

The Effects of Width and Thickness on Strength, Energy Absorption and Transition Temperature for Internally Notched Flat Steel Plates

Prepared by

Samuel T. Carpenter, Wendell P. Roop, A. W. Zell, Ewald Kasten

Swarthmore College, Division of Engineering,
Swarthmore, Pa.

INTRODUCTION and SUMMARY

This study, designated as the Aspect Ratio Program, is an exploratory investigation of the effects of specimen geometry (width and thickness) on strength, energy absorption and transition temperature, using internally notched steel specimens tested in tension. The width and thickness of specimens were related by considering the Aspect Ratios (AR) of the specimens where AR represents the ratio of gross width of specimen to thickness of the plate. Specimens of equal AR were said to be geometrically similar, since notch length and acuity were also held in strict similitude.

The intent of this study was to obtain a separation of the geometrical from metallurgical effects in plates having variable "as rolled" thicknesses from the same heat. A systematic variation in AR in various plate thicknesses was made, utilizing two different steels. Assuming for a given thickness of a given steel that chemical and metallurgical effects would remain constant, the size effects noted could be attributed to geometry in the form of increased width. It was thought that data using specimens of different thicknesses but with equal AR and the same chemistry, would enable a determination to be made of the effects of metallurgical changes due to rolling. The latter comparison is dependent upon the validity of geometrical similarity of both elastic and plastic strains in all regions of the specimen, regardless of plate thickness.

Results of this study on internally notched specimens indicate that dimensional similarity of unstressed specimens does not necessarily guarantee similarity of such important physical relations as strength and unit energy absorption. These physical quantities were found to vary with both thickness and width.

With regard to strength, as determined by the maximum average unit stress on the net cross-section, comparisons of geometrically similar specimens show that the thicker plates have a definitely smaller unit resistance than thinner plates. For plates of equal width the strength of the plates shows small differences with varying thickness. On the whole the strength does not appear to depend greatly on thickness when width is not varied.

With regard to energy absorption, to maximum load, the data for geometrically similar specimens indicate that the thicker plates absorbed less energy per cubic inch of volume (termed unit energy) than thinner plates. However, for specimens of equal width the situation is reversed and the thicker plates absorb more unit energy than thinner plates.

The transition temperature for a given thickness of plate, metallurgical effects assumed constant, shows a trend upwards as the width of the plate increases. For small widths the thicker plates have higher transition temperatures than the thinner plates, considering either constant aspect ratio or width. The question here is what part of this increase in transition temperature is due to the geometrical effect of increased thickness and what part due to metallurgical differences. The effects of metallurgical differences can only be determined in the absence of geometrical effects. As it was found that dimensional similarity does not completely eliminate geometrical effects, the isolation of metallurgical effects may require comparison of the various thicknesses on some basis other than equality of aspect ratio.

A trend toward uniformity of strength and unit energy in the various plate thicknesses, as width is increased, would suggest that the effect of thickness is to modify the rate at which these uniform values are approached as width is increased.

The results of this study must be considered to be exploratory, disclosing the need of further study and investigation.

MATERIALS

The steel plates used in the aspect ratio program have been given the code designation T-1, T-2, and T-2R. The T-1* steel was furnished in 1/2", 3/4", 1" and $1\frac{1}{2}$" thicknesses, with all plates rolled

*The T-1 steel was given the plate code letter "G" in the report "Further Study of Navy Tear Test" by N. A. Kahn and E. A. Imbembo published in the Welding Journal, February, 1950.

from the same heat. The T-2 steel was received in 3/4", 1" and $1\frac{1}{2}$" thicknesses, all rolled from the same heat. T-2R designates the 3/4" thick plates obtained by re-rolling a portion of the $1\frac{1}{2}$" thick T-2 steel.

The chemical analysis for these steels is as follows:

Steel Code	C	Mn	P	S	Si
T-1	.16	.93	.013	.034	.020
T-2	.18	.72	.024	.026	.26

T-1 steel is termed a semi-killed steel of the ABS-B type and the T-2 steel is termed a silicon-aluminum killed, fine grained steel.

The T-2R steel was produced by re-rolling 2 pieces of T-2 steel $1\frac{1}{2}$" thick x 48" wide x 60" long. A reduction to 3/4" thickness was made without cross rolling in 3 passes while maintaining the 48" wide dimension. The $1\frac{1}{2}$" thick plates were in the soaking pit prior to rolling for one hour and fifteen minutes at a temperature of 2240°F. The finishing temperature was 1680°F. The surfaces of the re-rolled plates were excellent and relatively free from scale.

The grain size for these steels has been reported to this laboratory by Mr. N. A. Kahn* of the New York Naval Shipyard, as follows:

Steel Code	Plate Thickness	McQuaid-Ehn Grain Size
T-1	1/2"	1-4
T-1	3/4"	1-3
T-1	1"	1-3
T-1	$1\frac{1}{2}$"	8
T-2R	3/4"	7-8

* By letter

It has been further reported for the T-1 steel that a progressive decrease in the ferrite grain size was observed, with a decrease in plate thickness. The ferrite grain size for the T-2 steel has been reported as 5-7 and for the T-2R steel as 6-8.

The tensile physical properties of the steels as defined by yield stress and ultimate stress are given as follows based on ASTM standard full plate thickness specimens:

		Physical Properties	
		Unnotched Bars	
Steel Code	Plate Thickness	Yield Stress psi	Ultimate Stress psi
T-1	1/2"	41,000	67,200
	3/4"	35,800	63,200
	1"	37,200	71,000
	1½"	36,400	60,000
T-2	3/4"	39,600	67,000
	1"	40,000	67,000
	1½"	33,800	64,500
T-2R	3/4"	39,200	67,000

Test Specimens and Test Schedule

Figure 1 represents the typical specimen used. The radii of the drill holes at the ends of the internal notches are proportionate to plate thickness. The size of the drill hole used for various thicknesses of plate was as indicated in Figure 1.

The layout of the specimens from the plates furnished to this laboratory is shown in Figures 2 to 8b inclusive, for steels designated as T-1, T-2, and T-2R. When the program was first planned, a layout of the plates of T-1 steel was made to provide sufficient specimens of a given size distributed across the width of the plate to determine changes in transition temperature due to position within the plate. The 1/2" thick plates of T-1 steel were laid out to provide four longitudinal blocks or zones denoted as Block I, II, III and IV on Figure 2. The 3/4" thick plates were laid out in three blocks denoted as Block I, II, and III, the 1" thick plates laid out in five blocks denoted as I to V inclusive, and the $1\frac{1}{2}$" thick plates laid out in Blocks I, II, and III. It was hoped that if enough specimens of any aspect ratio were tested from any given block, statistical studies of the effect of position within the plate could be made. However, due to costs and time involved, this extensive testing program was completed only in the 1/2" thickness.

Figures 9, 10 and 11 show the schematic outline of the aspect ratio program as originally planned in which it was contemplated that tests would be made for specimens as wide as 30" in the $1\frac{1}{2}$" thickness. However, this program had to be curtailed. The blacked-out plates in the figures indicate the widths and thicknesses actually tested in this program.

The aspect ratios tested in the different thicknesses for the various steels are given in the following table:

TABLE 1

Aspect Ratios Tested

Steel Code	Thickness	Aspect Ratios
T-1	1/2"	4,8,16,19
	3/4"	4,8,12,16
	1"	4,8,12
	$1\frac{1}{2}$"	4,6
T-2	3/4"	4,8,12,16
	1"	4,6,8,12
	$1\frac{1}{2}$"	4,6
T-2R	3/4"	4,6,16,20

The specimens within any given plate layout have been identified by a letter and a number (see layout diagrams).

Measurement of Elongation

The elongations of the test specimen were measured in the direction of the tensile loading over a gage length equal to 3/4 the width of any individual specimen. The same clip gage instrumentation as described in a previous Progress Report[1*] was adapted to longer or shorter gage lengths by using extending or shortening bars.

Temperature Control

The test temperature was controlled by enclosing the test specimens in a plexiglass housing in which temperatures below room temperature were maintained by circulating air cooled by dry ice. Heating of the specimen above room temperature was accomplished by electric strip heaters placed in the temperature control chamber. A full description of the temperature control equipment was given in a previous Progress Report[1]. Test temperatures were chosen so as to

*Superscripts refer to references in Bibliography straddle the transition from shear to cleavage fracture.

TEST RESULTS

Data

The tables in Appendix I list the basic data obtained for test specimens of all steels, as follows: Test temperature; the load producing the visible crack at the notch, the maximum load, and the fracture load; and the energy input to each of the aforementioned loads in inch-lbs. In addition, the character of the observed fracture is given in terms of percentage of shear texture in the fracture surface. The energy to the visible crack loading has been designated as E, the energy to maximum load as E_1, and the energy to fracture as E_2. The tables also list the difference in energies E_2-E_1 where this quantity represents the strain energy absorption after the maximum load. All of the tabulated energies were obtained by finding the area under the load-elongation curves. Typical load-elongation curves are included in Appendix III of this report for two specimens for every aspect ratio tested, one curve referring to a specimen failing in shear and the other curve referring to a specimen in which cleavage failure occurred.

The basic data shown in the tables are graphically summarized in the figures given in Appendix II.

Average Maximum Unit Stress

Tables 2 and 3 list the average values of the nominal unit stress at maximum load for T-1, T-2, and T-2R steels in addition to the unit energy values. The nominal unit stress intensity is based on the

TABLE 2

T-1 STEEL

Summary of Unit Energy* and Average Unit Stress at Maximum Load

Values Based on Gross Gage Volume and Net Area

and the Average for all Specimens Exhibiting Either 100% or 0% Shear Failures

Thick-ness	Percent of Shear	AR 4 u	AR 4 psi	AR 6 u	AR 6 psi	AR 8 u	AR 8 psi	AR 12 u	AR 12 psi	AR 16 u	AR 16 psi	AR 19 u	AR 19 psi
1/2"	100%	4,480	71,000			2,610	63,050			1,870	58,100	1,700	54,730
	0%	4,520	71,900			2,400	63,570			1,220	56,300	910	52,940
3/4"	100%	3,720	67,940			2,460	59,940	1,820	57,000	1,610	55,080		
	0%	3,810	69,230			2,000	59,530	1,420	56,460	1,350	53,620		
1"	100%	3,090	61,720			2,320	55,420	1,860	52,550				
	0%	3,190	62,680			1,900	57,160	1,245	52,680				
1 1/2"	100%	2,800	59,130	2,250	56,300								
	0%	2,540	60,200	1,960	56,780								

* u, unit energy in inch-lbs. per cubic inch

TABLE 3

T-2 and T-2R STEELS

Summary of Unit Energy* and Average Unit Stress at Maximum Load

Values Based on Gross Gage Volume and Net Area

and the Average of all Specimens Exhibiting Either 100% or 0% Shear Failures

Thickness	Percent of Shear	AR 4 u	AR 4 psi	AR 6 u	AR 6 psi	AR 8 u	AR 8 psi	AR 12 u	AR 12 psi	AR 16 u	AR 16 psi	AR 20 u	AR 20 psi
T-2 Steel													
3/4"	100%	3,350	66,820			2,160	60,770	1,600	57,600	1,530	55,360		
	0%	2,870	68,150			1,410	59,000	1,090	56,900	890	54,200		
1"	100%	2,160	63,130	1,970	60,200	1,770	56,500	1,460	54,500				
	0%	2,750	63,830	---	---	1,660	59,000	970	54,890				
1 1/2"	100%	2,270	59,770	1,920	58,000								
	0%	2,270	61,250	1,570	57,530								
T-2R Steel													
3/4"	100%	2,970	63,630	2,750	61,360					1,550	55,000	1,340	53,800
	0%	---	---	---	---					770	52,800	---	----

* u, unit energy in inch-lbs. per cubic inch.

net cross-sectional area of the plate at the notch. The averages are separately given for all specimens exhibiting either a total shear failure or a total cleavage failure.

Unit Energy

The energy absorbing capacity of a given steel in different aspect ratios may be compared by considering average unit energy. Unit energy, designated as (u), as herein defined represents the result obtained by dividing the total energy input to maximum load by the volume of the plate between gage lines. The units of the computed unit energy are inch-lbs. per cubic inch of metal. The volume is equal to $3/4W \times Wt$ or $3/4W^2t$ (see Fig. 1) which may be termed "gross gage volume". Thus, (u) equals E1 $(3/4W^2t)$.

Table 2 summarizes the calculated average unit energies at maximum load for T-1 steel. The average unit energies are given only for specimens failing in 100% shear or 0% shear, with all specimens of either mode of failure being used in obtaining the average value. Table 3 similarly summarizes the limited results for T-2, and T-2R respectively.

No consideration has been given to energy absorbed beyond maximum load, but values are given in the tables of Appendix I.

DISCUSSION OF TEST RESULTS

Average Unit Stress

Average unit stress values at maximum load based on the net area at the notch, for T-1 steel, have been plotted in Figure 12 against aspect ratio. The results plotted were taken from Table 2 for the specimens failing in 100% shear, but specimens failing in 0% shear do not differ significantly from the fully ductile ones in specimens of these aspect ratios. The unit stress for a given thickness gradually falls with increasing aspect ratio. This reduction is due to increased width since metallurgy may be assumed constant for a given thickness.

The unit stress for a given aspect ratio decreases as thickness increases. The loss in strength of the thicker plates may be attributed to metallurgical effects if specimens of equal aspect ratio are similar in their strain patterns. However, the effect of non-similarity of strain patterns will not be considered at the present time.

From the results obtained by the University of California[2] it may be expected that the unit stress would reach an asymptotic value for plates of great width. This is probably due to the more uniform action of stress upon the net cross-section at the greater width.

In Figure 13, the unit stress values of Table 2 have been plotted against width rather than aspect ratio. Here it may be noted that unit stress decreases as width increases; but that variable thickness does not greatly affect unit stress. Comparatively, width appears to be a better basis for correlation than aspect ratio.

Unit Energy Absorption

Figure 14 is a plot of unit energy (u) versus aspect ratio for the 1/2", 3/4", 1" and $1\frac{1}{2}$" thick plates of T-1 steel. In plotting Figure 14 the data from Table 2 for the specimens failing in 100% shear has been used. The figure shows, for equal aspect ratios, that the 1/2" thick plate generally absorbs more energy per cubic inch than the thicker plates, with the differences due to plate thickness being less in the higher aspect ratios. If unit energy to maximum load is a criterion, then it can generally be stated that the thicker plates possess less ductility than thinner plates, when comparing equal aspect ratios.

The unit energy absorption for specimens failing in 0% shear shows the same trend as aspect ratio is increased as for specimens failing in 100% shear. However, the values of unit energy are lower for 0% shear failures than for the 100% shear failures at aspect ratios of 8 and greater. It should be noted (see Table 2) that at an aspect ratio of 4 the values of unit energy are nearly equal for 100% and 0% shear for a given thickness. This indicates that the local conditions at and around the notch for the narrowest specimen are the same regardless of the mode of fracture. This progress report does not present a further analysis of the energy variation for the specimens exhibiting 0% shear failure. Analytical work is now in progress to ascertain the significance of these phenomena.

The unit energy data given in Table 3 for T-2 and T-2R steels shows the same trends with regard to thickness and aspect ratio as for T-1 steel. The T-2 steel, however, appears to absorb in general less energy than T-1.

The T-2R steel, based only upon a few tests in 3/4" thickness, absorbs essentially the same energy as T-2 steel. Considering the overall results it may be concluded that in a given thickness changes in metallurgy or chemistry had little or no effect on energy absorption for these two steels.

An interesting comparison between unit energy to maximum load, width, and thickness is shown in Figure 15 for T-1 steel. The unit energy tends to become equal for a given width of plate as the thickness is increased from 1" to 1½". The question here is whether or not this is indicative that the detail mechanism of energy absorption may be nearly similar for the specimens of constant width in the 1" and 1½" thickness. Such similarity might imply identical plastic strain patterns generally throughout the specimen with the probability that conditions at the notch would become similar for specimens of equal width in 1" or 1½" thickness. If this should be true, then the transition temperatures of equal width specimens would be comparable instead of specimens of equal aspect ratio. Furthermore, if this assumption is true, the difference in transition temperature so found could then be attributed to metallurgical differences alone. No definite generalizations can be made from the results, hence these speculations must be considered only in the form of a query.

When the values of unit energy to maximum load for 100% shear failures are plotted on width rather than on aspect ratio, Figure 16, the values for constant thickness run closely parallel, the results for greater thicknesses lying above the smaller thicknesses rather than below them. In Figure 14, where values of unit energy were plotted against aspect ratio (Wt^{-1}), the greater thickness gave lower values of unit energy. Inferences from this fact might be drawn with respect to the strain patterns as affected by thickness, but these are left for later consideration.

In any case, it appears that by plotting on some function intermediate between Wt^{-1} and Wt^{0} the curves could be superimposed within the limits of experimental error.

Transition Temperatures

Transition temperatures have been established by two methods: First, a temperature range was determined, either the range within which the mode of fracture changes from shear to cleavage, or the range within which the energy absorption shows a marked decrease. This is the range of uncertainty as to the temperature below which ductile behaviour is not assured. Second, a single value of transition temperature, instead of range, was determined by selecting a temperature at which either the energy value to maximum load or percent of shear in the fracture is midway between their respective maximum and minimum values. In a number of instances the single value fails outside of the transition temperature range (see Tables 4 and 5).

Figure II-1 of Appendix II is typical of the test results of the entire program, where the energy E1 to maximum load is not significantly different in the fully ductile or the fully cleavage modes of failure. Only several exceptions to this statement have been noted. (It is to be recalled that in previous wide plate tests[1,2] where jeweler's hack-saw cut notches were used, there was a definite transition in energy to maximum load.) As a consequence, the erergy to maximum load cannot be used here to obtain a transition temperature except in a few cases shown in Tables 4 and 5. E2 and E2-E1 diagrams (Appendix II) do show an abrupt drop in energy levels in the transition zone and a transition temperature can be obtained by using either of them. However, in this program

TABLE 4

TRANSITION TEMPERATURES

T-1 STEEL

Plate Thickness	Aspect Ratio	Block No.	Transition Temperature Range ° F: Based on energy to max. load	Based on appearance of fracture as defined by % of shear	All Blocks Combined, based on appearance	Single Point Transition Temp. °F based on appearance
½"	4	I	Indeterminate	-20 to zero		
		II	"	-40 to -30		
		III	"	-35 to -25	-20 to zero	-10
		IV	"	-40 to -30		
	8	II	Indeterminate	-10 to zero	-10 to zero	-10
	16	I	zero to +10	zero to +10		
		II	Indeterminate	+10 to +20		
		III	zero to +10	zero to +10	+10 to 20	- 2
		IV	Indeterminate	-10 to zero		
	19	I	Insufficient Data			
		II	-20 to -10	-20 to -10	-10 to zero	- 8
		III	-10 to zero	-10 to zero		
3/4"	4	II	Indeterminate	-20 to zero	-20 to zero	-23
	8	II	Indeterminate	zero to +10	zero to +10	zero
	12	II	zero to +10	zero to +10	zero to +10	+ 5
	16	I	Indeterminate	-20 to -10		
	16	II	"	+30 to +40	+30 to 40	+15
1"	4	II	Indeterminate	+10 to +20	+10 to +20	+13
	8	II	"	+10 to +20	+10 to +20	+13
	12	IV V	+30 to +40	+30 to +40	+30 to +40	+28
1½"	4	I	Indeterminate	+40 to +50		
		II	"	+40 to 50	+50 to 60	+44
		III	"	+50 to +60		
	6	II	"	+50 to +60	50 to 60	+50

TABLE 5

TRANSITION TEMPERATURES

T-2 and T-2R STEELS

Plate Thickness	Aspect Ratio	Transition Temperature Range °F: Based on Energy to max. load	Transition Temperature Range °F: Based on appearance of fracture as defined by % of shear	Single Point Transition Temp. °F based on appearance as defined by % of shear
		T-2 STEEL		
3/4"	4	Indeterminate	-20 to -10	-17
	8	"	-10 to - 5	-18
	12	"	-10 to zero	- 5
	16	"	+10 to +20	+ 2
1"	4	"	-10 to zero	- 7
	6	"	+10 to +20	+10
	8	"	+30 to +40	+33
	12	zero to +20	zero to +20	+13
$1\frac{1}{2}$"	4	Indeterminate	+30 to +40	+30
	6	"	+60 to +75	+68
		T-2R STEEL		
3/4"	4	(Insufficient Data)		
	6	(Insufficient Data)		
	16	Indeterminate	+40 to +50	+38
	20	"	+35 to +50	+38

these latter two diagrams will not determine transition temperature any better than the percentage of shear diagram. For this reason the appearance of the fracture (as defined by the percentage of shear) has been used to determine transition temperature range and single values of the transition temperature. Transition temperature results so found are shown in Table 4 for T-1 steel and in Table 5 for T-2 and T-2R steels.

In Table 4 relating to the T-1 steel, note that the transition temperatures have been given for the various thicknesses, aspect ratios and blocks indicating position within the plate, as indicated on the plate layout figures. The transition temperature was indeterminate by a consideration of energy to maximum load in all except six instances. The transition temperature did not vary significantly from block to block for the 1/2" thick plate or for the 3/4" thick plate except that the transition temperature was quite different in blocks I and II for the Aspect Ratio 16. No reasons have been formulated to explain this exception. It was thought best to incorporate all of the data from the various blocks and determine the overall transition temperature for each thickness from these composite results. Table 4 summarizes the transition temperature ranges and the single values of transition temperature where both are based on the appearance of the fracture.

Figure 17 is a plot of the single values of transition temperature for T-1 steel against aspect ratio for the four plate thicknesses involved. It will be noted that transition temperature for any given (AR) is affected by a change in thickness with the thicker plates (with one exception at AR 4 for the 3/4" thick plate) showing the higher transition temperatures. For a given thickness of plate the transition temperatures also generally increase with an increase in the aspect ratio.

Figure 18 represents a repetition of Figure 17 with a second parameter, the width of the test specimens, added. In order to complete this diagram, an extrapolation of the test results in $1\frac{1}{2}"$ thickness was made to widths of 4 and 10 inches. With the two parameters, thickness and width of specimen shown together, it is clearly indicated that as width is increased, for a given thickness, the transition temperatures also increase. This increase in transition temperature due to width can only be accounted for by a modifying of the strain conditions at the notch since metallurgical effects may be assumed to remain constant for a particular plate thickness.

Due to a combination of metallurgical and geometrical causes, transition temperature rises with increasing plate thickness. Also, increased thickness causes a decrease in the average stress at maximum load for geometrically similar specimens. Perhaps these two facts may be coupled together by referring the degree of localization of stress or strain at the notch to thickness.

When the transition temperatures are plotted on width, as in Figure 19, rather than on width divided by thickness, the curves for the different thicknesses, although not reversing in order as they were in plotting unit energy values, are seen to rise less steeply and appear to be more nearly parallel. This might be considered to indicate that the geometrical effect of width had in this way been more completely eliminated than in Figure 17. Residual differences between different thicknesses on the energy scale would then be attributed to non-geometrical (metallurgical) causes.

The limited results of tests on T-2 steel (Figure 20) exhibit the same trends previously noted for T-1 steel. The transition temperature for t = 3/4" is about 10° lower than for T-1 steel. Here, this difference may certainly be attributed to metallurgy alone. The 1" and $1\frac{1}{2}$" thicknesses, however, have a transition temperature of about the same as for T-1 steel. Insufficient tests prevent any general conclusion or firm comparisons.

Limited tests on T-2R steel indicate that the transition temperature of the re-rolled 3/4" thick plates are about 40° higher than for T-2 steel. (See Figure 20). It is evident that metallurgical changes took place which increased the notch-sensitivity of the T-2 steel. (See grain size classifications under section entitled "Materials").

CORRELATION WITH TESTS BY OTHERS

The University of California[2] has reported on wide plate tests for steel plates of 3/4" thickness in widths varying from 12 to 108", or interpreted in terms of aspect ratio, tests were made with AR varying from 16 to 144. Although only a few tests were made in the greater widths, there is an indication that the transition temperature rose as the width of the plate was increased, with a trend toward constant transition temperatures at great widths. This is in keeping with the trend found in this investigation. It can be inferred from the test of the 1/2" and the 3/4" thick plates of this investigation that plate widths of around 12" are nearly wide enough to establish a value for transition temperatures of internally notched specimens of great width.

The University of California(2) reported investigations made on geometrically similar specimens. The specimens reported were edge notched, with the thickness varying from 1/2" to 1 1/8". The thickness was the as rolled plate thickness in each instance. Since the width of the 1/2" thick specimen was only 2", it may be seen that the aspect ratio was in the lower range, whereas the tests reported herein cover aspect ratios up to and including 20. However, the trend in transition temperature shown by the California tests, namely, that transition temperature may be expected to increase with plate thickness, confirms the results of this investigation. Other California(2) tests using 3" wide edge notched specimens with thickness varying from 1/2" to 1 1/8", all machined from 1 1/8" thick plates, show that with constant width and varying thickness the transition temperature is generally lower for the thinner plates. The same type of specimen using plates of "as rolled" thicknesses showed more or less the same trend with the exception that the transition temperatures are lower than for the specimens machined from a single plate.

Professor E. R. Parker has reported(3) on work performed at the University of California concerning the action of geometrically similar specimens which were all machined from an annealed plate originally 1¼" thick. The specimens were 3", 6", and 12" wide and 3/16", 3/8" and 3/4" thick. The stress raiser was a square hole in the center of the plate with its sides at 45 degrees to the longitudinal axis of the plate. The radii at the corners of the square hole were made proportional to plate thickness. Professor Parker points out that geometrically similar notched specimens exhibit a marked size effect. This statement was made with the assumption that the specimens were metallurgically similar, and that the size effects must be due to geometry. Not enough evidence is presented to permit a study of the trends and transition temperature. Professor Parker contends that geometric similarity is destroyed before the maximum load is reached. This is a contention which our investigation supports, since it is felt that after the crack at the notch has become visible, the notch acuity is essentially the same in all specimens and that the original dimensional similarity is destroyed.

CONCLUSIONS

The tentative conclusions permitted on the basis of test results of internally notched specimens are as follows:

1. With plates rolled from the same heat the thick plates shift from shear to cleavage fracture at a higher temperature than thinner plates.
2. Transition temperatures, as judged by appearance of the fracture, for plates of constant thickness (metallurgy constant) increase as width increases, tending to become uniform for large widths.
3. The average unit stress at maximum load of geometrically similar notched plates indicates that thicker plates will withstand a smaller stress intensity than thinner plates. The average unit stress at maximum load for plates of equal width but of different thicknesses tends toward the same value regardless of thickness.

4. Unit energy absorption to maximum load for specimens failing in 100% shear decreases with increased thickness for dimensionally similar specimens; for plates of equal width but of different thickness the thicker plates have a unit energy absorption greater than thinner plates.

5. Dimensional similarity of specimens defined by equal aspect ratios does not establish geometric similarity of strain patterns when judged by unit energy absorption for specimens failing in 100% shear.

6. Differences in unit energy and transition temperature in plates of different thickness due to non-geometrical (metallurgical) causes are not completely segregated in comparisons made at equal aspect ratio. It now appears that instead of aspect ratio $(w \cdot t^{-1})$, another function such as $(w \cdot t^{-n})$, where $1 > n > 0$, may serve better for segregating the geometric from the metallurgical effects.

BIBLIOGRAPHY

1. S. T. Carpenter, W. P. Roop, N. Barr, E. Kasten & A. Zell, Swarthmore College, "Progress Report on Twelve-Inch Flat Plate Tests", Serial No. SSC-21, April 15, 1949 to the Bureau of Ships, U. S. Navy.

2. H. E. Davis, G. E. Troxell, E. R. Parker, A. Boodberg, M. P. O'Brien, University of California, "Final Report on Causes of Cleavage Fracture in Ship Plate, Flat Plate Tests and Additional Tests on Large Tubes", Serial No. SSC-8, January 17, 1947, to Bureau of Ships, U. S. Navy.

3. E. R. Parker, "The Effect of Section Size on the Fracture Strength of Mild Steel" in "Fracturing of Metals", p. 82, American Society of Metals, 1948.

ACKNOWLEDGMENTS

The investigation herein reported has been under the direct supervision of S. T. Carpenter. Captain W. P. Roop, USN (Retired) has been a constant adviser and collaborator. The testing has been done under the supervision of A. W. Zell and E. Kasten.

Theodore Bartholomew, Eugene Urban and Lawrence Robbins prepared all specimens and assisted in testing. Drawings of the report were made by John Calvin, Roy Bosshardt and Henry Rueger. Mrs. Ruth Sommer has performed all stenographic duties.

The investigators are deeply indebted to Dr. Finn Jonassen, Project Coordinator, and Dr. William Baldwin, Chairman of the Ship-Structure Advisory Committee, and to the members of the Committee, for much helpful advice.

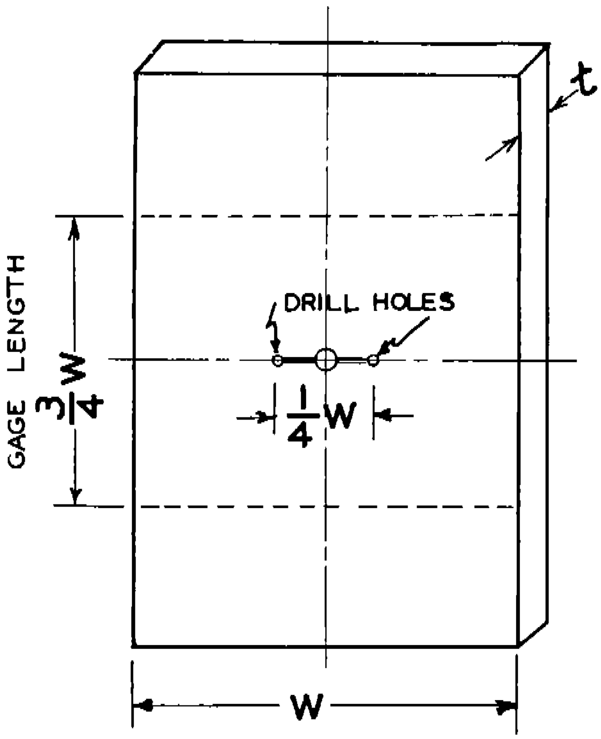

ASPECT RATIO $= \frac{W}{t}$

t	DIA. OF DRILL HOLES
$\frac{1}{2}$"	$\frac{1}{32}$"
$\frac{3}{4}$"	$\frac{3}{64}$"
1"	$\frac{1}{16}$"
$1\frac{1}{2}$"	$\frac{3}{32}$"

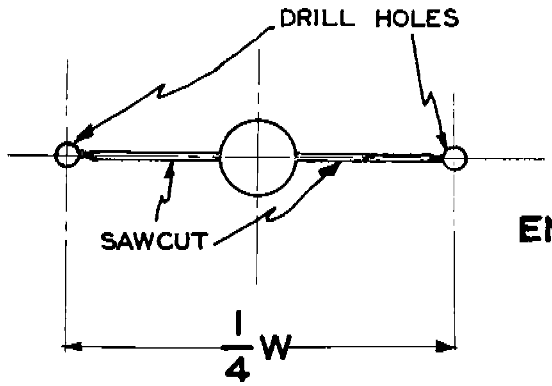

ENLARGED VIEW

FIG. 1

TYPICAL SPECIMEN

SWARTHMORE COLLEGE

9-6-49

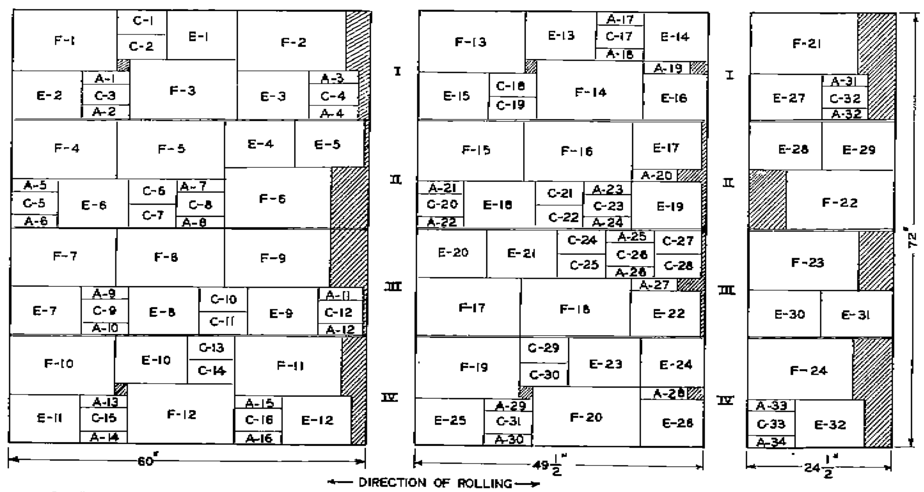

← DIRECTION OF ROLLING →

A – 2" x 8"
C – 4" x 8"
E – 8" x 12"
F – 9½" x 18"

STEEL T-1

FIG. 2

½" PLATE LAYOUT T-1

SWARTHMORE COLLEGE

9-7-49

SCALE – 0.5" = 8"

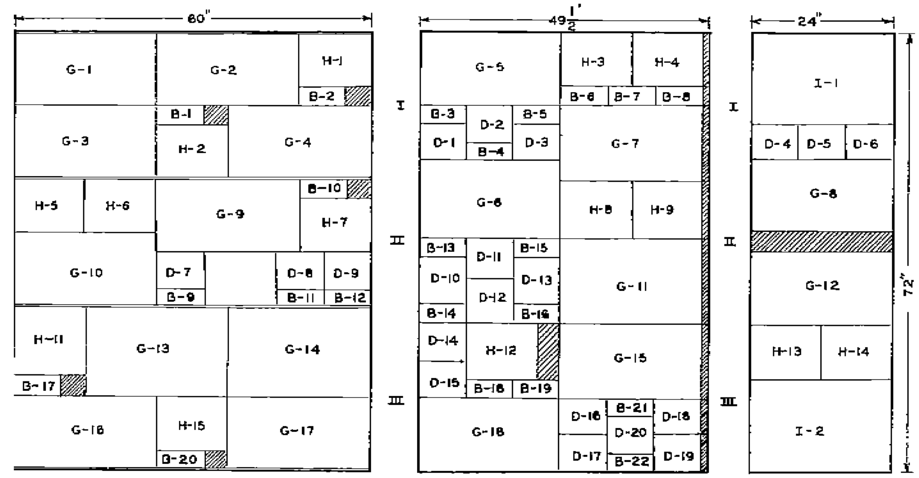

B – 3" x 8"
D – 6" x 8"
H – 9" x 12"
G – 12" x 24"
I – 15" x 24"

← DIRECTION OF ROLLING →

STEEL T-1

FIG. 3

¾" PLATE LAYOUT T-1

SWARTHMORE COLLEGE

9-7-49

SCALE – 0.5" = 8"

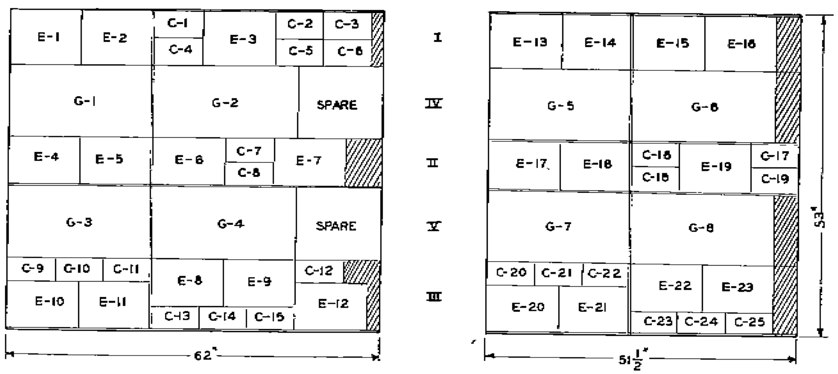

← DIRECTION OF ROLLING →

STEEL T-1

C – 4" x 8"
E – 8" x 12"
G – 11½" x 24"

FIG. 4

1" PLATE LAYOUT T-1

SWARTHMORE COLLEGE

9-6-49

SCALE – 0.5" = 8"

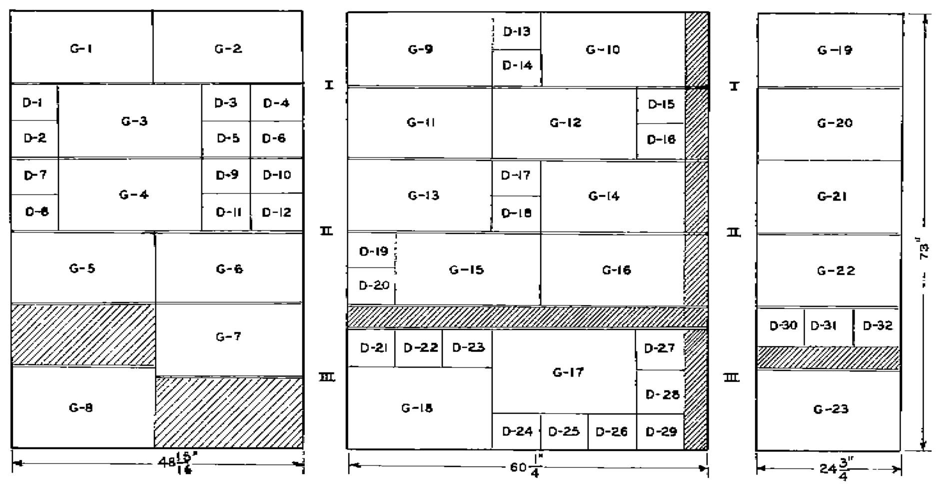

D – 6" x 8"
G – 12" x 24"

← DIRECTION OF ROLLING →

STEEL T-1

FIG. 5

1½" PLATE LAYOUT T-1

SWARTHMORE COLLEGE

9-7-49

SCALE – 0.5" = 8"

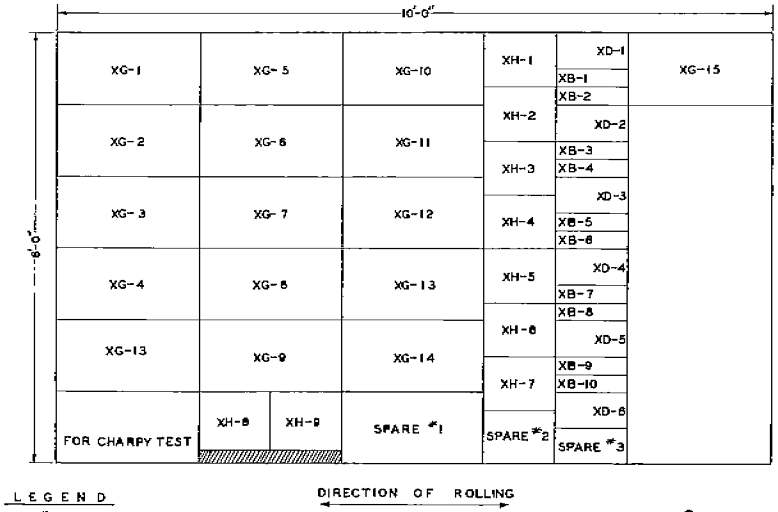

LEGEND
XG-3/4" X 12" X 24"
XH-3/4" X 9" X 12"
XD-3/4" X 6" X 12"
XB-3/4" X 3" X 12"

FIG. 6
3/4" PLATE LAYOUT
STEEL T-2
SWARTHMORE COLLEGE
6-29-50

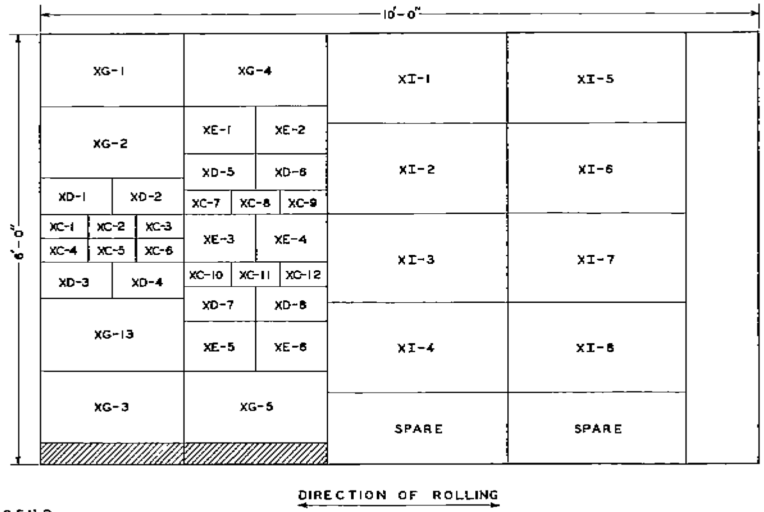

LEGEND
XG- 1" X 12" X 24"
XD- 1" X 6" X 12"
XE- 1" X 8" X 12"
XC- 1" X 4" X 8"
XI- 1" X 15" X 30"

FIG. 7
1" PLATE LAYOUT
STEEL T-2
SWARTHMORE COLLEGE
6-28-50

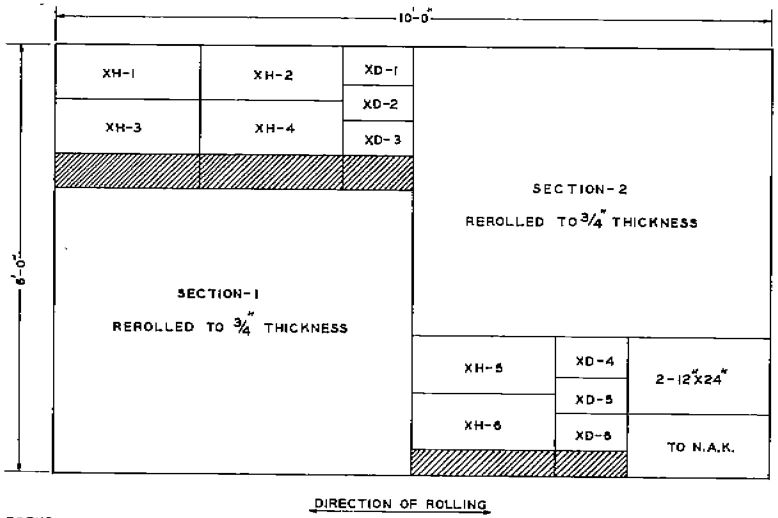

LEGEND
XD-6"X12"
XH-9"X24"

FIG. 8A
1½" PLATE LAYOUT
STEEL T-2
SWARTHMORE COLLEGE

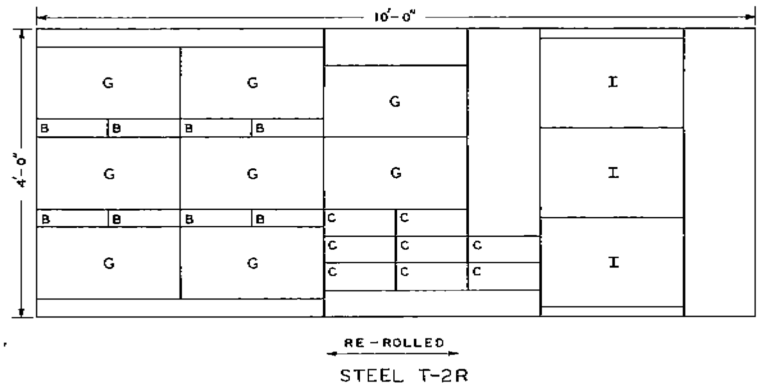

LEGEND:

	AR
B - 3" X 12"	4
C - 4½" X 12"	6
G - 12" X 24"	16
I - 15" X 24"	20

SCALE: 3/4" = 1'-0"

FIG. 8B
3/4" PLATE LAYOUT
FOR RE-ROLLED T-2 STEEL

SWARTHMORE COLLEGE
9-12-50

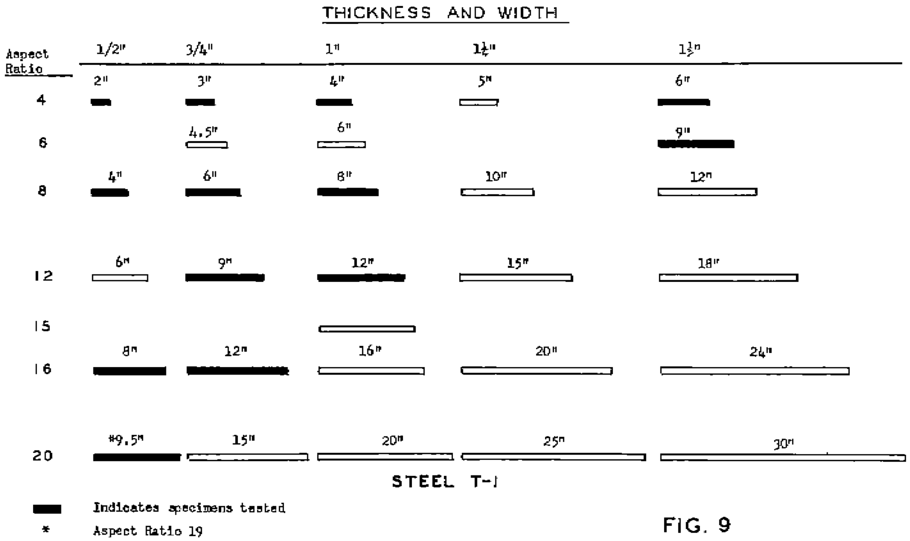

FIG. 9
ASPECT RATIO PROGRAM T-1
SWARTHMORE COLLEGE

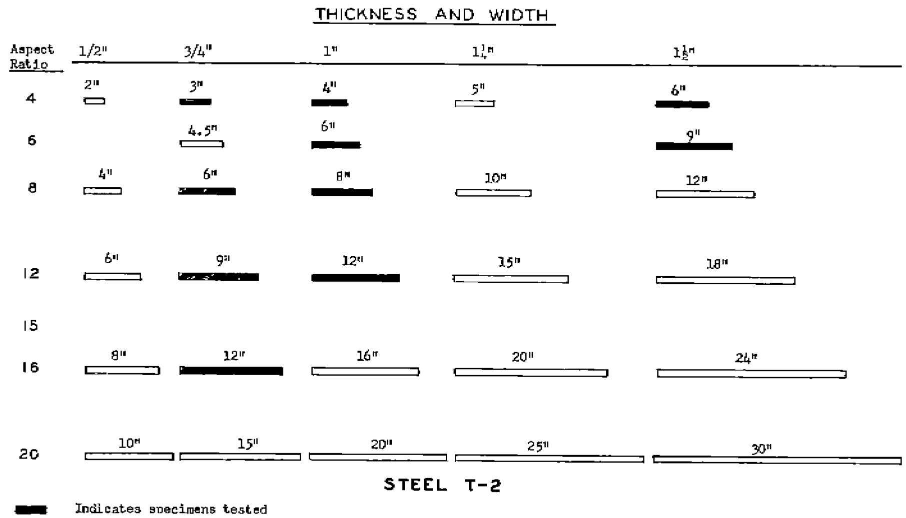

FIG. 10
ASPECT RATIO PROGRAM T-2
SWARTHMORE COLLEGE

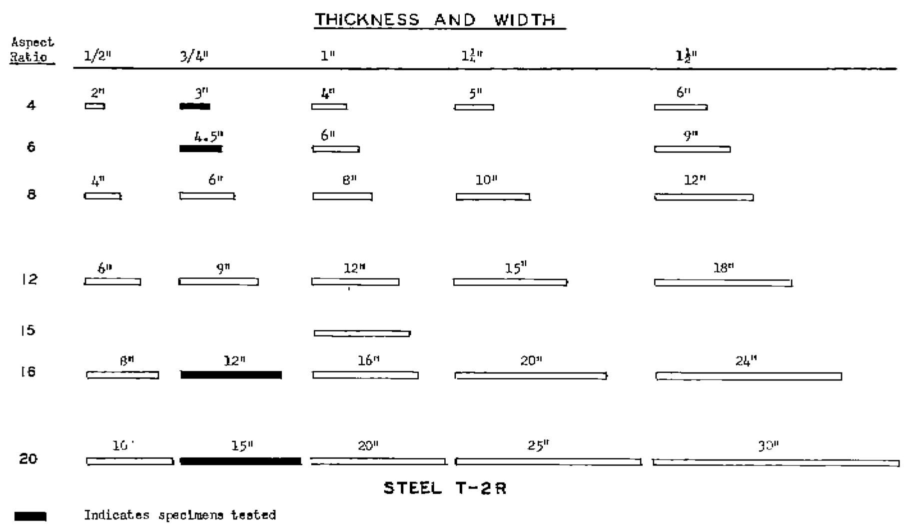

FIG. 11
ASPECT RATIO PROGRAM T-2R
SWARTHMORE COLLEGE

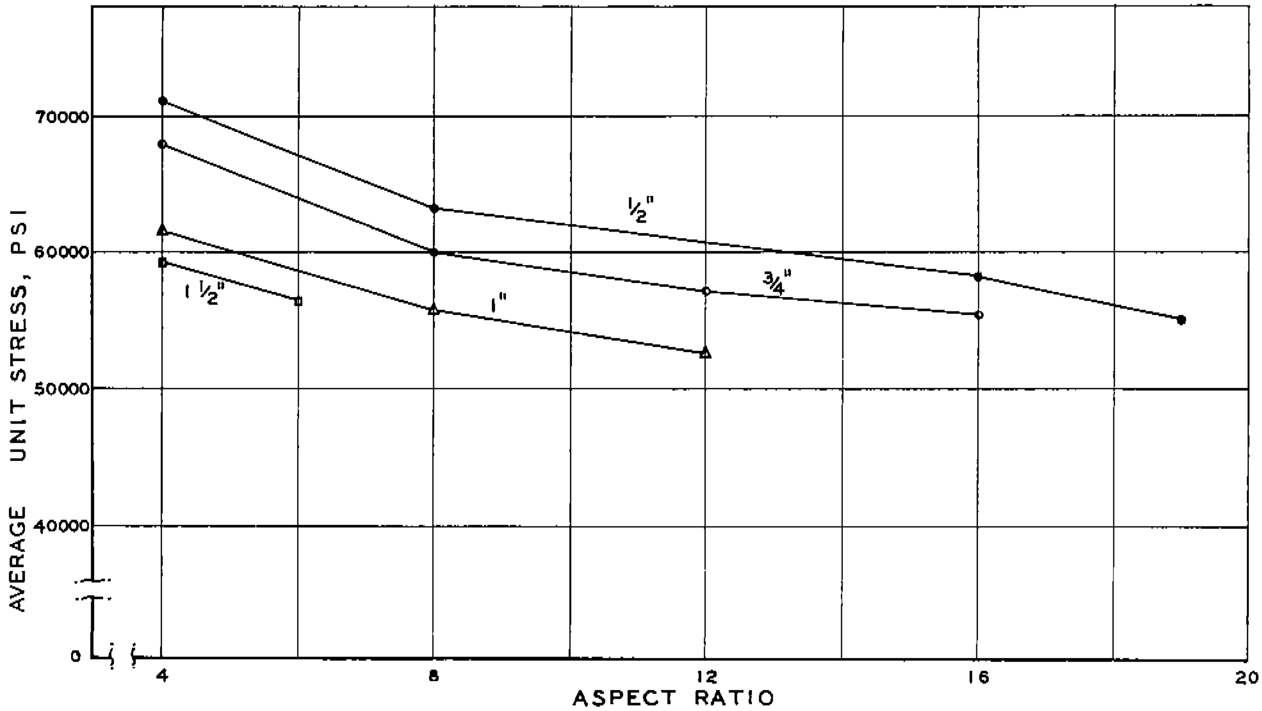

FIG. 12 VARIATION IN UNIT STRESS AT MAXIMUM LOAD FOR VARIABLE THICKNESS AND ASPECT RATIO, T-1 STEEL, 100% SHEAR FAILURES.

SWARTHMORE COLLEGE

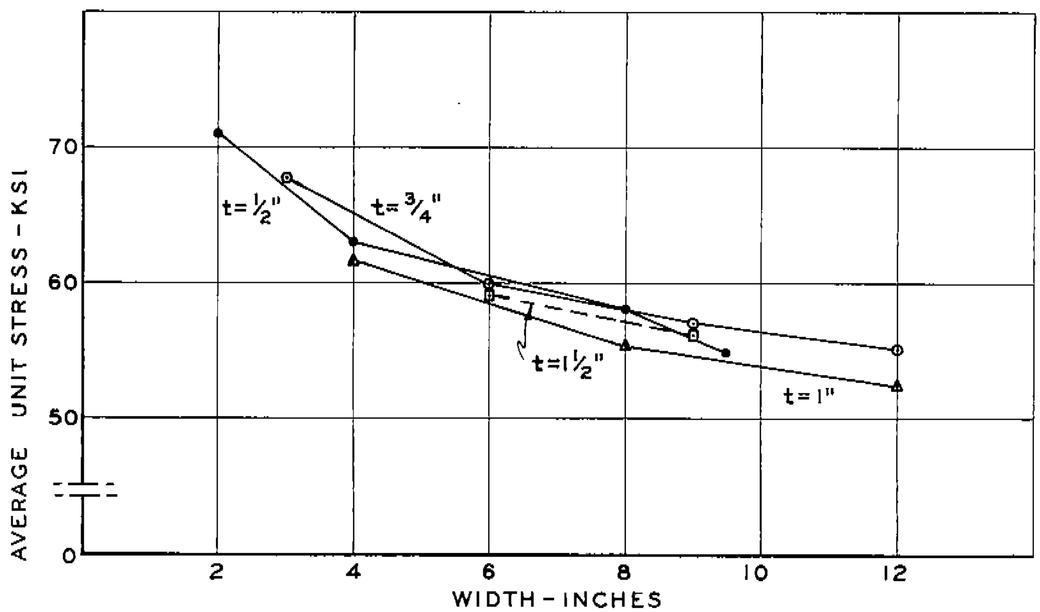

FIG. 13 VARIATION IN UNIT STRESS AT MAXIMUM LOAD FOR VARYING WIDTH AND THICKNESS, T-1 STEEL, 100% SHEAR FAILURES

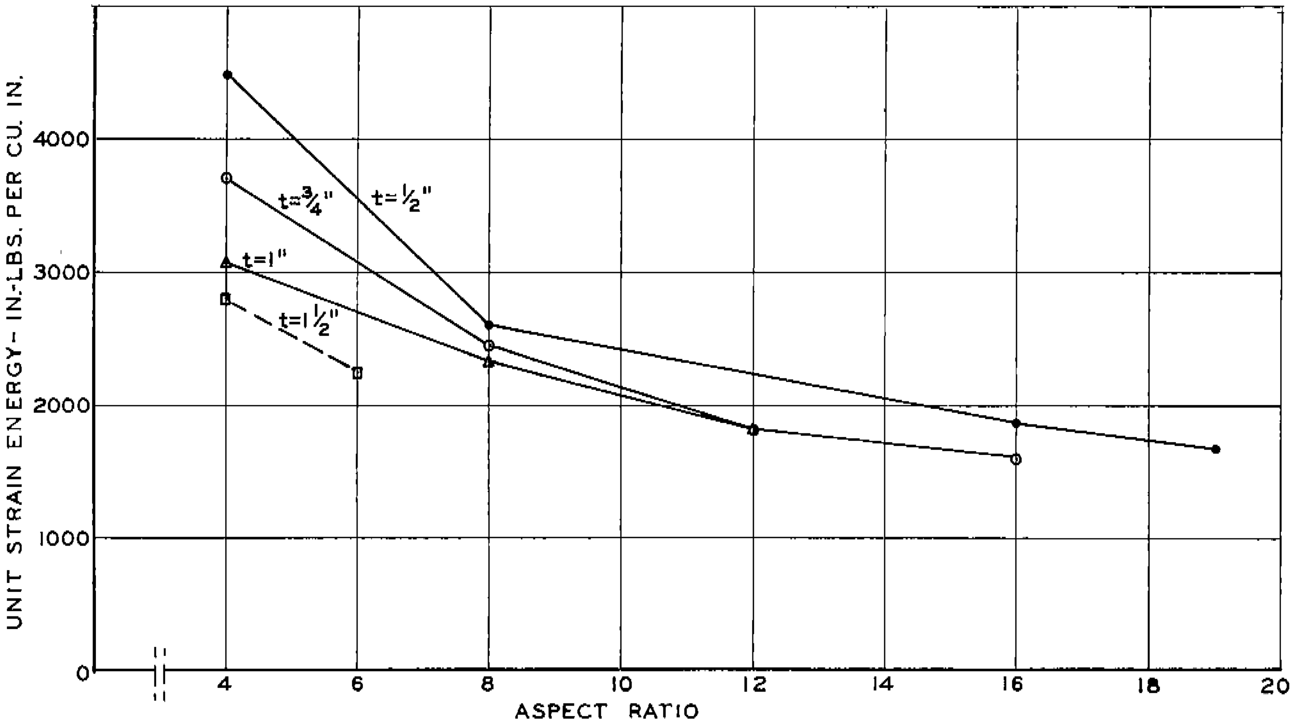

FIG. 14 AVERAGE UNIT STRAIN ENERGY TO MAXIMUM LOAD FOR VARYING ASPECT RATIO AND THICKNESS, T-1 STEEL, 100% SHEAR FAILURES

SWARTHMORE COLLEGE

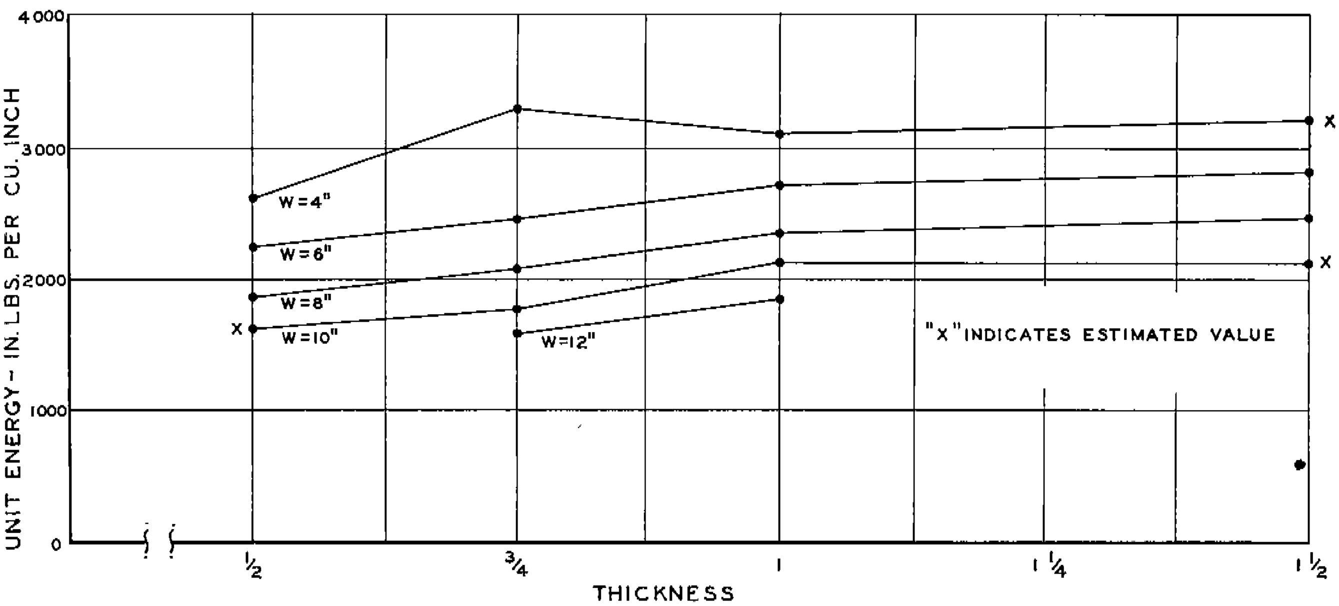

FIG. 15 AVERAGE UNIT ENERGY TO MAXIMUM LCAD. VARIATION FOR T-1 STEEL WITH VARYING THICKNESS AND WIDTH. 100% SHEAR FAILURES.

SWARTHMORE COLLEGE

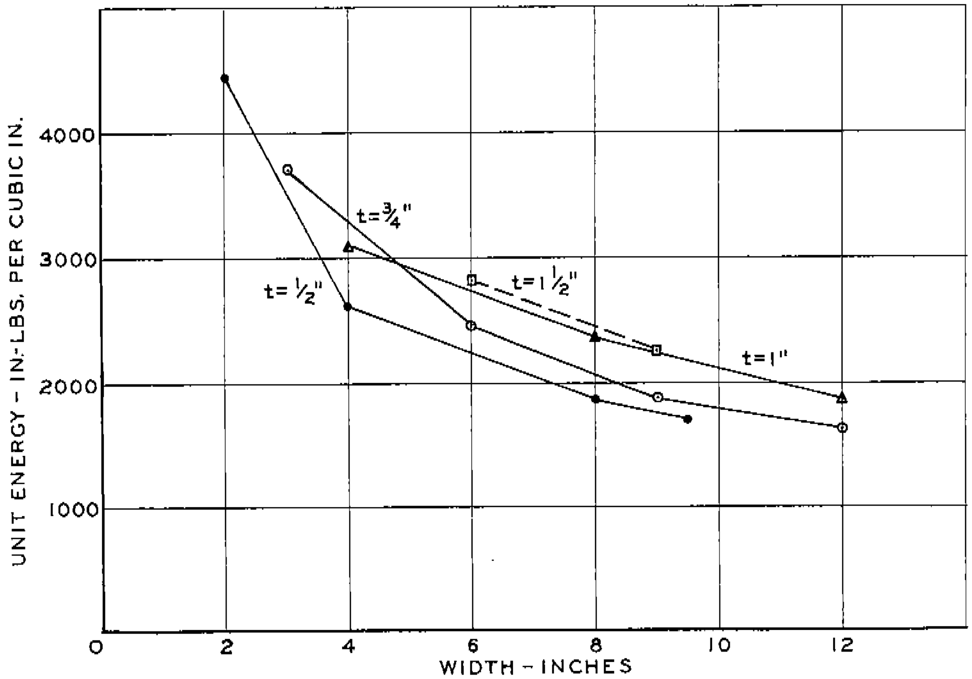

FIG. 16 AVERAGE UNIT STRAIN ENERGY TO MAXIMUM LOAD FOR VARYING WIDTH AND THICKNESS, T-1 STEEL, 100% SHEAR FAILURES

SWARTHMORE COLLEGE

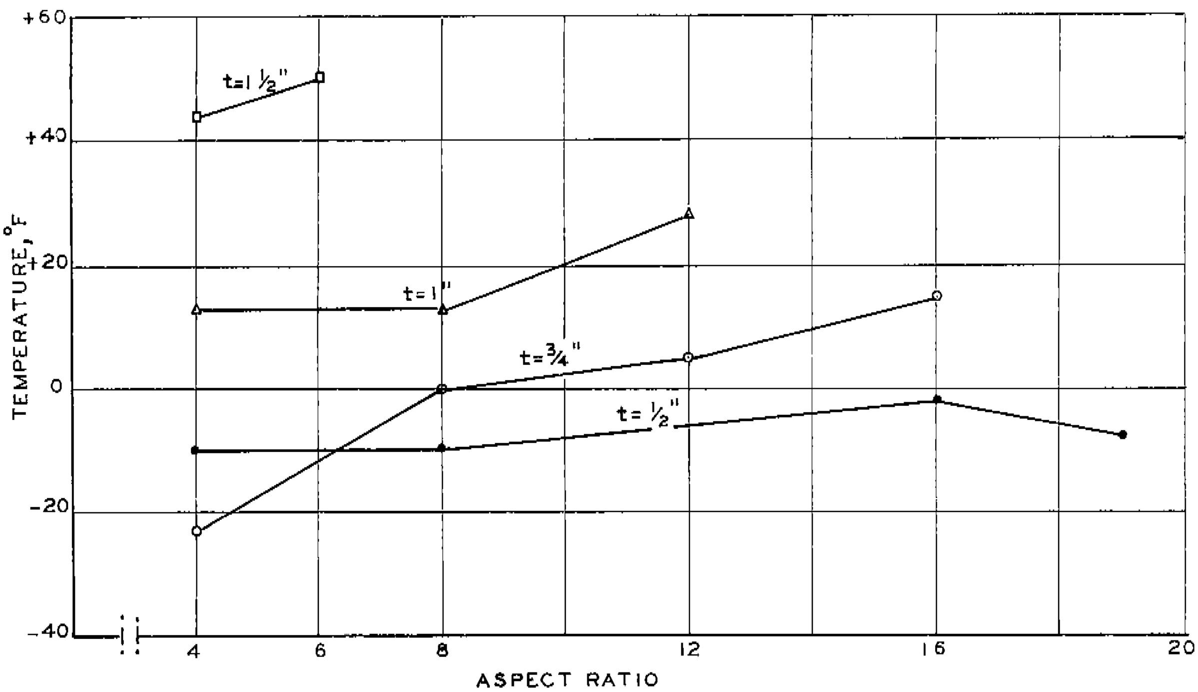

FIG. 17 TRANSITION TEMPERATURE FOR T-1 STEEL WITH VARYING ASPECT RATIO & THICKNESS

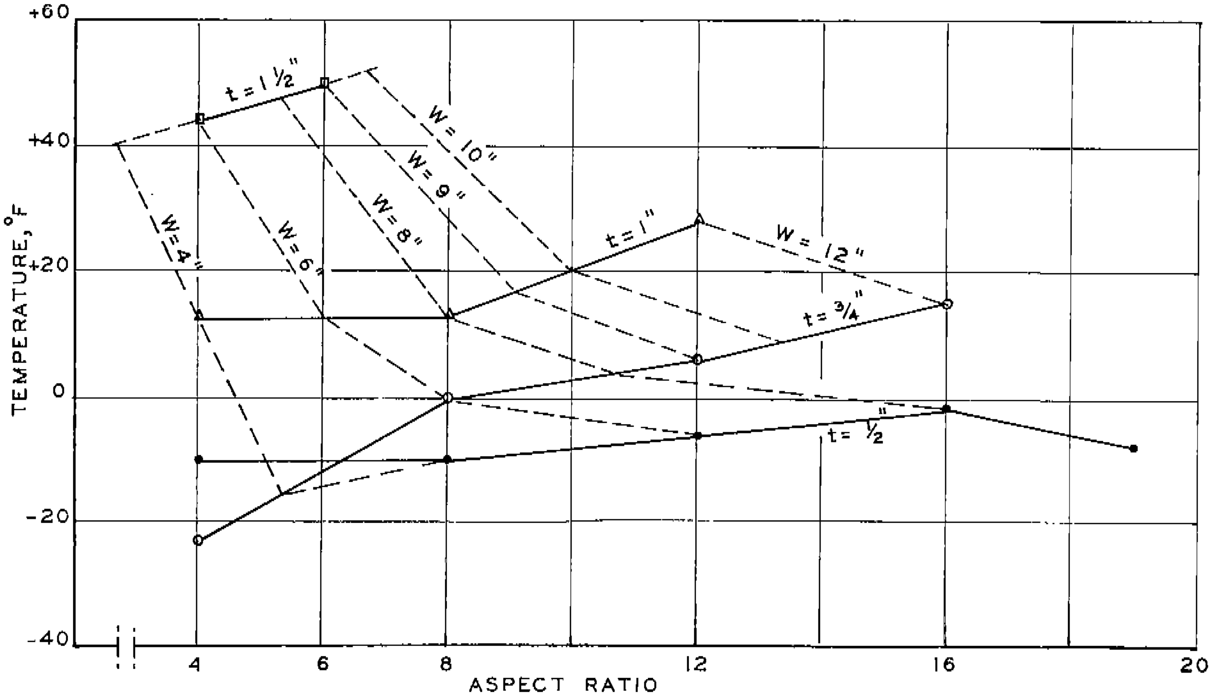

FIG. 18 TRANSITION TEMPERATURES FOR T-1 STEEL, SHOWING EFFECT OF ASPECT RATIO, THICKNESS AND WIDTH OF SPECIMEN.

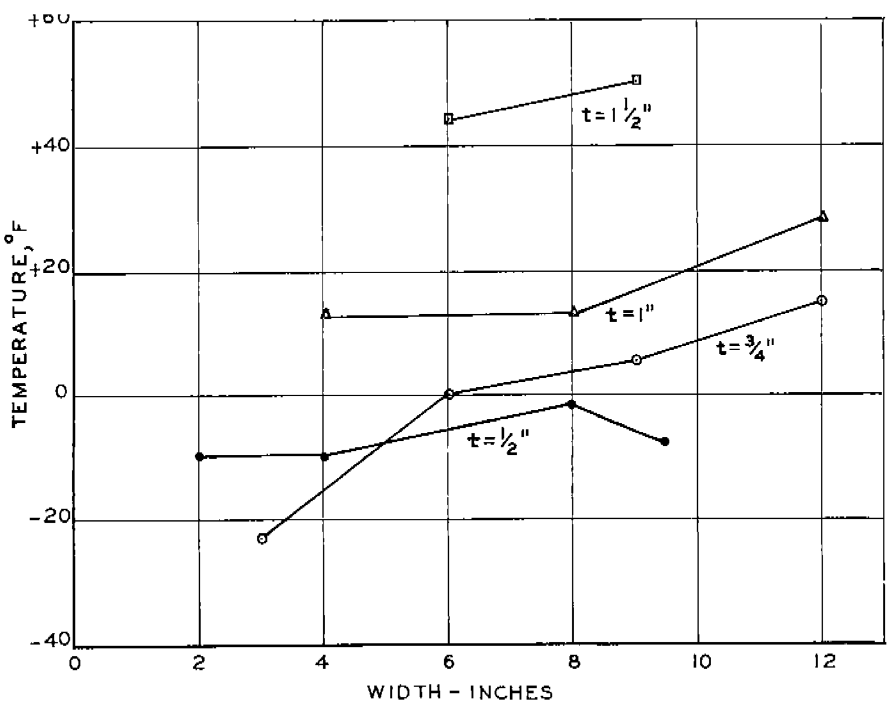

FIG. 19 TRANSITION TEMPERATURE FOR T-1 STEEL WITH VARYING WIDTH AND THICKNESS

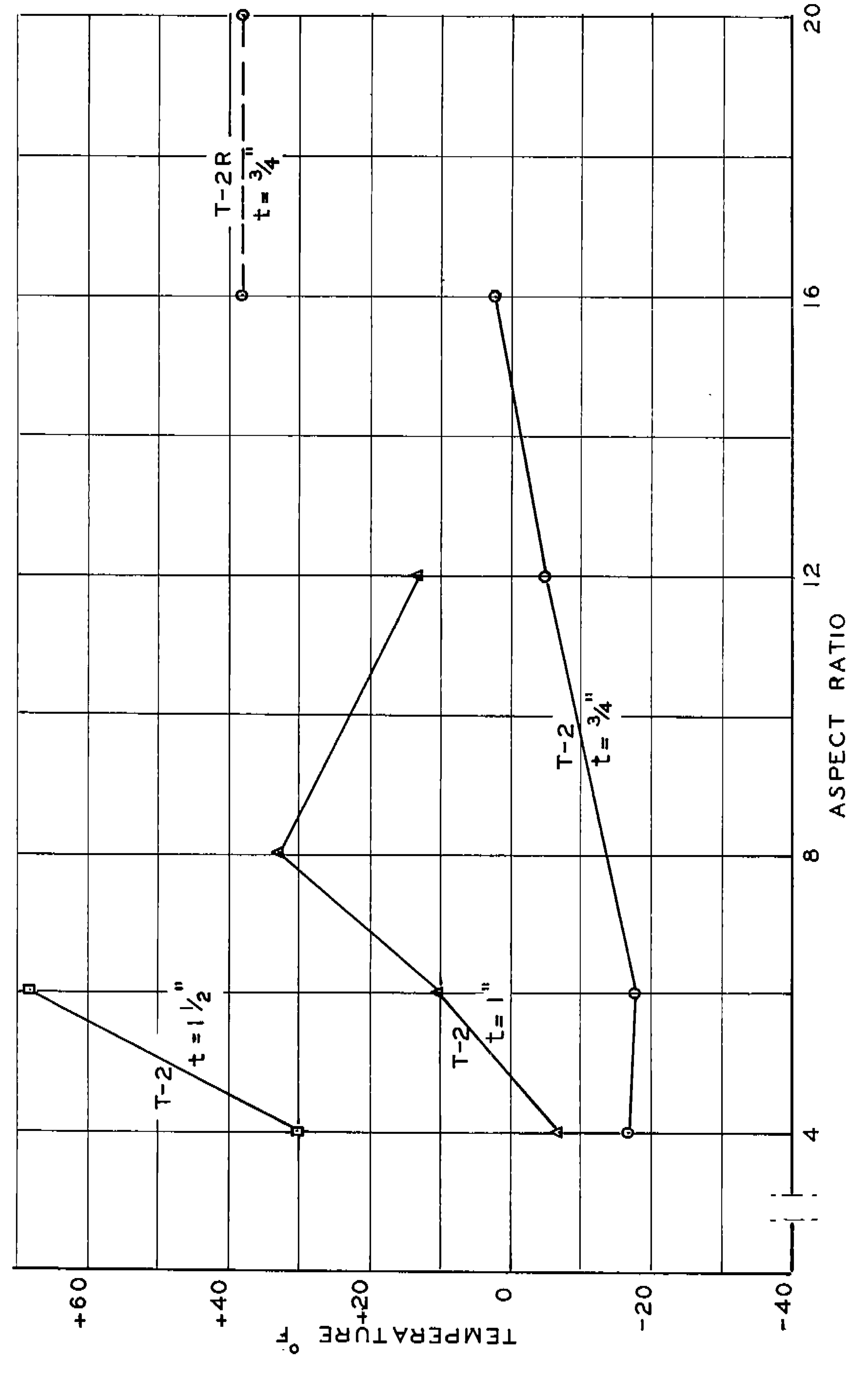

FIG. 20 TRANSITION TEMPERATURES FOR T-2 AND T-2R STEELS WITH VARYING ASPECT RATIO AND THICKNESS.

SWARTHMORE COLLEGE

APPENDIX I

TABLES OF BASIC DATA

TABLE I-1

Aspect Ratio 4

Code: T-1 Specimen Size: 1/2" x 2"

Block No.	Spec. No.	Temp. Deg F	To Visible Crack Energy E in.lbs.	To Visible Crack Load lbs.	To Maximum Load Energy E1 in.lbs.	To Maximum Load Load lbs.	To Fracture Energy E2 in.lbs.	To Fracture Load lbs.	Energy Difference E2 - E1 in.lbs.	% Shear	Internal Notch W/4 Acuity
I	A-3	0	2,740	46,500	6,400	52,000	14,300	14,000	7,900	100	1/32" notch
"	A-2	-10	3,000	47,200	6,500	53,800	7,350	53,600	850	0	"
"	A-32	-10	3,200	47,500	6,750	52,900	14,700	17,000	7,950	100	"
"	A-1	-18	3,200	48,300	6,500	53,300	8,500	50,000	2,000	8	"
"	A-4	-20	3,250	47,300	6,350	53,600	11,600	41,000	5,250	30	"
"	A-31	-20	3,500	49,000	6,300	53,200	6,300	53,200	0	0	"
"	A-17	-20	2,700	46,500	6,350	53,000	13,800	17,000	7,450	100	"
"	A-18	-64	3,850	48,200	7,850	54,000	7,850	54,000	0	0	"
II	A-5	0	1,690	42,200	6,060	51,600	13,370	13,000	7,310	100	"
"	A-22	-25	1,990	42,800	6,800	53,200	14,200	15,000	7,400	100	"
"	A-6	-32	1,760	42,800	6,760	53,700	13,680	13,000	6,920	100	"
"	A-23	-35	2,100	42,000	7,250	53,500	7,250	53,300	0	0	"
"	A-24	-40	1,850	42,600	7,350	54,400	7,350	54,400	0	0	"
"	A-7	-52	1,960	42,500	6,870	54,700	6,870	54,700	0	0	"

TABLE I-1a

Aspect Ratio 4 Continued

Code: T-1 Specimen Size: 1/2" x 2"

Block No.	Spec. No.	Temp. Deg. F	To Visible Crack Energy E in.lbs.	To Visible Crack Load lbs.	To Maximum Load Energy E1 in.lbs.	To Maximum Load Load lbs.	To Fracture Energy E2 in.lbs.	To Fracture Load lbs.	Energy Difference E2 - E1 in.lbs.	% Shear	Internal Notch W/4 Acuity
III	A-9	0	1,300	43,200	6,350	53,900	12,300	13,000	5,950	100	1/32" hole
"	A-25	-25	2,400	44,900	7,300	54,500	15,100	13,000	7,800	100	"
"	A-10	-35	1,950	43,500	7,500	55,000	14,400	16,000	6,900	100	"
"	A-11	-35	2,100	44,500	6,200	53,500	6,200	53,500	0	0	"
"	A-26	-40	2,500	44,100	6,800	54,100	6,800	54,100	0	0	"
"	A-12	-40	2,200	44,200	6,200	54,400	6,200	54,400	0	0	"
IV	A-13	0	2,800	45,500	5,850	51,800	14,300	12,000	8,450	100	"
"	A-14	-20	3,350	47,500	7,200	53,100	16,950	13,000	9,750	100	"
"	A-15	-20	3,350	47,300	6,600	52,800	15,400	17,000	8,800	100	"
"	A-16	-32	3,600	48,800	6,700	53,800	15,300	17,000	8,600	100	"
"	A-30	-42	4,000	48,300	6,700	53,200	6,700	53,200	0	0	"
"	A-33	-55	3,000	46,500	7,400	54,200	16,500	16,000	9,100	100	"
"	A-29	-60	3,200	47,300	6,000	54,000	6,000	54,000	0	0	"
"	A-34	-64	2,800	48,200	7,500	54,000	8,000	53,700	500	0	"

TABLE I-2

Aspect Ratio 8

Code: T-1 Specimen Size: 1/2" x 4"

Block No.	Spec. No.	Temp. Deg. F	To Visible Crack Energy E in.lbs.	To Visible Crack Load lbs.	To Maximum Load Energy E1 in.lbs.	To Maximum Load Load lbs.	To Fracture Energy E2 in.lbs.	To Fracture Load lbs.	Energy Difference E2 - E1 in.lbs.	% Shear	Internal Notch W/4 Acuity
I	C-3	0	4,250	76,500	13,750	95,200	13,750		0	0	1/32" hole
II	C-8	21	3,750	72,500	14,500	93,700	37,000	16,000	22,500	100	"
"	C-6	0	3,500	73,700	16,250	94,800	40,000	25,000	23,750	100	"
"	C-20	0	3,370	73,900	15,000	94,800	40,500	20,000	25,500	100	"
"	C-23	-10	3,750	73,700	17,000	95,000	40,700	16,000	23,700	100	"
"	C-5	-10	3,500	71,600	15,000	95,500	15,000	95,500	0	0	"
"	C-7	-20	3,750	74,400	18,100	97,700	28,250	83,000	10,150	25	"

TABLE I-3

Aspect Ratio 16

Code: T-1 Specimen Size: 1/2" x 8"

Block No.	Spec. No.	Temp. Deg. F	To Visible Crack Energy E in.lbs.	To Visible Crack Load lbs.	To Maximum Load Energy E1 in.lbs.	To Maximum Load Load lbs.	To Fracture Energy E2 in.lbs.	To Fracture Load lbs.	Energy Difference E2 - E1 in.lbs.	% Shear	Internal Notch W/4 Acuity
I	E-13	+10	11,000	136,500	45,000	168,300	117,000	20,000	72,000	100	1/32" hole
"	E-14	0	11,500	140,300	50,000	173,100	125,000	26,000	75,000	100	"
"	E-27	0	9,500	138,500	32,500	172,000	32,500	172,000	0	0	"
"	E-3	0	12,000	143,600	46,500	177,000	119,000	15,000	72,500	100	"
"	E-1	-10	10,000	140,000	44,000	177,400	118,000	22,000	74,000	100	"
"	E-16	-10	9,000	136,800	20,000	160,500	20,000	160,500	0	0	"
"	E-2	-20	10,000	139,200	33,500	173,000	33,500	173,000	0	0	"
"	E-15	-21	10,000	140,600	33,250	175,200	33,250	175,200	0	0	"
II	E-17	40	6,800	132,300	39,400	172,500	112,300	20,000	72,900	100	"
"	E-29	30	7,000	133,300	43,300	172,500	101,200	15,000	57,900	100	"
"	E-28	20	10,000	139,200	43,000	173,900	108,000	20,000	65,000	100	"
"	E-5	10	7,500	133,000	27,100	166,500	27,100	166,500	0	0	"
"	E-19	10	8,500	132,800	31,000	169,000	31,000	169,000	0	0	"
"	E-4	0	6,600	133,300	50,900	179,800	64,700	170,000	13,800	16	"
"	E-6	0	6,300	132,800	54,000	177,700	103,000	94,000	49,000	35	"
"	E-18	-30	6,500	139,500	28,000	170,500	28,000	170,500	0	0	"

TABLE I-3a

Aspect Ratio 16 Continued

Code: T-1 Specimen Size: 1/2" x 8"

Block No.	Spec. No.	Temp. Deg. F	To Visible Crack		To Maximum Load		To Fracture		Energy Difference E2 - E1 in.lbs.	% Shear	Internal Notch W/4 Acuity
			Energy E in.lbs.	Load lbs.	Energy E1 in.lbs.	Load lbs.	Energy E2 in.lbs.	Load lbs.			
III	E-7	30	9,200	135,300	43,000	172,900	101,000	20,000	58,000	100	1/32" hole
"	E-9	10	7,500	133,800	43,000	176,300	109,000	60,900	66,000	100	"
"	E-8	0	7,500	134,200	48,500	175,400	113,500	17,700	65,000	100	"
"	E-21	0	7,000	133,700	37,500	173,500	37,500	173,500	0	0	"
"	E-20	-10	8,500	136,800	36,500	174,500	36,500	174,500	0	0	"
"	E-30	-10	6,000	134,000	20,500	160,000	20,500	160,000	0	0	"
IV	E-10	0	11,500	140,500	46,500	175,600	116,500	25,000	70,000	100	"
"	E-12	-10	10,500	135,700	33,000	167,500	33,000	167,500	0	0	"
"	E-23	-10	8,000	135,000	41,000	176,000	41,000	176,000	0	8	"
"	E-11	-20	11,000	138,500	52,500	172,600	80,000	130,500	27,500	45	"
"	E-25	-20	7,500	135,000	48,000	176,700	126,500	29,000	78,500	100	"
"	E-26	-25	5,500	135,000	29,500	166,700	29,500	166,700	0	0	"
"	E-32	-35	7,500	135,000	27,500	167,000	27,500	167,000	0	0	"

TABLE I-4

Aspect Ratio 19

Code: T-1 Specimen Size: 1/2" x 9.5"

Block No.	Spec. No.	Temp. Deg F	To Visible Crack		To Maximum Load		To Fracture		Energy Difference E2 - E1 in.lbs.	% Shear	Internal Notch W/4 Acuity
			Energy E in.lbs.	Load lbs.	Energy E1 in.lbs.	Load lbs.	Energy E2 in.lbs.	Load lbs.			
I	F-1	10	9,500	153,000	67,000	201,000	159,000	30,000	92,000	100	1/32" hole
II	F-6	20	8,500	154,800	64,000	203,500	155,000	30,000	91,000	100	"
"	F-4	0	7,500	154,000	70,450	206,300	160,000	25,000	89,550	100	"
"	F-22	-10	5,000	154,500	61,000	205,000	152,000	21,000	91,000	100	"
"	F-5	-20	9,500	160,200	32,250	194,700	32,250	194,700	0	0	"
III	F-7	0	8,000	160,000	62,500	206,500	156,000	16,000	93,500	100	"
"	F-9	0	9,500	159,700	55,000	207,000	148,000	30,000	93,000	100	"
"	F-17	-10	9,500	163,600	29,000	195,000	29,000	195,000	0	0	"
"	F-18	-10	9,000	162,800	61,000	208,000	75,000	205,000	14,000	10	"
"	F-23	-20	6,000	162,000	46,000	207,500	46,000	207,500	0	0	"
"	F-8	-60	4,000	174,500	28,000	197,000	28,000	197,000	0	0	"

TABLE I-5

Aspect Ratio 4

Code: T-1 Specimen Size: 3/4" x 3"

Block No.	Spec. No.	Temp. Deg. F	To Visible Crack Energy E in.lbs.	To Visible Crack Load lbs.	To Maximum Load Energy E1 in.lbs.	To Maximum Load Load lbs.	To Fracture Energy E2 in.lbs.	To Fracture Load lbs.	Energy Difference E2 - E1 in.lbs.	% Shear	Internal Notch W/4 Acuity
II	B-15	0	5,500	88,000	18,650	110,300	42,500	27,000	23,850	100	.046" Hole
	B-16	-20	6,250	90,300	18,650	112,200	44,000	30,000	25,350	100	"
	B-4	-20	6,000	92,100	19,400	113,000	39,000	23,000	19,600	100	"
	B-10	-20	6,075	92,300	18,300	113,600	19,470	113,400	1,170	0	"
"	B-12	-20	5,125	89,600	17,500	112,900	42,500	27,000	25,000	100	"
	B-14	-30	6,250	88,800	21,300	114,500	21,300	114,500	0	0	"
	B-1	-30	4,400	87,700	17,250	114,500	17,250	114,500	0	0	"
	B-9	-30	5,525	90,000	18,750	113,900	23,150	111,000	4,400	10	"
"	B-11	-40	6,000	94,000	19,425	114,300	20,500	114,000	1,075	0	"

TABLE I-6

Aspect Ratio 8

Code: T-1 Specimen Size: 3/4" x 6"

Block No.	Spec. No.	Temp. Deg. F	To Visible Crack Energy E in.lbs.	To Visible Crack Load lbs.	To Maximum Load Energy E1 in.lbs.	To Maximum Load Load lbs.	To Fracture Energy E2 in.lbs.	To Fracture Load lbs.	Energy Difference E2 - E1 in.lbs.	% Shear	Internal Notch W/4 Acuity
II	10	10	17,500	165,000	54,000	200,000	118,000	40,000	64,000	100	.046" Hole
	12	0	18,000	165,300	44,000	195,500	44,000	195,500	0	0	"
	1	0	18,000	168,800	47,500	202,400	119,000	15,000	71,500	100	"
	11	-10	19,000	167,000	38,000	196,000	38,000	196,000	0	0	"
"	7	-10	18,000	167,800	50,000	202,900	124,000	33,500	74,000	100	"
	13	-20	17,760	168,500	48,400	202,500	122,000	35,000	73,600	100	"
	8	-20	18,000	169,300	46,000	202,200	116,000	37,000	70,000	100	"
	3	-30	15,000	168,500	40,000	205,000	40,000	205,000	0	0	"
"	9	-40	19,300	175,800	38,600	205,900	38,600	205,900	0	0	"

TABLE I-7

Aspect Ratio 12

Code: T-1 Specimen Size: 3/4" x 9"

Block No.	Spec. No.	Temp. Deg. F	To Visible Crack Energy E in.lbs.	To Visible Crack Load lbs.	To Maximum Load Energy E1 in.lbs.	To Maximum Load Load lbs.	To Fracture Energy E2 in.lbs.	To Fracture Load lbs.	Energy Difference E2 - E1 in.lbs.	% Shear	Internal Notch W/4 Acuity
II	H-8	20	16,900	218,800	80,600	285,300	212,500	45,000	131,900	100	.046" Hole
	H-6	10	16,500	221,200	90,000	284,000	200,200	40,000	110,200	100	"
	H-7	10	17,500	222,200	78,000	285,700	219,000	20,000	141,000	100	"
	H-5	0	16,500	224,400	58,000	281,900	58,000	281,900	0	0	"
	H-10	-10	16,000	220,500	73,000	279,500	73,000	279,500	0	0	"
"	H-9	-20	19,500	230,000	62,800	285,500	62,800	285,500	0	0	"

TABLE I-8

Aspect Ratio 16

Code: T-1 Specimen Size: 3/4" x 12"

Block No.	Spec. No.	Temp. Deg. F	To Visible Crack Energy E in.lbs.	To Visible Crack Load lbs.	To Maximum Load Energy E1 in.lbs.	To Maximum Load Load lbs.	To Fracture Energy E2 in.lbs.	To Fracture Load lbs.	Energy Difference E2 - E1 in.lbs.	% Shear	Internal Notch W/4 Acuity
I	G-1	30	23,000	284,400	136,000	369,000	350,000	50,000	214,000	100	.046" Hole
	G-2	20	23,000	282,800	135,500	369,100	322,500	109,000	187,000	100	"
	G-5	0	21,500	284,800	129,000	379,500	354,000	63,200	225,000	100	"
"	G-3	-10	20,000	287,800	129,000	373,400	341,000	54,000	212,000	100	"
	G-4	-20	22,000	286,800	121,500	375,500	121,500	375,500	0	5	"
"	G-7	-20	24,000	294,800	87,000	359,000	87,000	359,000	0	0	"
II	G-6	+40	16,200	266,800	127,300	362,400	338,600	35,000	211,300	100	"
	G-8	30	26,000	280,000	138,000	366,500	138,000	366,500	0	0	"
	G-12	20	25,000	281,400	134,000	365,700	365,000	15,000	231,000	100	"
"	G-15	20	22,000	276,400	123,000	364,000	327,000	66,000	204,000	100	"
	G-10	10	26,300	285,500	94,800	352,500	94,800	352,500	0	0	"
	G-11	0	17,400	275,500	145,700	370,900	145,700	370,900	0	0	"
"	G-9	-10	23,500	283,900	80,000	347,500	80,000	347,500	0	0	"

TABLE I-9

Aspect Ratio 4

Code: T-1 Specimen Size: 1" x 4" x 8"

Block No.	Spec. No.	Temp. Deg F	To Visible Crack Energy E in.lbs.	To Visible Crack Load lbs.	To Maximum Load Energy E1 in.lbs.	To Maximum Load Load lbs.	To Fracture Energy E2 in.lbs.	To Fracture Load lbs.	Energy Difference E2 - E1 in.lbs.	% Shear	Internal Notch W/4 Acuity
II	C-7	30	20,000	164,900	40,000	183,000	95,000	33,000	55,000	100	1/16" hole
"	C-18	20	17,500	164,300	37,000	185,000	89,000	42,000	52,000	100	"
"	C-19	15	16,000	164,200	34,500	187,500	87,000	45,000	52,500	100	"
"	C-8	10	18,000	167,300	37,000	186,400	37,000	186,400	0	0	"
"	C-16	0	15,000	157,400	40,000	187,300	45,000	186,600	5,000	0	"
"	C-17	-10	20,000	172,700	38,000	190,500	38,000	190,500	0	0	"

TABLE I-10

Aspect Ratio 8

Code: T-1 Specimen Size: 1" x 8"

Block No.	Spec. No.	Temp. Deg F	To Visible Crack Energy E in.lbs.	To Visible Crack Load lbs.	To Maximum Load Energy E1 in.lbs.	To Maximum Load Load lbs.	To Fracture Energy E2 in.lbs.	To Fracture Load lbs.	Energy Difference E2 - E1 in.lbs.	% Shear	Internal Notch W/4 Acuity
II	E-4	74	32,000	263,200	96,000	325,000	244,000	40,000	148,000	100	1/16" hole
"	E-6	30	28,000	261,500	115,000	335,600	270,000	45,000	155,000	100	"
"	E-7	20	35,000	268,500	125,000	337,000	281,000	50,000	156,000	100	"
"	E-5	10	29,000	263,000	113,000	341,000	173,000	307,000	60,000	25	"
"	E-19	10	30,500	273,900	100,400	343,400	200,600	250,000	100,000	25	"
"	E-18	0	31,000	274,000	92,000	341,000	92,000	341,000	0	0	"
"	E-17	-10	31,000	280,200	91,000	345,000	91,000	345,000	0	0	"

TABLE I-11

Aspect Ratio 12

Code: T -1 Specimen Size: 1" x 12" x 24"

Block No.	Spec. No.	Temp. Deg F	To Visible Crack: Energy E in.lbs.	To Visible Crack: Load lbs.	To Maximum Load: Energy E1 in.lbs.	To Maximum Load: Load lbs.	To Fracture: Energy E2 in.lbs.	To Fracture: Load lbs.	Energy Difference E2 - E1 in.lbs	% Shear	Notch $\frac{W}{4}$ acuity
IV	G-5	40	32,000	357,800	214,000	481,100	599,000	22,000	385,000	100	1/16" hole
"	G-1	30	39,000	358,400	194,000	483,000	512,000	79,000	318,000	100	"
"	G-2	30	39,000	368,000	200,000	487,400	395,000	363,000	195,000	55	"
"	G-6	30	35,000	359,000	203,500	488,500	218,500	487,000	15,000	10	"
V	G-3	75	30,000	326,000	198,000	449,500	549,000	20,000	351,000	100	"
"	G-7	50	42,500	363,900	198,000	478,700	502,000	55,000	304,000	100	"
"	G-8	20	30,000	354,800	122,000	468,400	122,000	468,400	0	0	"
"	G-4	10	31,000	358,000	147,000	480,000	147,000	480,000	0	0	"

TABLE I-12

Aspect Ratio 4

Code: T-1 Specimen Size: $1\frac{1}{2}$" x 6"

Block No.	Spec. No.	Temp. Deg. F	To Visible Crack: Energy E in.lbs.	To Visible Crack: Load lbs.	To Maximum Load: Energy E1 in.lbs.	To Maximum Load: Load lbs.	To Fracture: Energy E2 in.lbs.	To Fracture: Load lbs.	Energy Difference E2 - E1 in.lbs.	% Shear	Internal Notch $\frac{W}{4}$
I	D-15	20	38,500	332,300	104,000	406,900	104,000	406,900	0	0	3/32" Hole
"	D-3	20	33,400	329,000	109,500	405,000	109,500	405,000	0	0	"
"	D-4	20	35,000	333,500	110,000	404,000	157,000	384,500	47,000	5	"
"	D-6	30	38,500	331,500	90,000	399,000	90,000	399,000	0	0	"
"	D-5	35	45,000	340,500	115,000	398,300	250,000	13,000	140,000	100	"
"	D-2	40	46,000	348,500	108,500	402,000	108,500	402,000	0	0	"
"	D-14	50	40,000	336,000	110,000	401,300	255,000	145,000	145,000	100	"
"	D-16	50	33,000	318,300	119,000	398,800	235,500	125,000	116,500	100	"
"	D-13	-65	28,200	343,000	83,400	427,600	84,250	426,000	850	0	"
II	D-9	0	32,500	328,500	116,000	415,500	116,000	415,500	0	0	"
"	D-17	20	35,000	322,000	116,000	406,500	116,000	406,500	0	0	"
"	D-19	30	44,000	343,500	110,000	403,500	263,000	145,000	153,000	100	"
"	D-20	30	40,300	342,000	100,200	403,000	100,200	403,000	0	0	"
"	D-10	40	44,000	339,000	106,000	396,000	106,000	396,000	0	0	"
"	D-18	40	44,000	339,000	115,200	401,800	262,000	135,000	146,800	100	"
"	D-8	40	42,000	337,700	119,000	405,000	125,000	402,000	6,000	5	"
"	D-11	50	41,600	336,000	112,000	399,000	244,000	135,000	132,000	100	"
"	D-12	60	35,000	320,000	118,000	392,500	285,000	120,000	167,000	100	"
"	D-7	76	40,000	327,000	114,000	388,000	246,000	125,000	132,000	100	"

TABLE I-12a

Aspect Ratio 4

Code: T-1 Specimen Size: $1\frac{1}{2}$" x 6"

Block No.	Spec. No.	Temp. Deg. F	To Visible Crack Energy E in.lbs.	To Visible Crack Load lbs.	To Maximum Load Energy E1 in.lbs.	To Maximum Load Load lbs.	To Fracture Energy E2 in.lbs.	To Fracture Load lbs.	Energy Difference E2 - E1 in.lbs.	% Shear	Internal Notch W/4 Acuity
III	D-23	30	34,000	324,500	107,800	404,400	107,800	404,400	0	0	3/32" hole
"	D-28	30	36,000	334,300	111,000	404,500	111,000	404,500	0	0	"
"	D-24	32	24,000	301,000	106,000	408,000	252,000	145,000	146,000	100	"
"	D-27	40	27,500	309,000	110,000	400,200	133,000	398,800	23,000	5	"
"	D-26	50	32,000	325,300	100,600	403,900	176,000	350,000	75,400	20	"
"	D-25	60	34,000	322,500	120,000	399,700	288,000	100,000	168,000	100	"
"	D-29	60	36,000	328,300	112,000	400,000	245,000	140,000	133,000	100	"
"	D-21	20	14,000	267,000	25,000	303,000	25,000	303,000	0	0	J.H.Saw cut
"	D-22	83	8,000	236,300	100,000	369,300	256,000	120,000	156,000	100	"
"	*4 G-17	50	6,500	247,600	45,000	338,500	45,000	338,500	0	0	"
"	*5 G-17	60	6,200	237,500	85,000	375,000	85,000	375,000	0	5	"
"	*6 G-17	75	8,500	234,500	58,000	348,000	58,000	348,000	0	0	"
"	*3 G-17	90	8,000	233,400	89,000	361,500	243,000	110,000	154,000	100	"

* Cut from G-17

TABLE I-13

Aspect Ratio 6

Code: T-1 Specimen Size: $1\frac{1}{2}$" x 9"

Block No.	Spec. No.	Temp. Deg F	To Visible Crack Energy E in.lbs.	To Visible Crack Load lbs.	To Maximum Load Energy E1 in.lbs.	To Maximum Load Load lbs.	To Fracture Energy E2 in.lbs.	To Fracture Load lbs.	Energy Difference E2 - E1 in.lbs.	% Shear	Internal Notch W/4 Acuity
II	18	77	100,000	507,500	210,000	564,000	568,000	185,000	358,000	100	3/32" hole
"	5	60	67,000	459,500	200,000	564,000	440,000	190,000	240,000	100	"
"	13	50	84,000	495,000	165,000	568,000	165,000	568,000	0	0	"
"	4	50	70,000	480,200	205,000	568,500	477,000	155,000	272,000	100	"
"	16	40	64,500	463,000	206,000	578,500	534,000	150,000	328,000	100	"
"	14	30	70,000	480,000	193,000	579,000	193,000	579,000	0	0	"
"	15	40	71,000	479,000	203,000	574,000	203,000	574,000	0	3	"

TABLE I-14

Aspect Ratio 4

Code: T-2 Specimen Size: 3/4" x 3" x 12"

Spec. No.	Temp. Deg. F	To Visible Crack: Energy E in.lbs.	To Visible Crack: Load lbs.	To Maximum Load: Energy E1 in.lbs.	To Maximum Load: Load lbs.	To Fracture: Energy E2 in.lbs.	To Fracture: Load lbs.	Energy Difference E2 - E1 in.lbs.	% Shear	Internal Notch W/4 Acuity
XB-9	0	5,000	94,000	17,000	112,500	36,750	20,000	19,750	100	.046" Hole
XB-1	-10	5,000	93,500	16,500	112,000	38,375	35,000	21,875	100	"
XB-3	-20	5,500	94,000	18,250	114,200	25,000	108,600	6,750	20	"
XB-8	-20	5,750	96,700	16,000	113,000	37,000	52,000	21,000	60	"
XB-7	-30	5,500	94,300	13,625	114,000	13,625	114,000	0	0	"
XB-6	-40	4,500	89,000	15,000	115,000	15,000	115,000	0	0	"

TABLE I-15

Aspect Ratio 8

Code: T -2 Specimen Size: 3/4" x 6" x 12"

Spec. No.	Temp. Deg. F.	To Visible Crack: Energy E in.lbs.	To Visible Crack: Load lbs.	To Maximum Load: Energy E1 in.lbs.	To Maximum Load: Load lbs.	To Fracture: Energy E2 in.lbs.	To Fracture: Load lbs.	Energy Difference E2 - E1 in.lbs.	% Shear	Internal Notch W/4 Acuity
XD-5	+10	10,000	161,700	44,000	204,500	103,000	40,000	59,000	100	.046" Hole
XD-1	0	12,000	165,000	43,000	207,300	112,000	25,000	69,000	100	"
XD-6	- 5	10,000	161,800	44,000	204,800	102,000	40,000	58,000	100	"
XD-3	-10	13,000	168,500	45,500	206,500	54,000	198,000	8,500	15	"
XD-2	-20	12,500	169,500	46,500	208,900	49,500	206,500	3,000	15	"
XD-4	-30	10,000	164,000	28,500	199,000	28,500	199,000	0	0	"

TABLE I-16

Aspect Ratio 12

Code T - 2 Specimen Size: 3/4" x 9" x 12"

Spec. No.	Temp. Deg. F	To Visible Crack		To Maximum Load		To Fracture		Energy Difference E2 - E1 in.lbs.	% Shear	Internal Notch W/4 Acuity
		Energy E in.lbs.	Load lbs.	Energy E1 in.lbs.	Load lbs.	Energy E2 in.lbs.	Load lbs.			
XH-9	+10	15,000	229,500	68,500	284,700	185,000	45,000	116,500	100	.046" hole
XH-1	0	16,250	226,300	77,500	291,300	163,500	70,000	86,000	100	"
XH-7	- 5	15,000	231,500	76,000	293,500	155,000	215,000	79,000	50	"
XH-8	-10	15,000	231,700	42,000	276,500	42,000	276,500	0	0	"
XH-3	-20	16,500	230,800	71,000	293,000	79,000	281,500	8,000	10	"
XH-5	-30	16,250	235,700	57,500	293,000	57,500	293,000	0	0	"

TABLE I-17

Aspect Ratio 16

Code: T - 2 Specimen Size 3/4" x 12" x 24"

Spec. No.	Temp. Deg	To Visible Crack		To Maximum Load		To Fracture		Energy Difference E2 - E1 in. lbs.	% Shear	Internal Notch W/4 Acuity
		Energy E in.lbs.	Load lbs.	Energy E1 in.lbs.	Load lbs.	Energy E2 in.lbs.	Load lbs.			
10	30	21,000	292,400	116,000	370,400	336,000	25,000	220,000	100	.046" hole
6	20	20,000	296,000	126,000	375,000	300,000	45,000	174,000	100	"
15	20	21,000	301,200	130,000	374,500	279,000	200,000	144,000	55	"
1	20	18,000	296,500	130,000	375,800	300,000	60,000	170,000	100	"
11	10	20,000	294,500	116,500	374,500	291,000	118,000	174,500	75	"
3	10	20,000	295,000	140,000	376,200	272,000	182,000	132,000	60	"
13	10	23,000	301,600	66,000	352,800	66,000	352,800	0	0	"
4	0	31,000	309,000	113,000	379,500	126,000	378,000	13,000	10	"
5	0	18,000	294,500	117,000	378,500	207,000	323,000	90,000	30	"
14	0	24,000	302,600	120,000	378,000	164,000	364,500	44,000	15	"
2	-20	18,000	300,000	140,000	386,700	146,000	381,000	6,000	10	"
12	-20	23,500	304,100	124,500	382,000	129,500	380,000	5,000	10	"
8	-30	21,000	308,800	122,500	391,200	122,500	391,200	0	10	"
9	-40	19,000	312,600	77,500	379,000	77,500	379,000	0	0	"

TABLE I-18

Aspect Ratio 4

Code: T-2 Specimen Size 1" x 4" x 8"

Spec. No.	Temp. Deg.	To Visible Crack Energy E in.lbs.	To Visible Crack Load lbs.	To Maximum Load Energy E1 in.lbs.	To Maximum Load Load lbs.	To Fracture Energy E2 in.lbs.	To Fracture Load lbs.	Energy Difference E2 - E1 in.lbs.	% Shear	Internal Notch W/4 Acuity
6	+20	9,000	153,400	29,000	187,000	71,500	25,000	42,500	100	1/16" hole
11	+10	12,000	163,000	25,500	187,500	68,000	33,000	42,500	100	"
9	0	10,500	165,000	24,500	191,700	71,500	35,000	47,000	100	"
7	0	12,500	168,500	25,000	191,500	70,000	30,000	45,000	100	"
8	-10	7,200	158,000	32,500	.193,000	56,500	167,500	24,000	30	"
1	-20	10,000	163,000	33,000	191,500	33,000	191,500	0	0	"

TABLE I-19

Aspect Ratio 6

Code T-2 Specimen Size: 1" x 6" x 8"

Block No.	Spec. No.	Temp. Deg F	To Visible Crack Energy E in.lbs.	To Visible Crack Load lbs.	To Maximum Load Energy E1 in.lbs.	To Maximum Load Load lbs.	To Fracture Energy E2 in.lbs.	To Fracture Load lbs.	Energy Difference E2 - E1 in.lbs.	% Shear	Internal Notch W/4 Acuity
	3	+20	16,000	225,000	54,000	270,000	131,000	45,000	77,000	100	.046 " hole
	1	20	22,000	240,000	53,500	271,800	138,000	41,000	84,500	100	"
	5	10	16,000	221,800	51,000	272,200	100,350	205,000	49,350	30	"
	4	10	17,500	237,200	55,000	271,000	65,000	259,000	10,000	22	"
	7	10	22,000	236,400	52,000	271,000	139,000	40,000	87,000	100	"
	6	0	18,500	235,000	57,500	273,200	98,500	215,000	41,000	33	"
	8	0	13,500	232,000	42,500	273,000	50,150	272,500	7,650	10	"
	2	-10	17,500	233,700	52,500	278,300	89,000	246,000	36,500	33	"

TABLE I-20

Aspect Ratio 8

Code: T - 2 Specimen Size 1" x 8" x 12"

Spec. No.	Temp. Deg. F	To Visible Crack Energy E in.lbs.	To Visible Crack Load lbs.	To Maximum Load Energy E1 in.lbs.	To Maximum Load Load lbs.	To Fracture Energy E2 in.lbs.	To Fracture Load lbs.	Energy Difference E2 - E1 in.lbs.	% Shear	Internal Notch W/4 Acuity
6	50	28,000	289,000	78,000	336,000	200,000	63,000	112,000	100	1/16" hole
4	40	26,400	293,600	92,500	342,600	200,000	78,000	107,500	100	"
1	30	20,500	280,500	88,000	346,500	147,000	287,000	62,500	30	"
2	10	19,500	281,800	88,000	346,800	198,000	130,000	110,000	70	"
3	-10	18,500	285,400	86,000	355,600	135,000	303,000	49,000	30	"
5	-20	17,000	292,900	80,000	354,100	80,000	353,500	0	0	"

TABLE I-21

Aspect Ratio 12

Code: T-2 Specimen Size: 1" x 12" x 24"

Spec. No.	Temp Deg F	To Visible Crack Energy E in.lbs.	To Visible Crack Load lbs.	To Maximum Load Energy E1 in.lbs.	To Maximum Load Load lbs.	To Fracture Energy E2 in.lbs.	To Fracture Load lbs.	Energy Difference E2 - E1 in.lbs.	% Shear	Internal Notch W/4 Acuity
5	50	47,000	417,000	152,500	488,300	372,500	130,000	220,000	100	1/16" hole
4	40	31,000	389,500	163,000	493,000	393,000	140,000	230,000	100	"
1	30	34,000	403,000	157,000	498,000	372,000	230,000	215,000	75	"
3	20	40,000	414,300	152,000	498,000	376,000	195,000	224,000	75	"
2	0	40,000	416,500	105,000	494,000	105,000	494,000	0	0	"

TABLE I-22

Aspect Ratio 4

Code: T-2 Specimen Size $1\frac{1}{2}$" x 6" x 12"

Spec. No.	Temp. Deg. F	To Visible Crack Energy E in.lbs.	To Visible Crack Load lbs.	To Maximum Load Energy E1 in.lbs.	To Maximum Load Load lbs.	To Fracture Energy E2 in.lbs.	To Fracture Load lbs.	Energy Difference E2 - E1	% Shear	Internal Notch $\frac{W}{4}$ Acuity
XD-2	10	30,000	345,600	98,000	423,400	133,000	397,000	35,000	10	3/32" drill hole
XD-1	20	30,000	343,000	92,000	413,500	92,000	413,500	0	0	"
XD-4	30	36,000	354,500	95,000	415,000	208,000	215,000	113,000	50	"
XD-3	40	28,000	331,800	100,000	413,200	210,000	170,000	110,000	100	"
XD-5	76	35,000	334,500	94,000	400,900	224,000	145,000	130,000	100	"
XD-6	100	37,000	341,200	82,000	396,400	222,000	145,000	140,000	100	"

TABLE I-23

Aspect Ratio 6

Code: T-2 Specimen Size $1\frac{1}{2}$" x 9" x 24"

Spec. No.	Temp. Deg. F	To Visible Crack Energy E in.lbs.	To Visible Crack Load lbs.	To Maximum Load Energy E1 in.lbs.	To Maximum Load Load lbs.	To Fracture Energy E2 in.lbs.	To Fracture Load lbs.	Energy Difference E2 - E1	% Shear	Internal Notch $\frac{W}{4}$ Acuity
XH-6	30	52,000	501,000	155,000	598,500	182,000	597,500	27,000	10	3/32" drill hole
XH-5	40	52,000	498,000	160,000	593,500	390,000	175,000	230,000	100	"
XH-1	60	62,000	497,200	143,000	581,000	143,000	581,000	0	0	"
XH-3	75	60,000	492,500	190,000	578,700	443,000	145,000	253,000	100	"

TABLE I-24

Aspect Ratio 4

Code: T-2R

Specimen Size 3/4" x 3" x 12"

Spec. No.	Temp. Deg. F	To Visible Crack		To Maximum Load		To Fracture		Energy Difference E2 - E1	% Shear	Internal Notch W/4 Acuity
		Energy E in.lbs.	Load lbs	Energy E1 in.lbs.	Load lbs.	Energy E2 in.lbs.	Load lbs.			
B-1	75	6,250	100,700	13,500	106,800	34,750	22,000	21,250	100	.046" drill hole
B-4	74	9,000	100,500	16,250	107,000	36,200	21,000	19,950	100	"

TABLE I-25

Aspect Ratio 6

Code: T-2R

Specimen Size 3/4" x 4½" x 12"

Spec. No.	Temp. Deg. F	To Visible Crack		To Maximum Load		To Fracture		Energy Difference E2 - E1	% Shear	Internal Notch W/4 Acuity
		Energy E in.lbs.	Load lbs.	Energy E1 in.lbs.	Load lbs.	Energy E2 in.lbs.	Load lbs.			
7	85	11,000	130,200	23,000	154,300	65,000	30,000	42,000	100	.046" drill hole
4	73	10,000	129,300	32,500	152,500	75,000	31,000	42,500	100	"

TABLE I-26

Aspect Ratio 16

Code: T-2R Specimen Size 3/4" x 12" x 24"

Spec. No.	Temp. Deg. F	To Visible Crack Energy E in.lbs.	To Visible Crack Load lbs.	To Maximum Load Energy E1 in.lbs.	To Maximum Load Load lbs.	To Fracture Energy E2 in.lbs.	To Fracture Load lbs.	Energy Difference E2 - E1 in. lbs.	% Shear	Internal Notch W/4 Acuity
GR-4	60	29,000	308,800	110,000	367,700	310,000	140,000	200,000	100	.046" Hole
GR-7	50	26,000	302,800	142,000	374,900	337,000	35,000	195,000	100	"
GR-3	40	27,000	309,500	124,000	376,900	285,000	215,000	161,000	60	"
GR-1	30	25,000	305,000	57,500	345,000	57,500	345,000	0	0	"
GR-8	+10	27,500	311,500	138,000	384,500	138,000	384,500	0	10	"
GR-6	-10	27,000	310,000	129,000	382,800	147,000	380,000	18,000	15	"
GR-2	-20	20,500	307,800	68,000	368,000	75,000	368,000	7,000	0	"

TABLE I-27

Aspect Ratio 20

Code: T-2R Specimen Size 3/4" x 15" x 24"

Spec. No.	Temp. Deg F	To Visible Crack Energy E in.lbs.	To Visible Crack Load lbs.	To Maximum Load Energy E1 in.lbs.	To Maximum Load Load lbs.	To Fracture Energy E2 in.lbs.	To Fracture Load lbs.	Energy Difference E2 - E1 in. lbs.	% Shear	Internal Notch W/4 Acuity
I-1	+50	38,000	373,000	170,000	451,900	442,000	60,000	272,000	100	.046" drill hole
I-2	35	40,000	373,800	180,000	456,500	316,000	375,000	136,000	40	"
I-3	20	34,000	377,300	178,000	461,800	230,000	449,500	52,000	20	"

APPENDIX II

GRAPHICAL SUMMARIES OF BASIC DATA

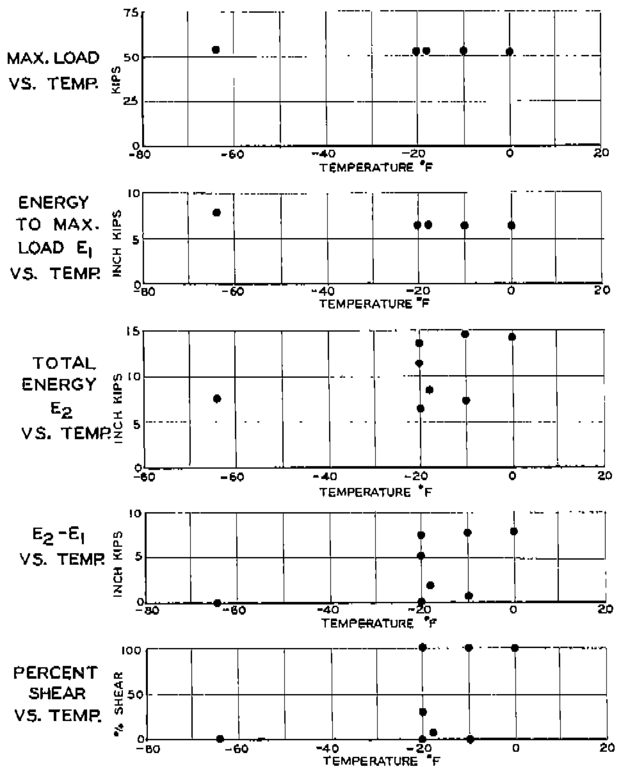

FIG. II-1
SPECIMENS – A
2" x 1/2" ASPECT RATIO 4
BLOCK I CODE T-1
SWARTHMORE COLLEGE
8-31-49

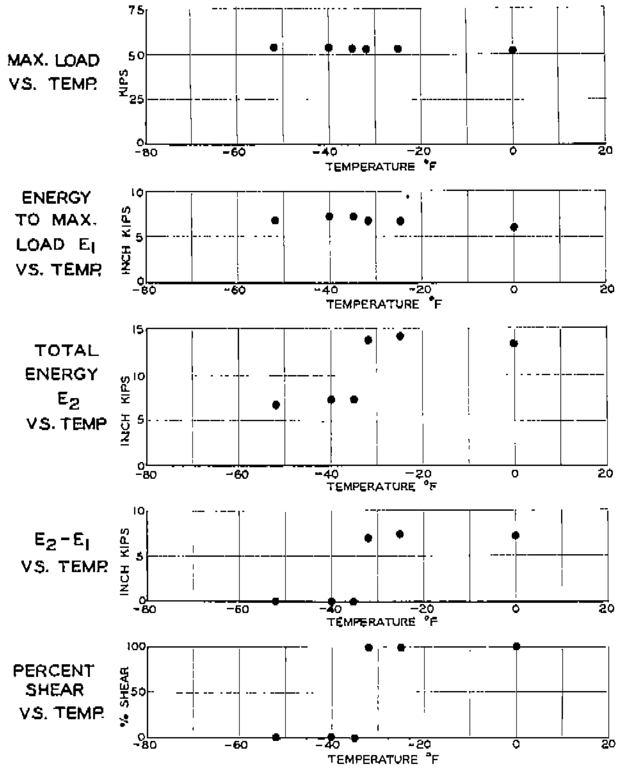

FIG. II-2
SPECIMENS – A
2" x 1/2" ASPECT RATIO 4
BLOCK II CODE T-1
SWARTHMORE COLLEGE
9-1-49

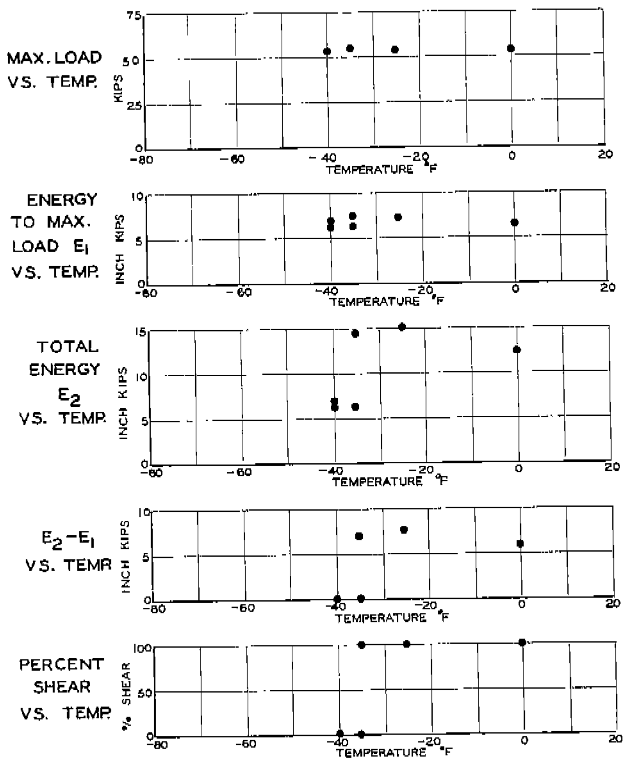

FIG. II-3
SPECIMENS – A
2" x 1/2" ASPECT RATIO 4
BLOCK III CODE T-1
SWARTHMORE COLLEGE
9-1-49

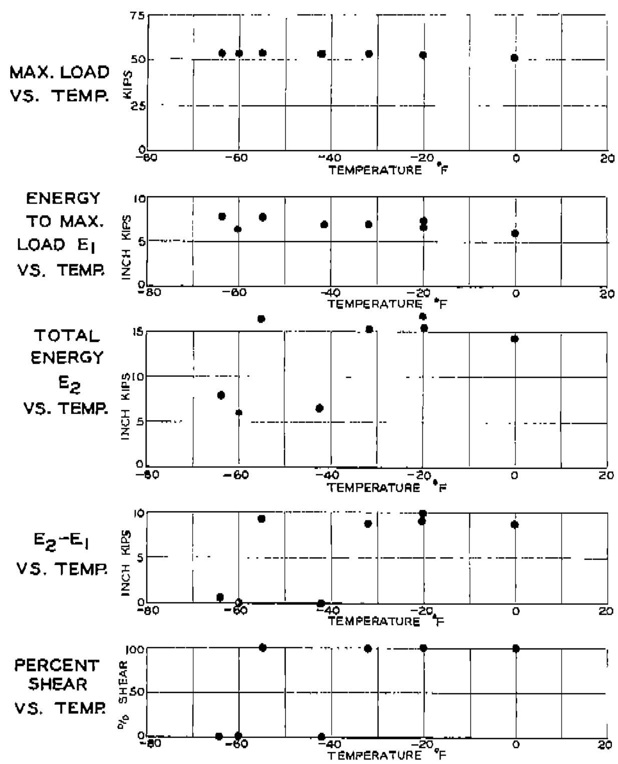

FIG. II-4
SPECIMENS – A
2" x 1/2" ASPECT RATIO 4
BLOCK IV CODE T-1
SWARTHMORE COLLEGE
9-1-49

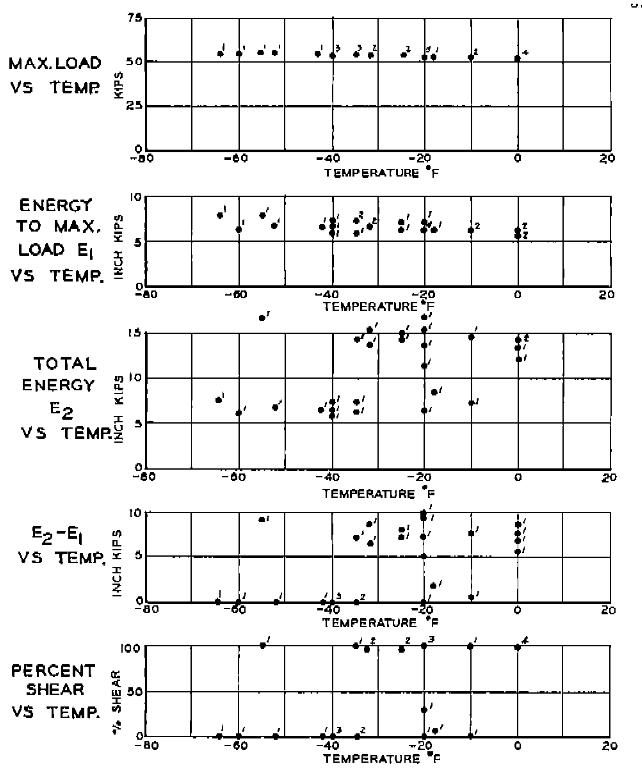

NOTE:
NUMBER ADJACENT TO PLOTTED POINT INDICATES NUMBER OF SPECIMENS.

FIG. II-5
SUMMARY FOR ALL BLOCKS
1/2" THICKNESS ASPECT RATIO 4
STEEL T-1
SWARTHMORE COLLEGE

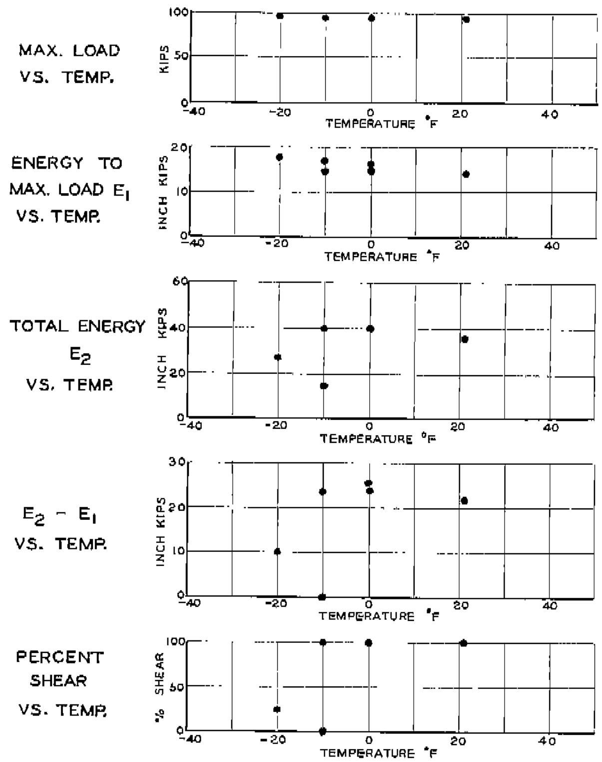

FIG. II-6
SPECIMENS-C
1/2" x 4" ASPECT RATIO 8
BLOCK II CODE T-1
SWARTHMORE COLLEGE
9-3-49

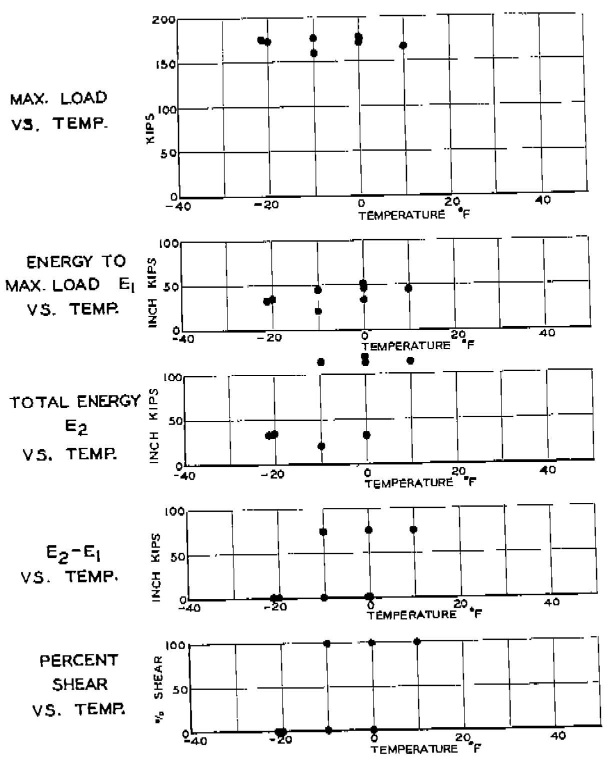

FIG. II-7
SPECIMENS-E
1/2" x 8" ASPECT RATIO 16
BLOCK I CODE T-1
SWARTHMORE COLLEGE
9-2-49

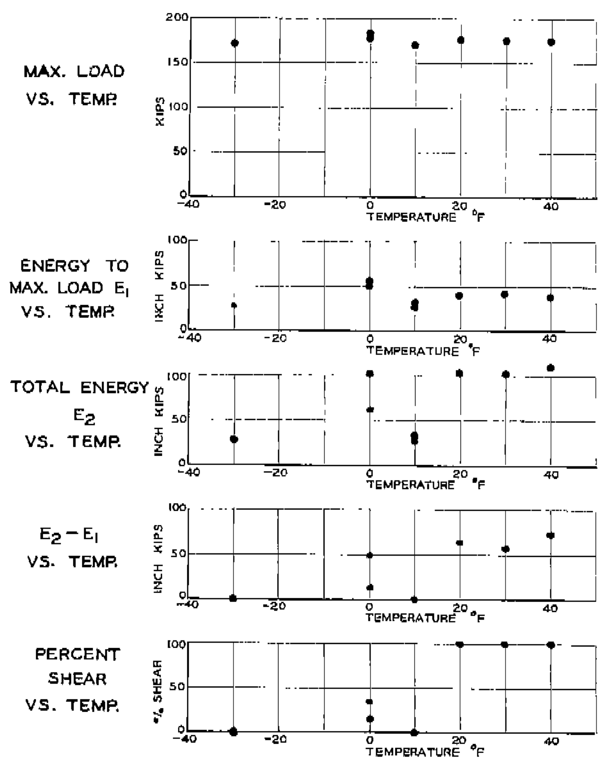

FIG. II-8
SPECIMENS-E
1/2" x 8" ASPECT RATIO 16
BLOCK II CODE T-1
SWARTHMORE COLLEGE
9-2-49

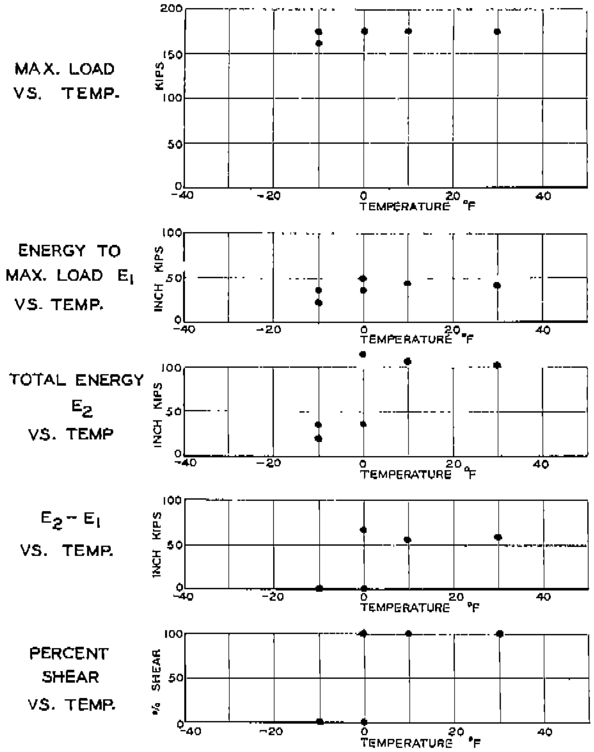

FIG. II-9
SPECIMENS-E
$\frac{1}{2}$" x 8" ASPECT RATIO 16
BLOCK III CODE T-1
SWARTHMORE COLLEGE
9-2-49

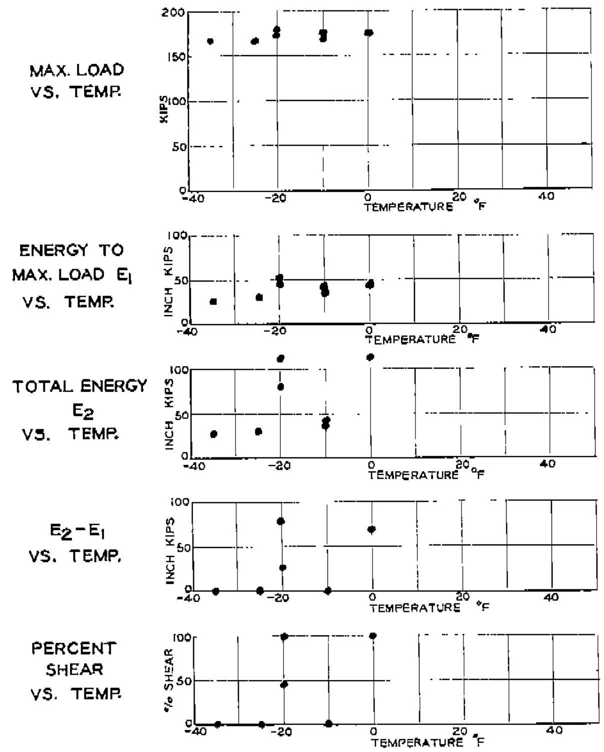

FIG. II-10
SPECIMENS-E
$\frac{1}{2}$" x 8" ASPECT RATIO 16
BLOCK IV CODE T-1
SWARTHMORE COLLEGE
9-2-49

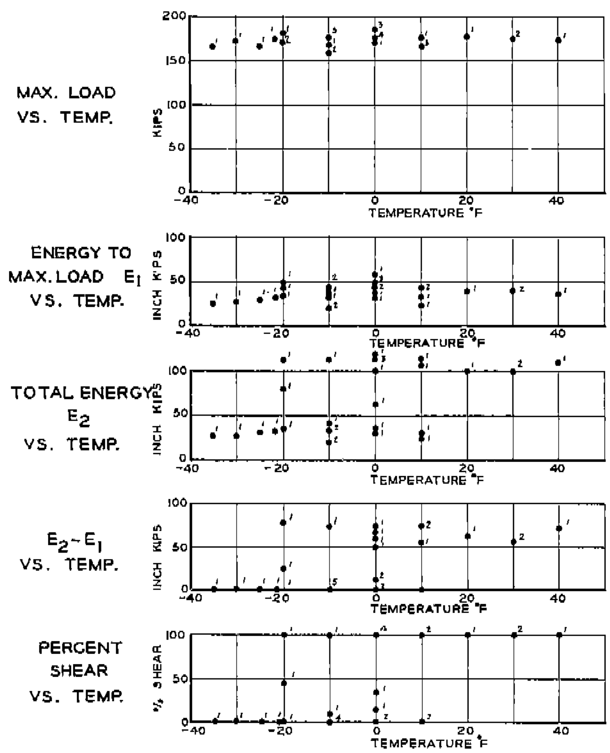

NOTE:
NUMBER ADJACENT TO PLOTTED POINT INDICATES NUMBER OF SPECIMENS.

FIG. II-11
SUMMARY FOR ALL BLOCKS
$\frac{1}{2}$" THICKNESS ASPECT RATIO 16
STEEL T-1
SWARTHMORE COLLEGE

REV. 9-21-51

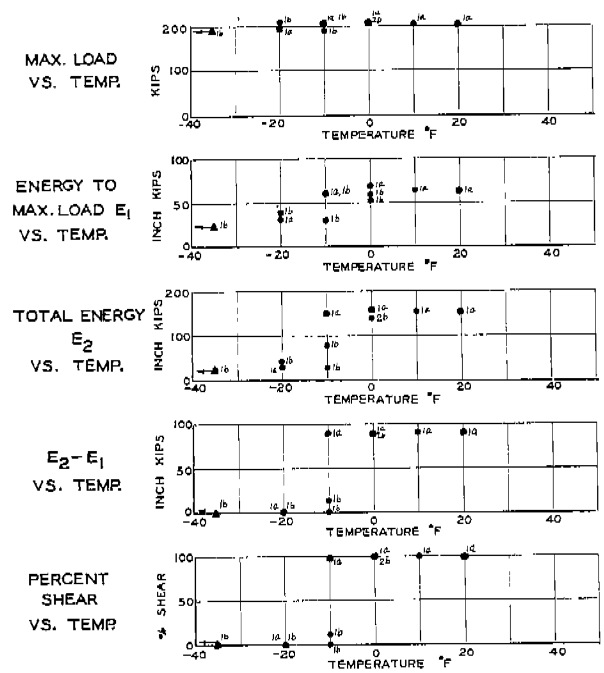

NOTE: NUMBERS ADJACENT TO PLOTTED POINT INDICATES NUMBER OF SPECIMENS. SUBSCRIPT "a" REFERS TO BLOCK II AND "b" REFERS TO BLOCK III SPECIMENS.

▲ - SPECIMEN TESTED AT -60°F

FIG. II-14
SPECIMENS-F
$\frac{1}{2}$" x 9.5" ASPECT RATIO 19
BLOCK II & III CODE T-1
SWARTHMORE COLLEGE
9-3-49

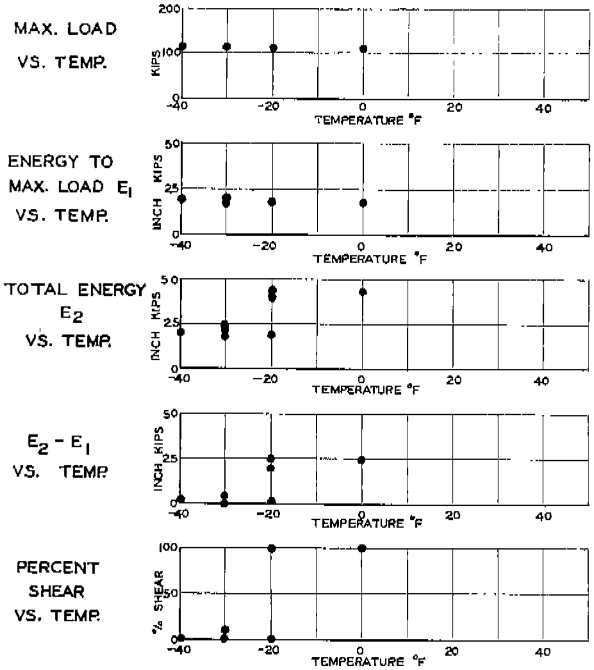

FIG. II-15

SPECIMENS-B

$\frac{3}{4}$" x 3" ASPECT RATIO 4
BLOCK II CODE T-1
SWARTHMORE COLLEGE
9-13-49

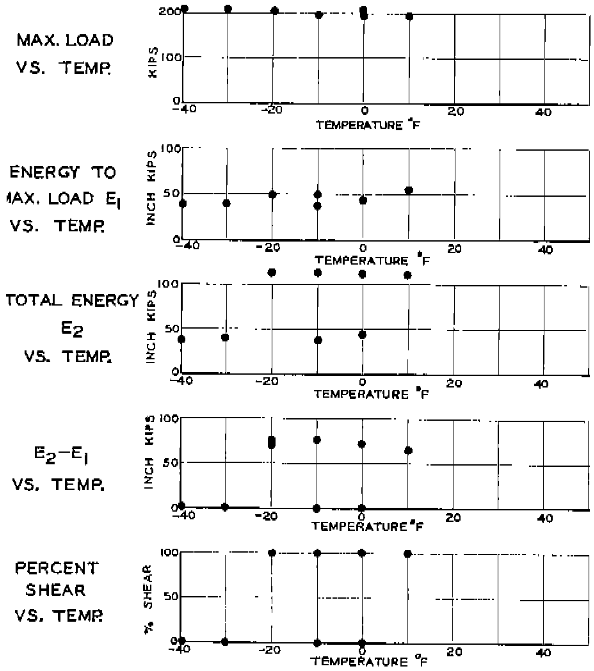

FIG. II-16

SPECIMENS-D

$\frac{3}{4}$" x 6" ASPECT RATIO 8
BLOCK II CODE T-1
SWARTHMORE COLLEGE
9-13-49

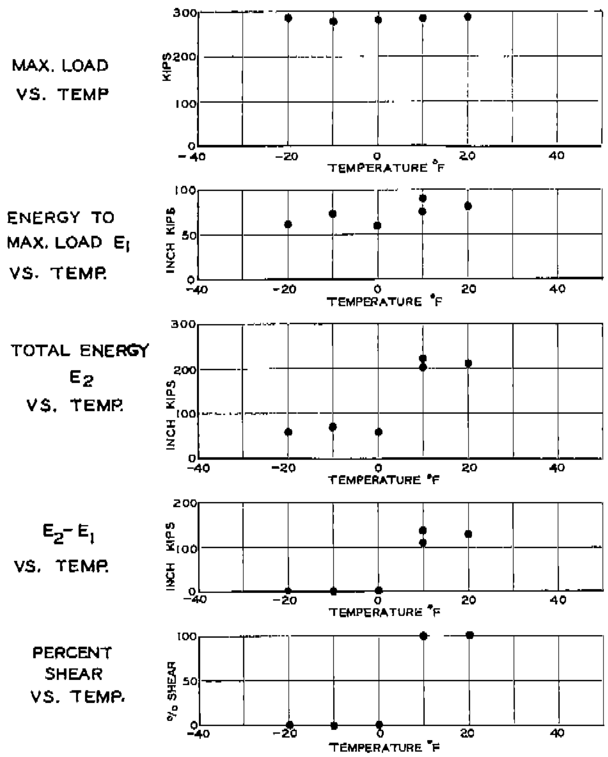

FIG. II-17

SPECIMENS-H

$\frac{3}{4}$" x 9" ASPECT RATIO 12
BLOCK II CODE T-1
SWARTHMORE COLLEGE
9-16-49

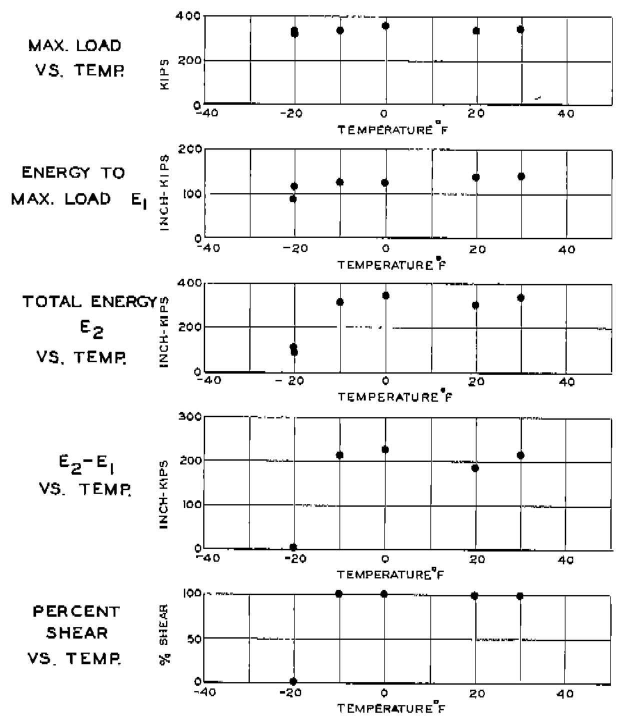

FIG. II-18

SPECIMENS-G

$\frac{3}{4}$" x 12" ASPECT RATIO 16
BLOCK I CODE T-1
SWARTHMORE COLLEGE
12-12-49

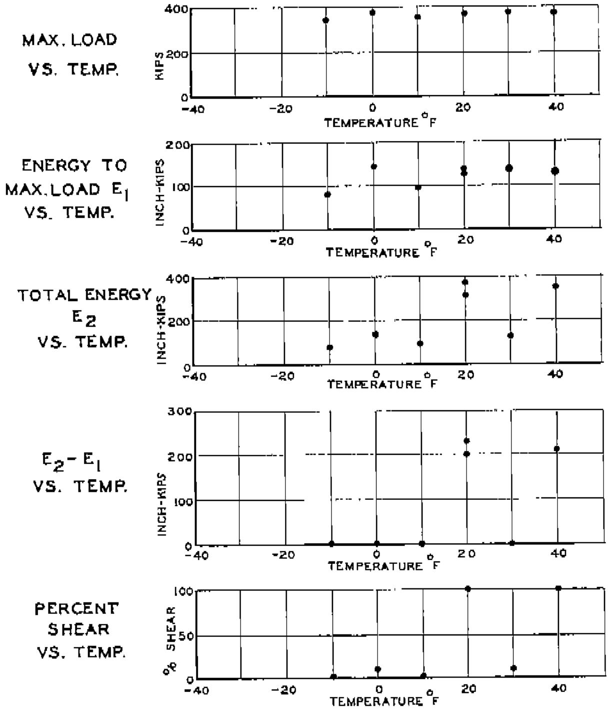

FIG. II-19
SPECIMENS G
3/4" x 12" ASPECT RATIO 16
BLOCK II CODE T-1
SWARTHMORE COLLEGE

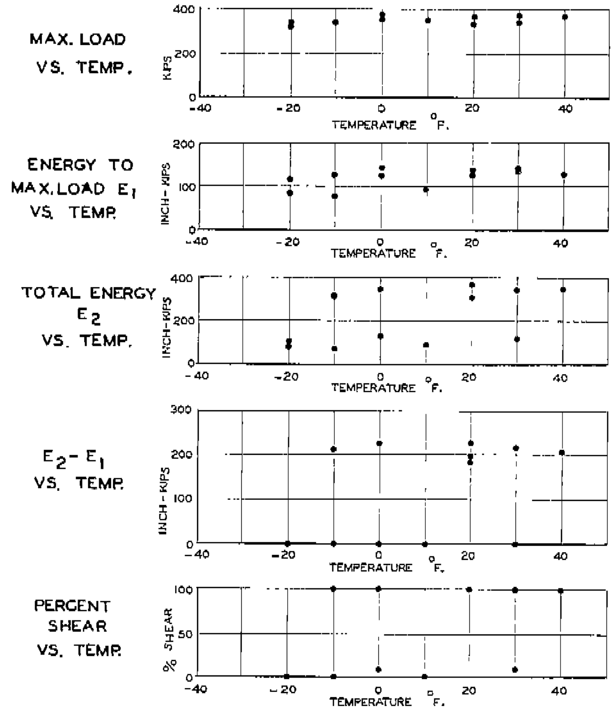

FIG. II-20
SPECIMENS - G
3/4" x 12" ASPECT RATIO 16
BLOCK III CODE T-1
SWARTHMORE COLLEGE

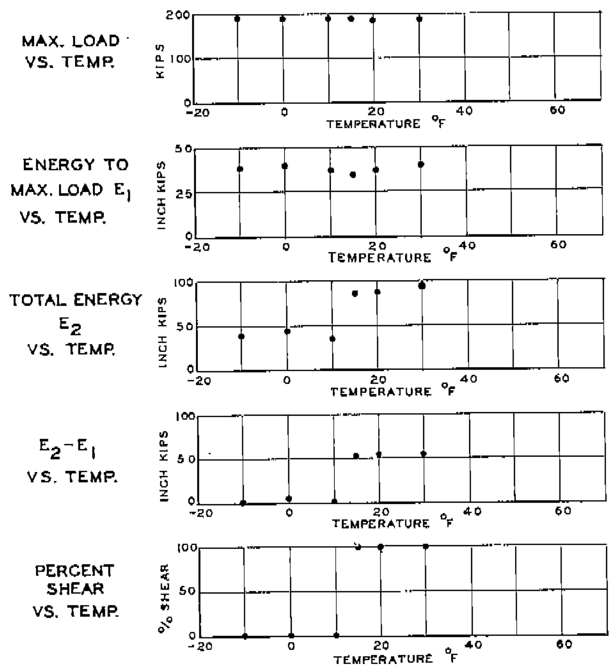

FIG. II-21
SPECIMENS - C
1" x 4" ASPECT RATIO 4
BLOCK II CODE T-1
SWARTHMORE COLLEGE
10-18-49

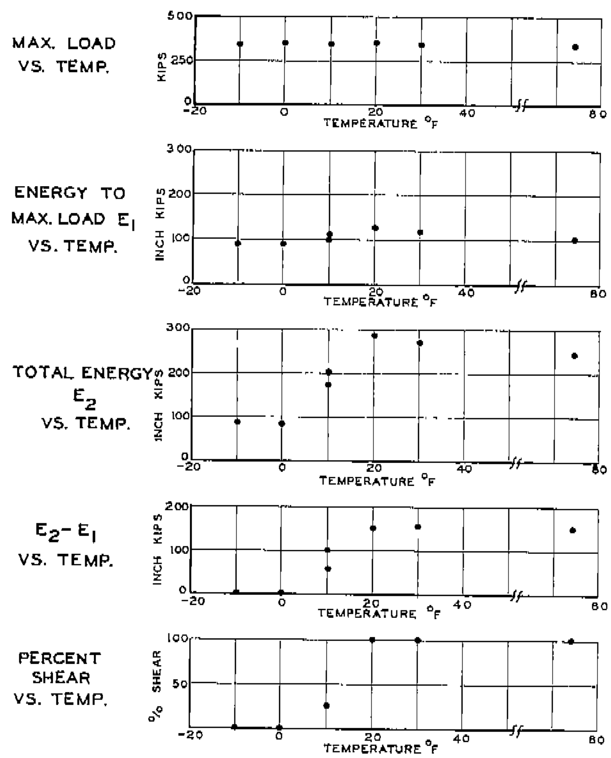

FIG. II-22
SPECIMENS - E
1 x 8 ASPECT RATIO 8
BLOCK II - CODE T-1
SWARTHMORE COLLEGE
9-7-49

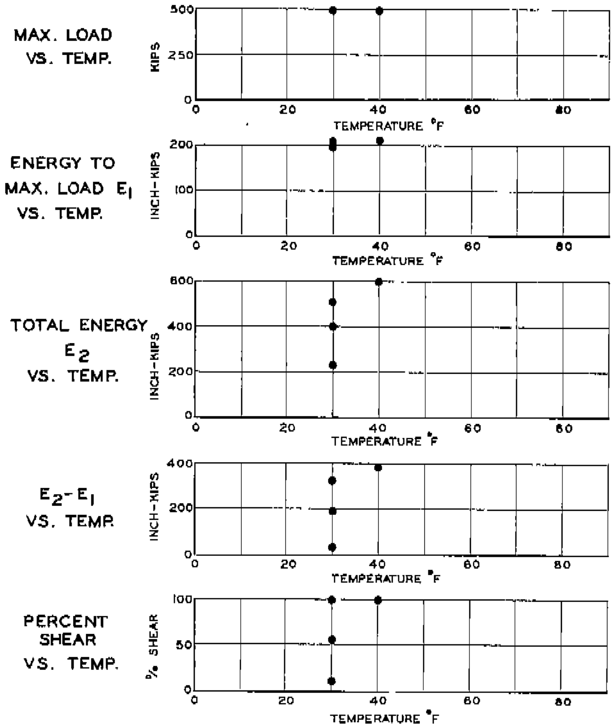

FIG. II-23

SPECIMENS-G

1" x 12" ASPECT RATIO 12

BLOCK III CODE T-1

SWARTHMORE COLLEGE

12-13-49

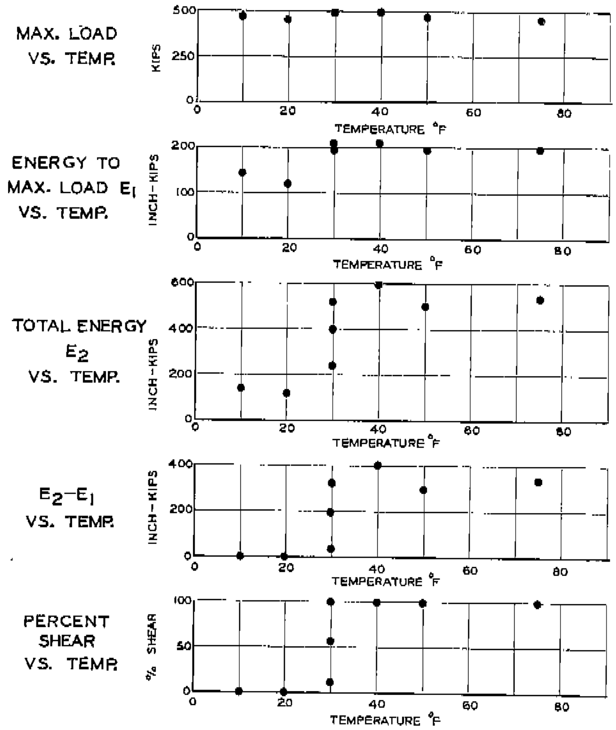

FIG. II-25

SPECIMENS-G

1" x 12" ASPECT RATIO 12

BLOCK IV & BLOCK V CODE T-1

SWARTHMORE COLLEGE

12-13-49

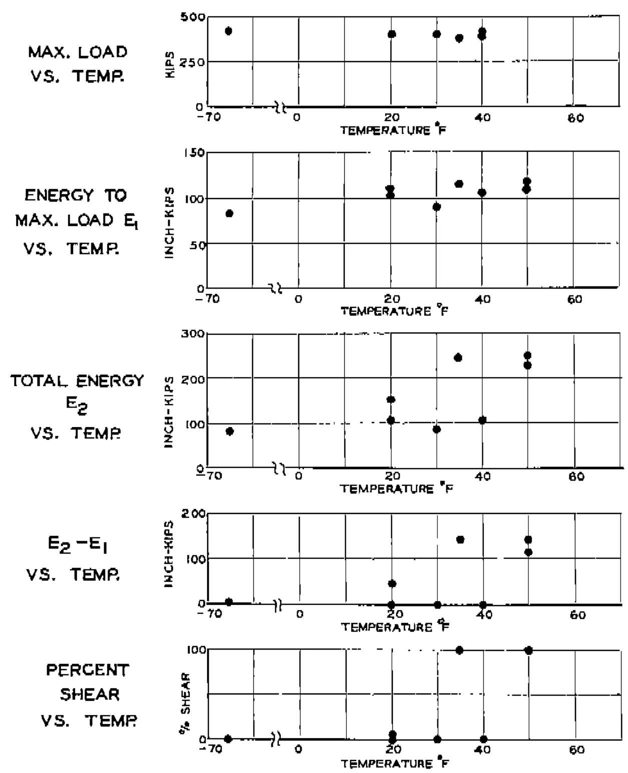

FIG. II-26

SPECIMENS-D

$1\frac{1}{2}$" x 6" ASPECT RATIO 4

BLOCK I CODE T-1

SWARTHMORE COLLEGE

10-21-49

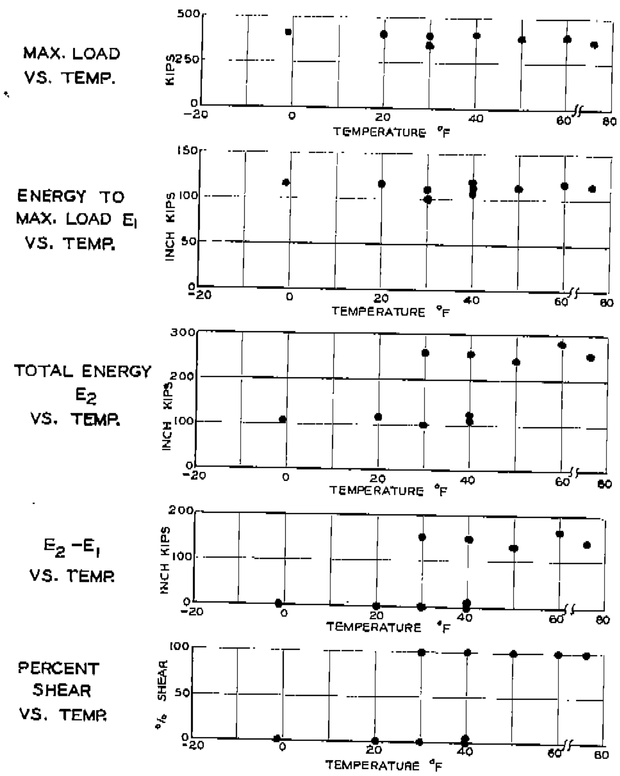

FIG. II-27

SPECIMENS-D

$1\frac{1}{2}$" x 6" ASPECT RATIO 4

BLOCK II CODE T-1

SWARTHMORE COLLEGE

9-3-49

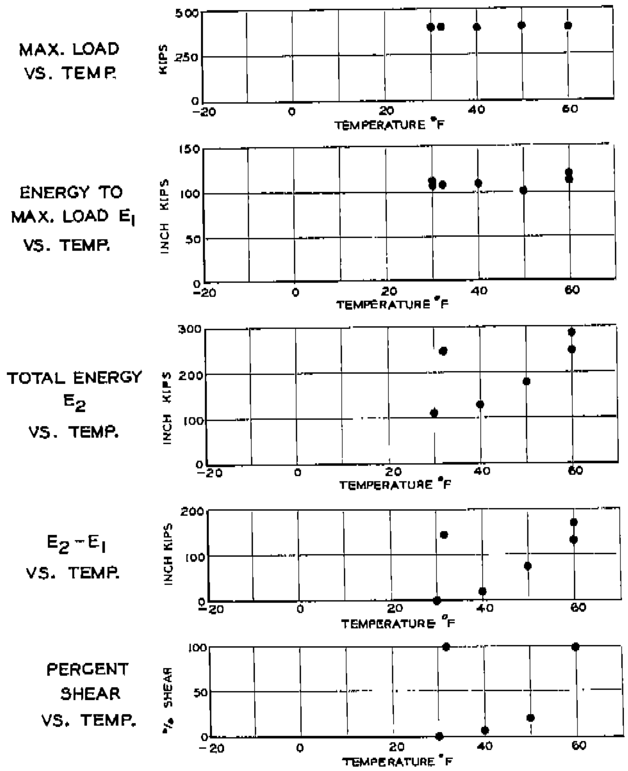

FIG. II-28

SPECIMENS-D
$1\frac{1}{2}$" x 6" ASPECT RATIO 4
BLOCK III CODE T-1
SWARTHMORE COLLEGE
10-25-49

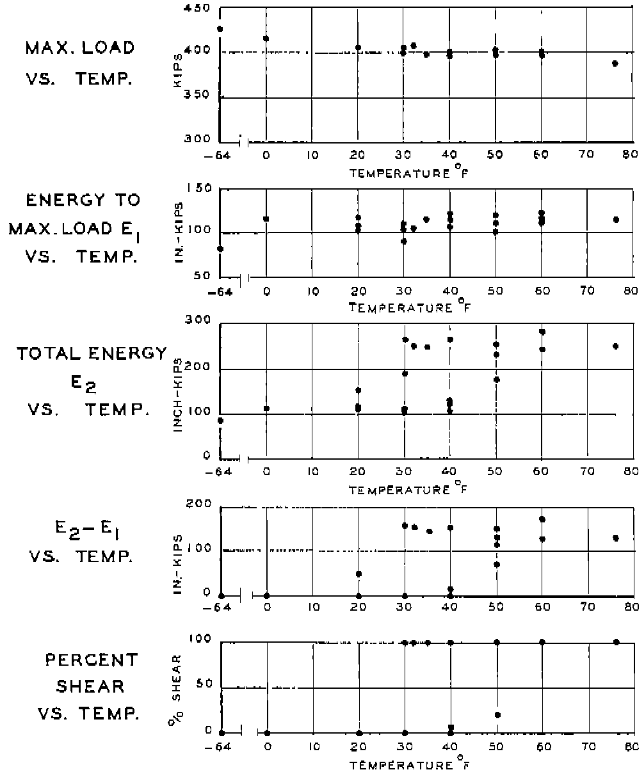

FIG. II-29 SPECIMENS - D
$1\frac{1}{2}$" x 6" ASPECT RATIO 4
BLOCKS I, II, III CODE T-1

SWARTHMORE COLLEGE

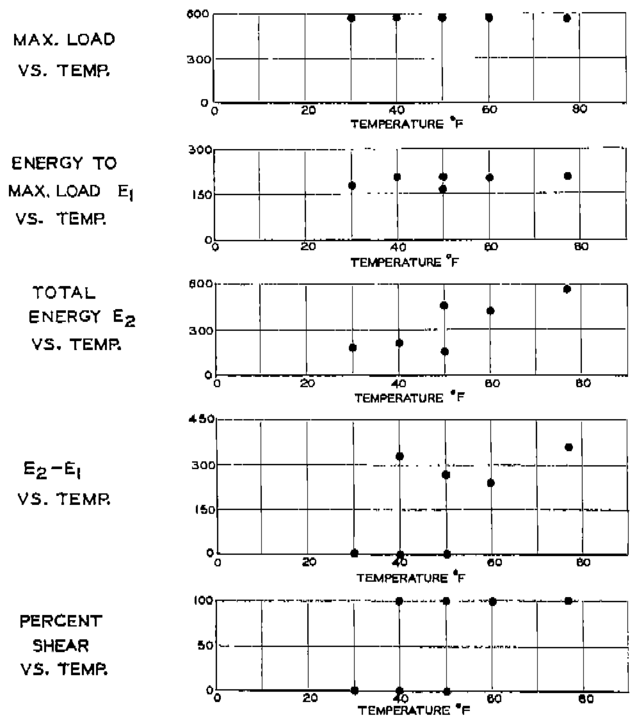

FIG. II-30
SPECIMENS-H
$1\frac{1}{2}$" x 9" ASPECT RATIO 6
CODE T-1
SWARTHMORE COLLEGE
1-10-50

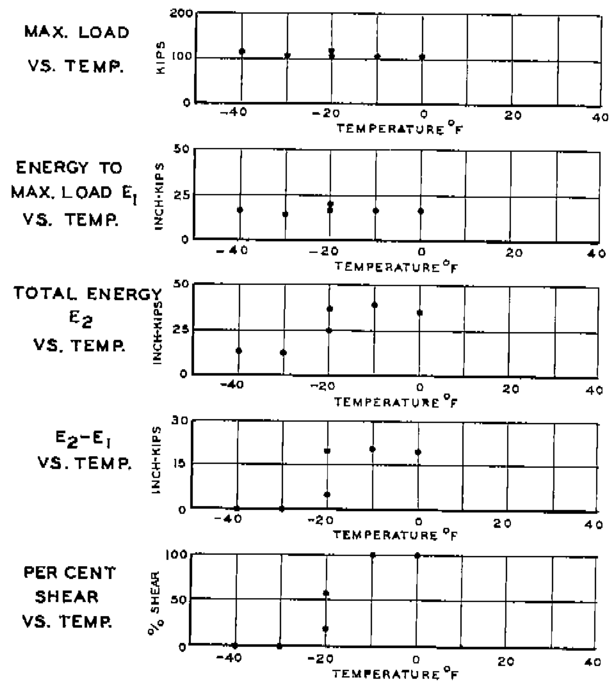

FIG. II-31
SPECIMENS B-T-2
3/4" x 3" ASPECT RATIO 4
SWARTHMORE COLLEGE
9-15-50

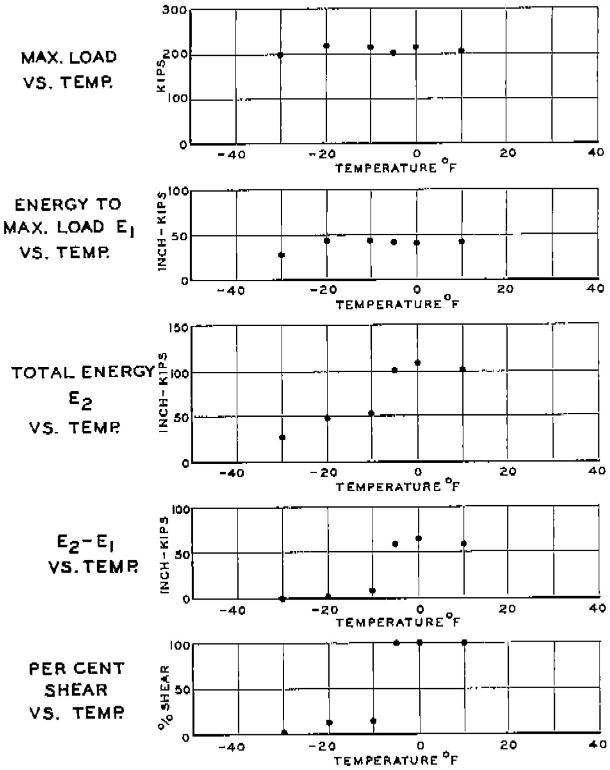

FIG. II-32
SPECIMENS D-T-2
3/4" x 6" ASPECT RATIO 8
SWARTHMORE COLLEGE
9-15-50

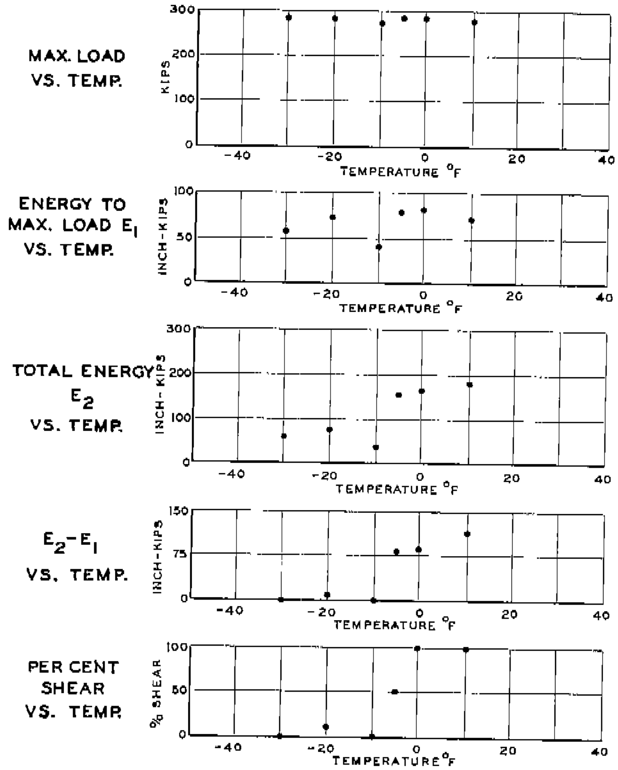

FIG. II-33
SPECIMENS H-T-2
3/4" x 9" ASPECT RATIO 12
SWARTHMORE COLLEGE
9-15-50

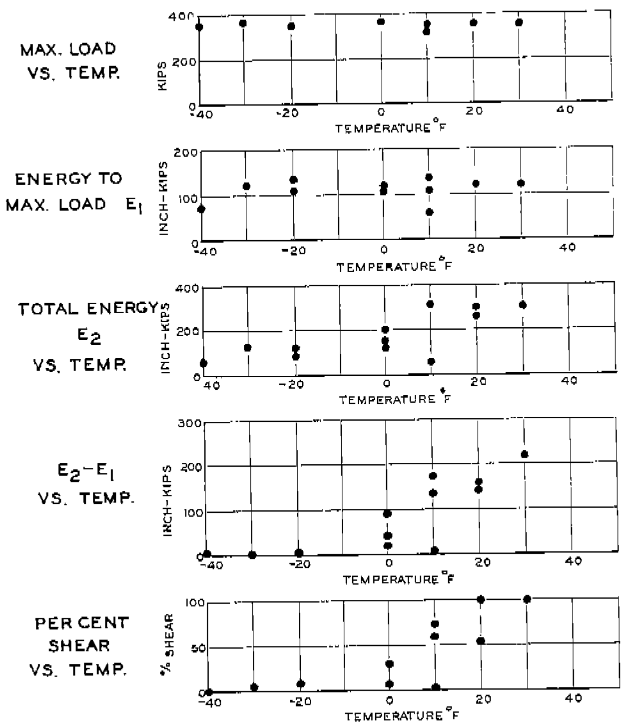

FIG. II-34
SPECIMENS-G
3/4" x 12" ASPECT RATIO 16
CODE T-2
SWARTHMORE COLLEGE
5-18-50

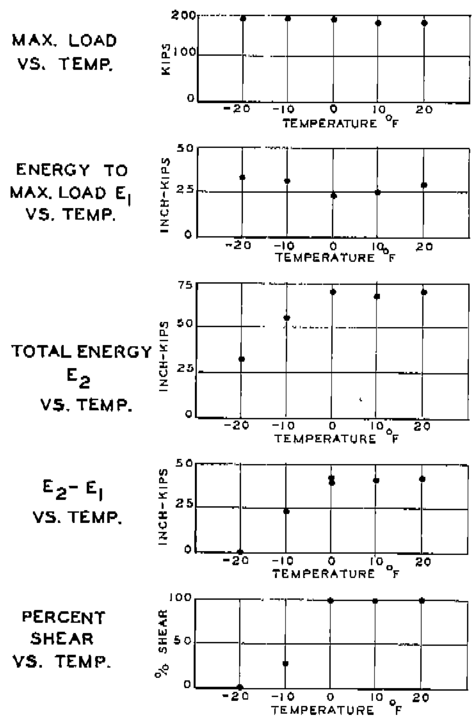

FIG. II-35
SPECIMEN-C
1" x 4" ASPECT RATIO 4
CODE T-2
SWARTHMORE COLLEGE

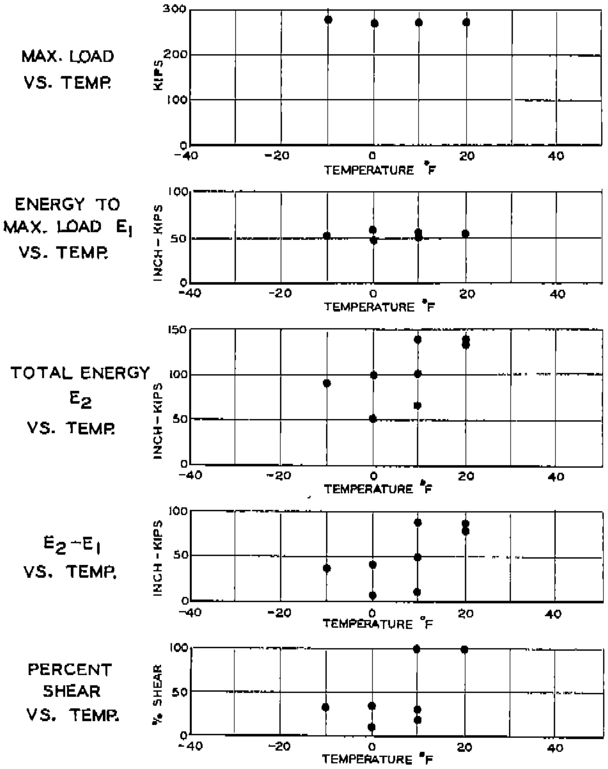

FIG. II-36

SPECIMENS- D-T-2

1" x 6" ASPECT RATIO 6

SWARTHMORE COLLEGE

4-27-50

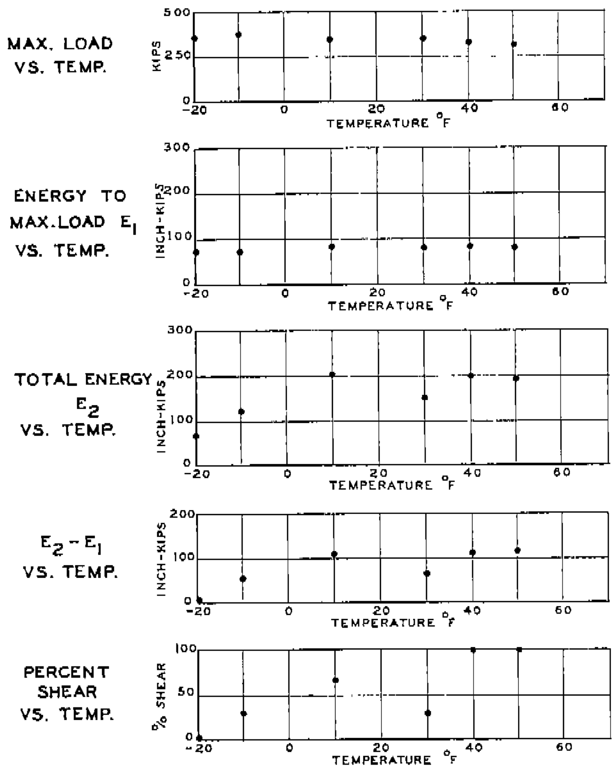

FIG. II-37

SPECIMENS E-T-2

1" x 8" ASPECT RATIO 8

CODE T-2

SWARTHMORE COLLEGE

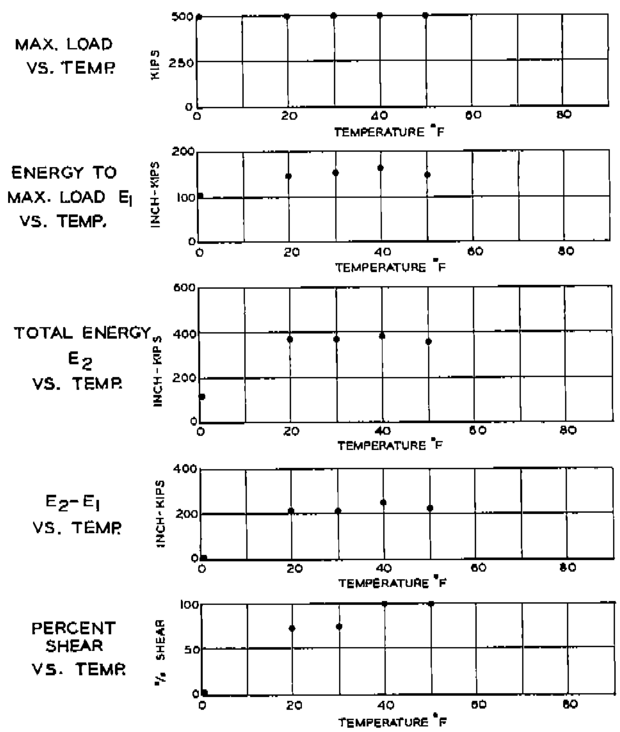

FIG. II-38

SPECIMENS G-T-2

1" x 12" ASPECT RATIO 12

SWARTHMORE COLLEGE

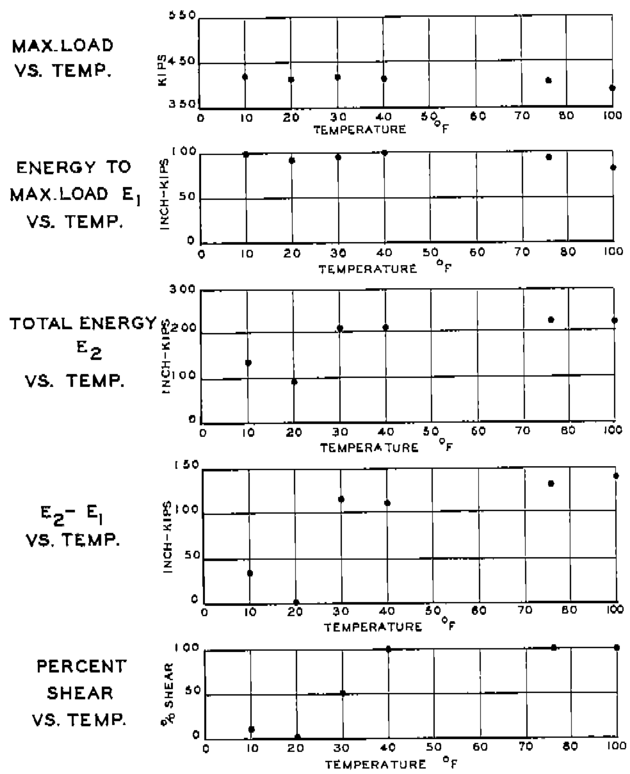

FIG. II-39

SPECIMENS D-T-2

1½" x 6" ASPECT RATIO 4

SWARTHMORE COLLEGE

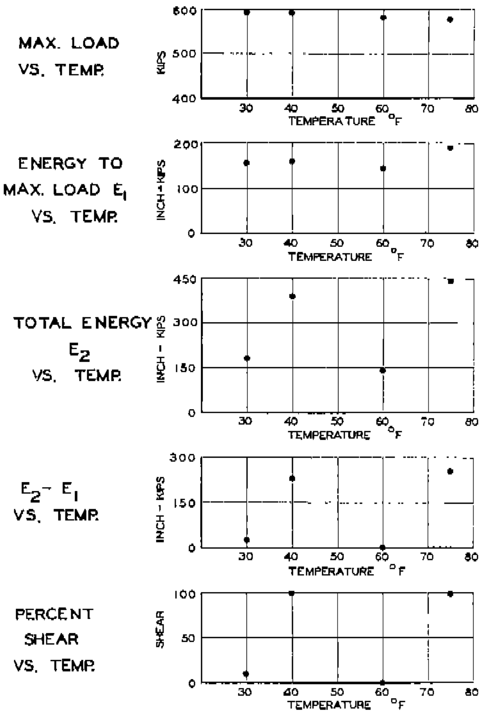

FIG. II - 40

SPECIMEN H-T-2

$1\frac{1}{2}$" x 9" ASPECT RATIO 6

SWARTHMORE COLLEGE

[illegible]

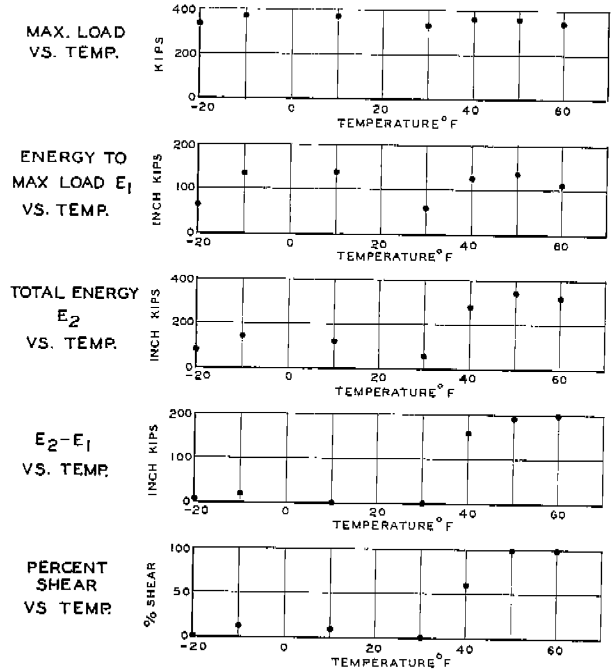

FIG. II-41

SPECIMENS-G

3/4" X 12" ASPECT RATIO 16

CODE T-2R

SWARTHMORE COLLEGE

11-4-50

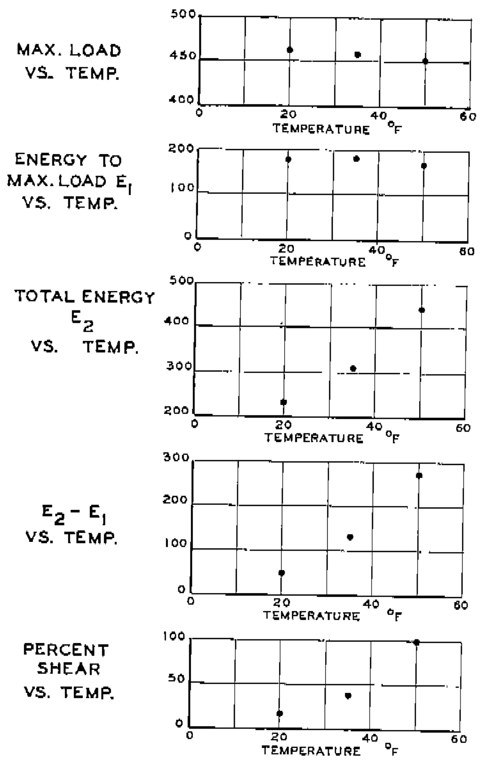

FIG. II-42

SPECIMEN - I

3/4" X 15" ASPECT RATIO 20

CODE T-2R

SWARTHMORE COLLEGE

APPENDIX III

LOAD-ELONGATION CURVES

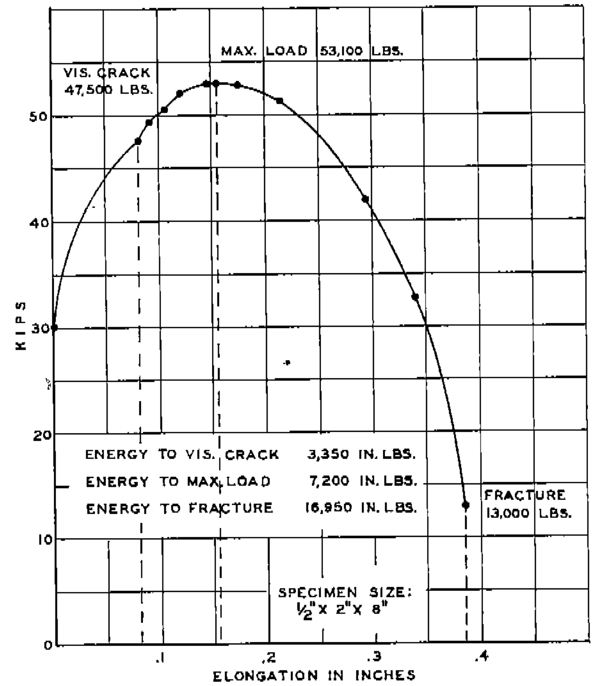

FIG. III-1
LOAD-ELONGATION CURVE
SPECIMEN A-14
CODE T-1
-20°F, 100% SHEAR

SWARTHMORE COLLEGE
11-18-50

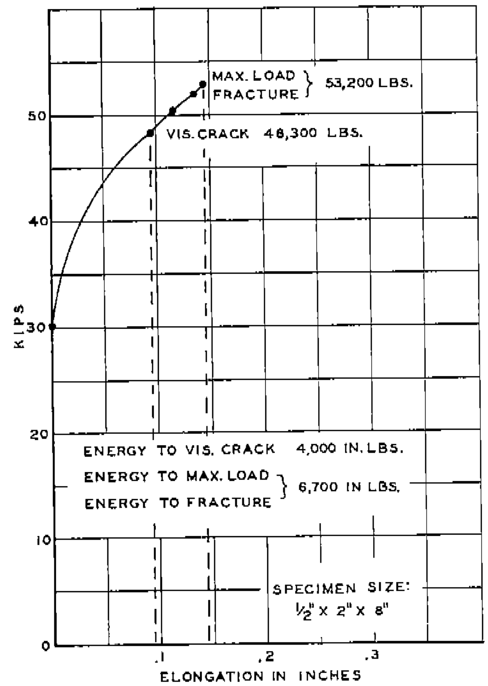

FIG. III-2
LOAD-ELONGATION CURVE
SPECIMEN A-30
CODE T-1
-42°F, 0% SHEAR

SWARTHMORE COLLEGE
11-18-50

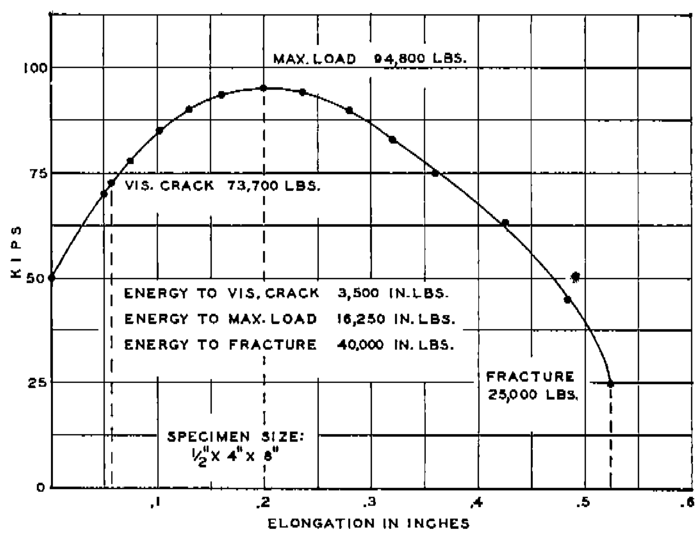

FIG. III-3
LOAD-ELONGATION CURVE
SPECIMEN C-6
CODE T-1
0°F, 100% SHEAR

SWARTHMORE COLLEGE
11-25-50

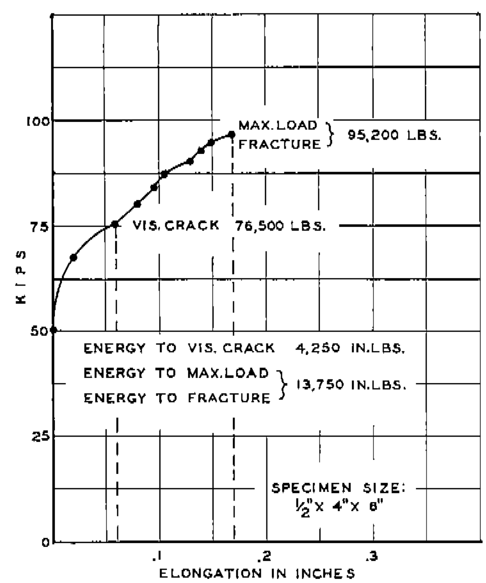

FIG. III-4
LOAD-ELONGATION CURVE
SPECIMEN C-3
CODE T-1
0°F, 0% SHEAR

SWARTHMORE COLLEGE
11-25-50

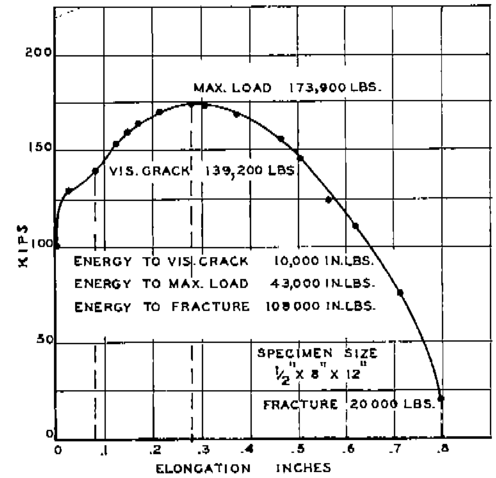

FIG. III-5

LOAD-ELONGATION CURVE

SPECIMEN E-28

CODE T-1

20°F, 100% SHEAR

SWARTHMORE COLLEGE

11-27-50

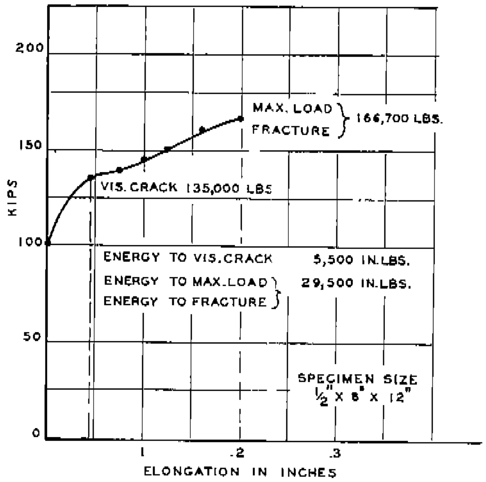

FIG. III-6

LOAD-ELONGATION CURVE

SPECIMEN E-26

CODE T-1

0°F, 0% SHEAR

SWARTHMORE COLLEGE

11-27-50

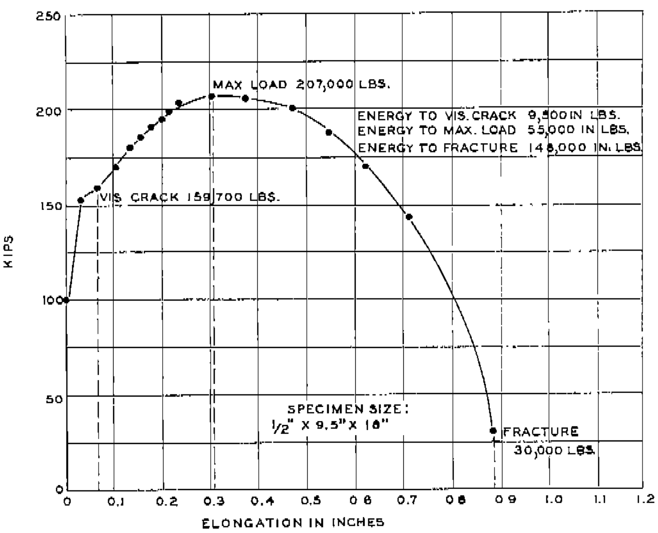

FIG. III-7

LOAD vs ELONGATION

CODE T-1 1/2" F-9

TEMP. 0°F 100% SHEAR

SWARTHMORE COLLEGE

2-13-50

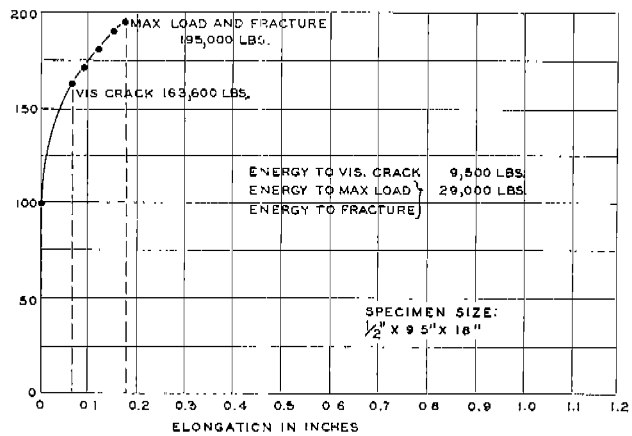

FIG. III-8

LOAD vs ELONGATION

CODE T-1 1/2" F-17

TEMP. -10°F 0% SHEAR

SWARTHMORE COLLEGE

2-15-50

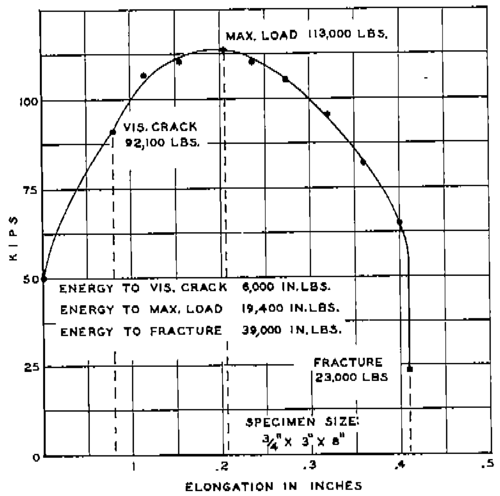

FIG. III-9

LOAD-ELONGATION CURVE
SPECIMEN B-4
CODE T-1
-20°F, 100% SHEAR

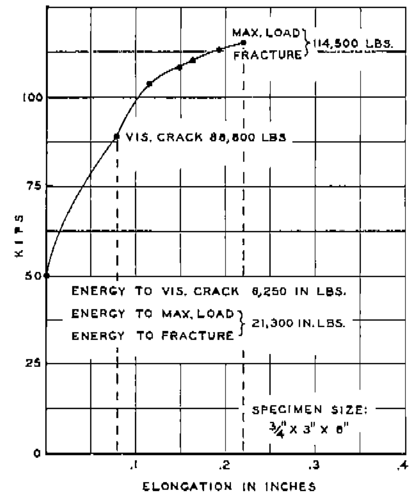

FIG. III-10

LOAD-ELONGATION CURVE
SPECIMEN B-14
CODE T-1
-30°F, 0% SHEAR

SWARTHMORE COLLEGE
12-2-50

SWARTHMORE COLLEGE
12-2-50

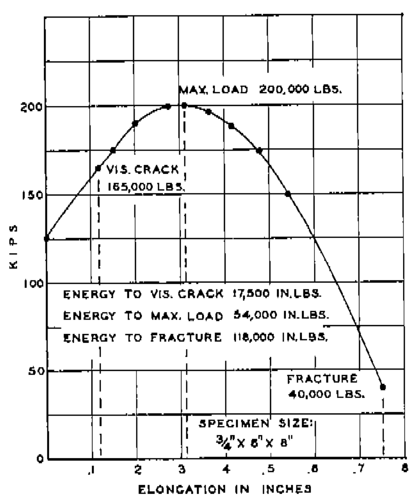

FIG. III-11

LOAD-ELONGATION CURVE
SPECIMEN D-10
CODE T-1
10°F, 100% SHEAR

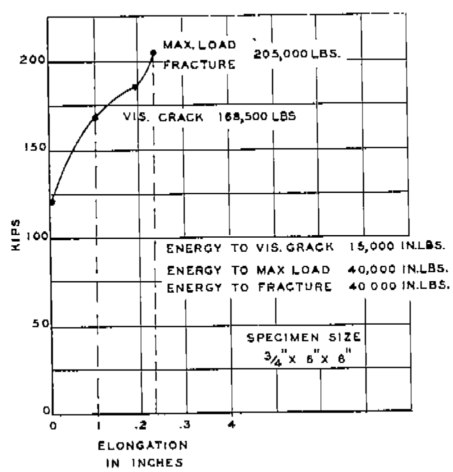

FIG. III-12

LOAD-ELONGATION CURVE
SPECIMEN D-3
CODE T-1
-30°F 100% SHEAR

SWARTHMORE COLLEGE
12-4-50

SWARTHMORE COLLEGE
12-2-50

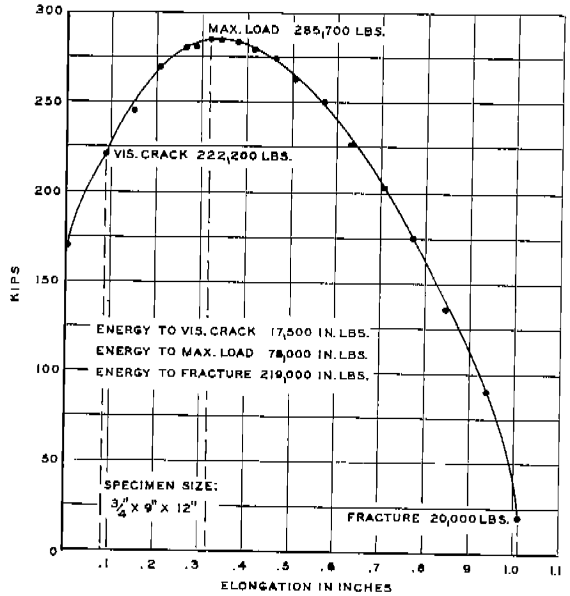

FIG. III-13 LOAD-ELONGATION CURVE
SPECIMEN H-7
CODE T-1
10°F, 100% SHEAR

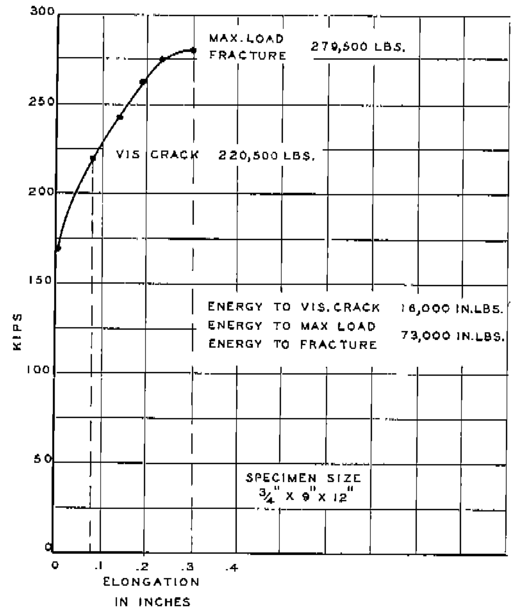

FIG. III-14 LOAD-ELONGATION CURVE
SPECIMEN H-10
CODE T-1
-10°F, 0% SHEAR

SWARTHMORE COLLEGE
12-4-50

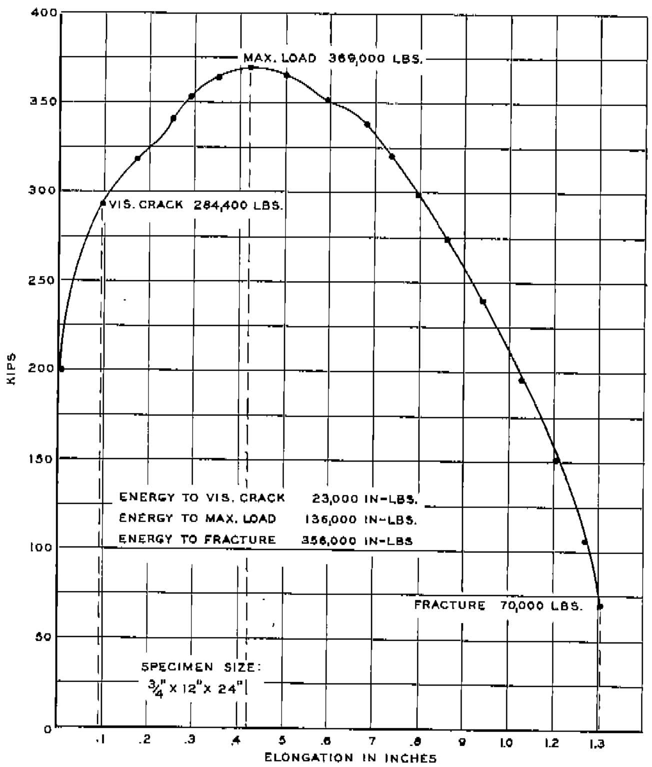

FIG. III-15 LOAD-ELONGATION CURVE
SPECIMEN G-1
CODE T-1
30°F, 100% SHEAR

SWARTHMORE COLLEGE
12-13-50

SWARTHMORE COLLEGE
12-5-50

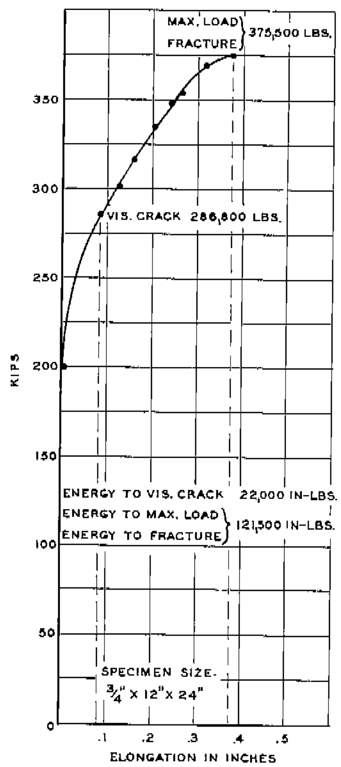

FIG. III-16 LOAD-ELONGATION CURVE
SPECIMEN G-4
CODE T-1
-20°F, 5% SHEAR

SWARTHMORE COLLEGE
12-13-50

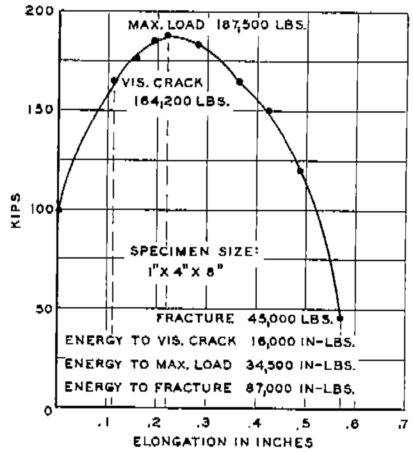

FIG. III-17

LOAD-ELONGATION CURVE
SPECIMEN C-19
CODE T-1
15°F, 100% SHEAR

SWARTHMORE COLLEGE
12-18-50

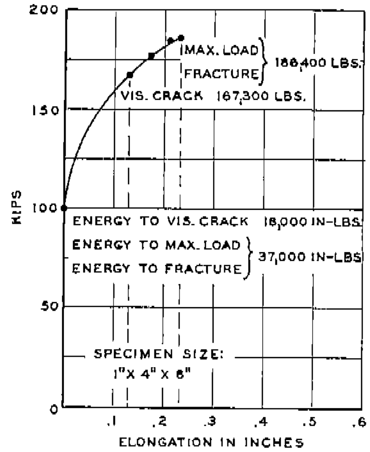

FIG. III-18

LOAD-ELONGATION CURVE
SPECIMEN C-8
CODE T-1
10°F, 0% SHEAR

SWARTHMORE COLLEGE
12-18-50

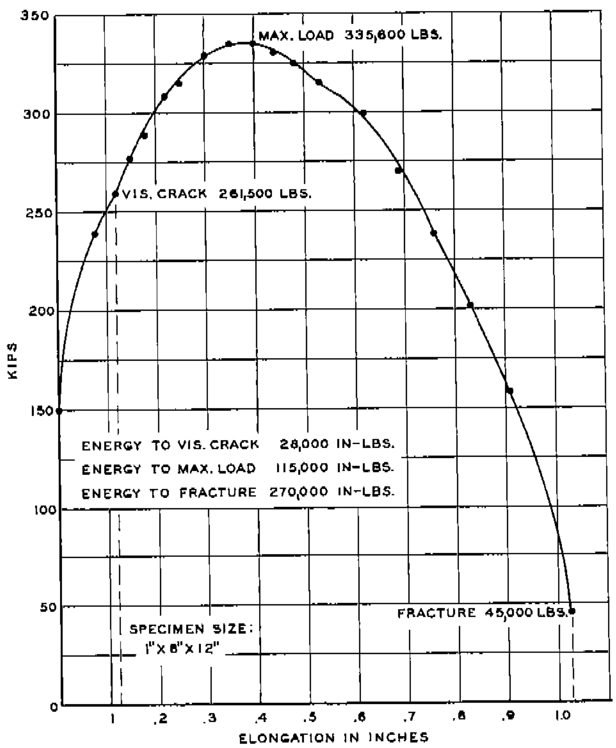

FIG. III-19

LOAD-ELONGATION CURVE
SPECIMEN E-6
CODE T-1
30°F, 100% SHEAR

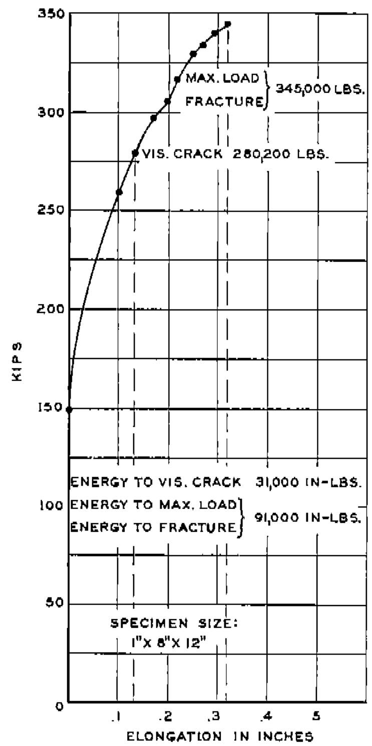

FIG. III-20

LOAD-ELONGATION CURVE
SPECIMEN E-17
CODE T-1
-10°F, 0% SHEAR

SWARTHMORE COLLEGE
12-13-50

SWARTHMORE COLLEGE
12-13-50

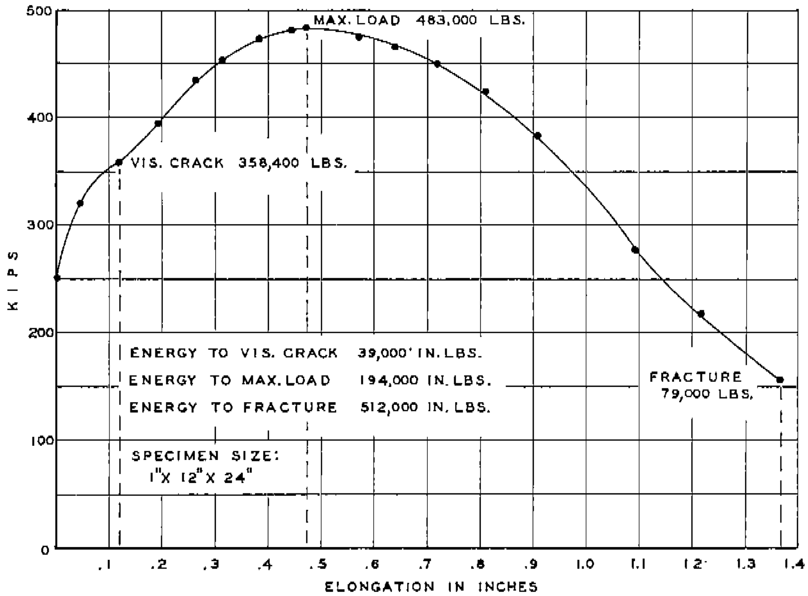

FIG. III-21
LOAD-ELONGATION CURVE
SPECIMEN G-1
CODE T-1
30°F, 100% SHEAR

SWARTHMORE COLLEGE
12-23-50

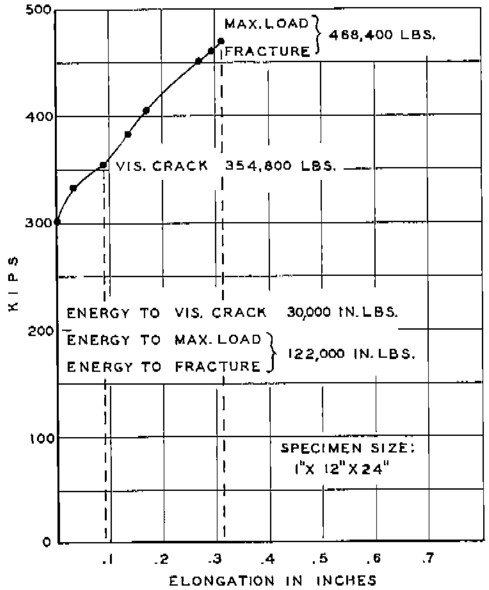

FIG. III-22
LOAD-ELONGATION CURVE
SPECIMEN G-8
CODE T-1
20°F, 0% SHEAR

SWARTHMORE COLLEGE
12-23-50

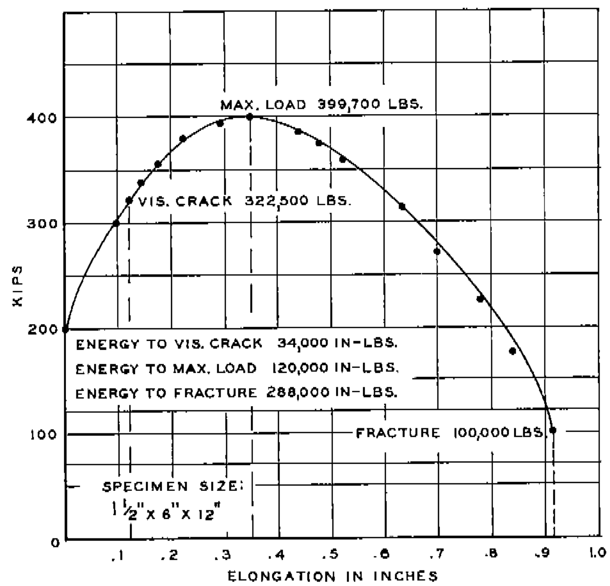

FIG. III-23
LOAD-ELONGATION CURVE
SPECIMEN D-25
CODE T-1
60°F, 100% SHEAR

SWARTHMORE COLLEGE

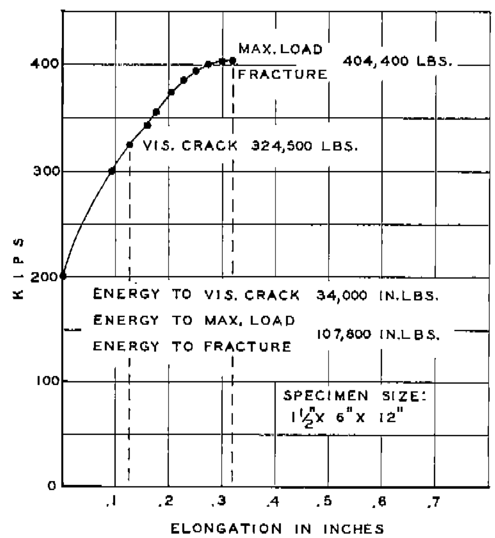

FIG. III-24
LOAD-ELONGATION CURVE
SPECIMEN D-23
CODE T-1
30°F, 0% SHEAR

SWARTHMORE COLLEGE
12-23-50

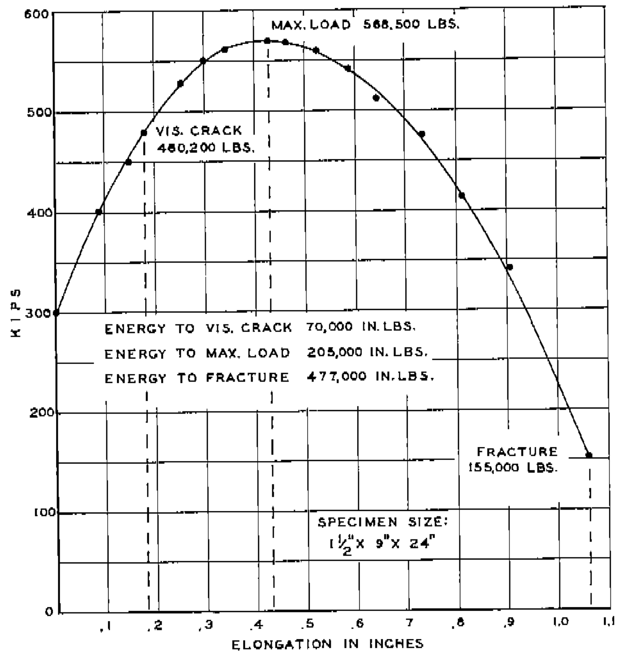

FIG. III-25
LOAD-ELONGATION CURVE
SPECIMEN GH-4
CODE T-1
50°F, 100% SHEAR

SWARTHMORE COLLEGE
1-6-51

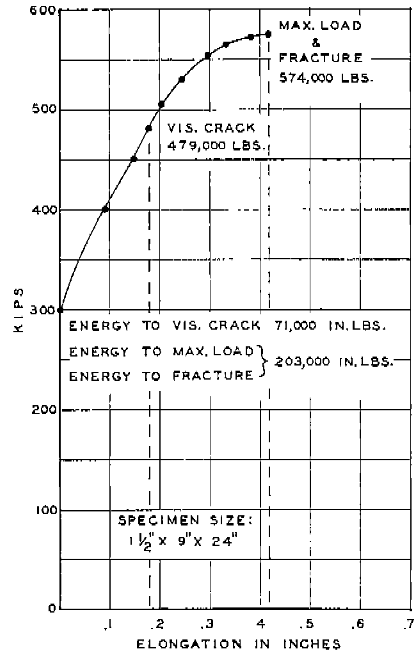

FIG. III-26
LOAD-ELONGATION CURVE
SPECIMEN GH-15
CODE T-1
40°F, 3% SHEAR

SWARTHMORE COLLEGE
1-6-51

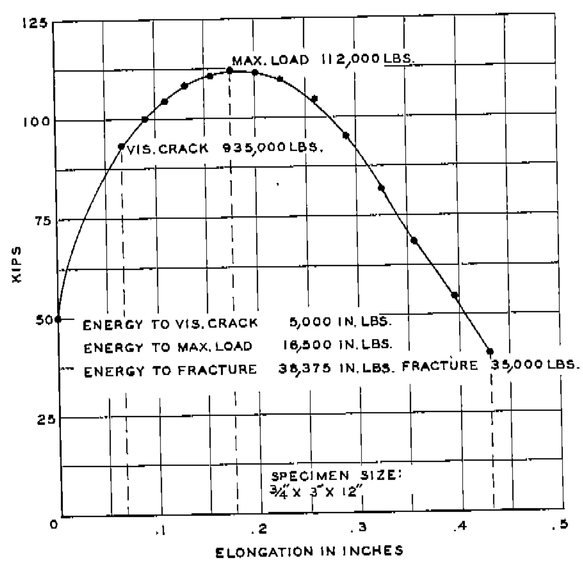

FIG. III-27 LOAD ELONGATION CURVE
SPECIMEN ¾"XB-1, T-2
-10°F, 100% SHEAR

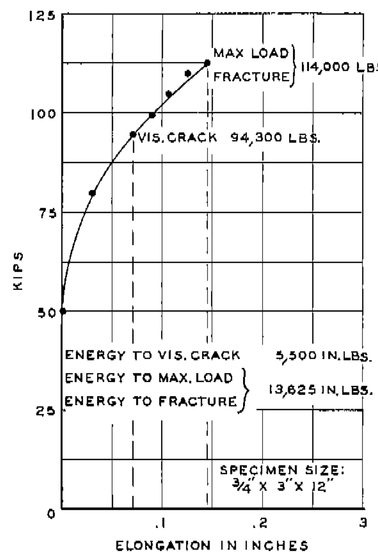

FIG. III-28 LOAD ELONGATION CURVE
SPECIMEN ¾"XB-7, T-2
-30°F, 0% SHEAR

SWARTHMORE COLLEGE
11-1-50

SWARTHMORE COLLEGE
11-1-50

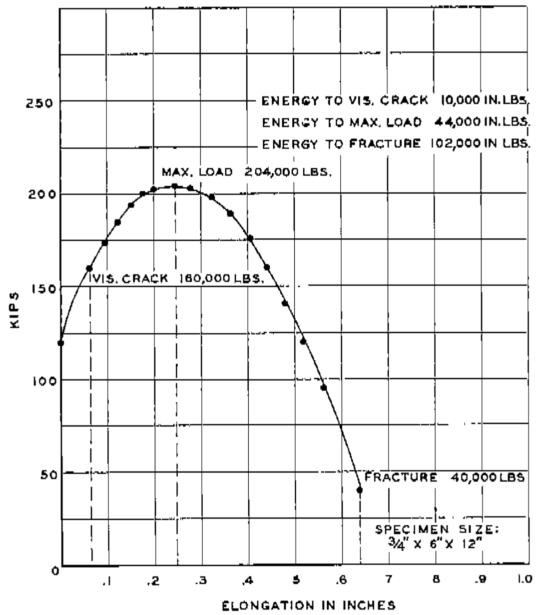

FIG. III-29 LOAD ELONGATION CURVE
SPECIMEN XD-6, T-2
-5°F, 100% SHEAR

SWARTHMORE COLLEGE
11-1-50

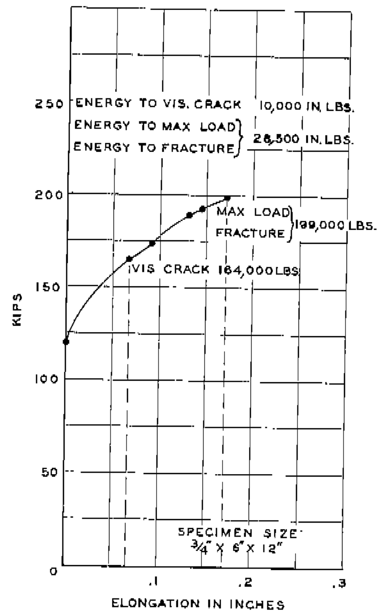

FIG. III-30 LOAD ELONGATION CURVE
SPECIMEN 3/4" XD-4, T-2
-30°F, 0% SHEAR

SWARTHMORE COLLEGE
11-1-50

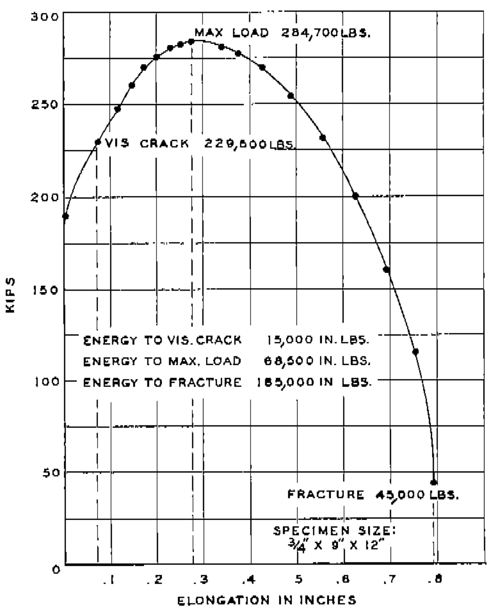

FIG. III-31 LOAD ELONGATION CURVE
SPECIMEN 3/4" XH-9, T-2
10°F, 100% SHEAR

SWARTHMORE COLLEGE
11-1-50

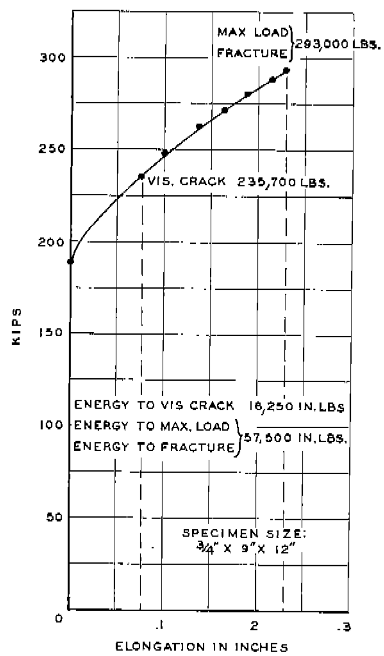

FIG. III-32 LOAD ELONGATION CURVE
SPECIMEN 3/4" XH-5, T-2
-30°F, 0% SHEAR

SWARTHMORE COLLEGE
11-1-50

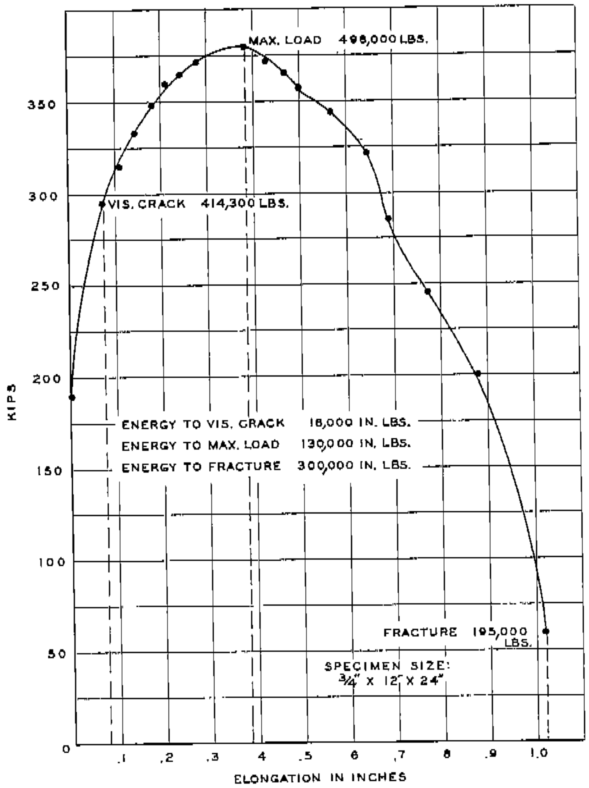

FIG. III-33 LOAD ELONGATION CURVE
SPECIMEN 3/4" XG-1, T-2
20°F, 100% SHEAR

SWARTHMORE COLLEGE
11-1-50

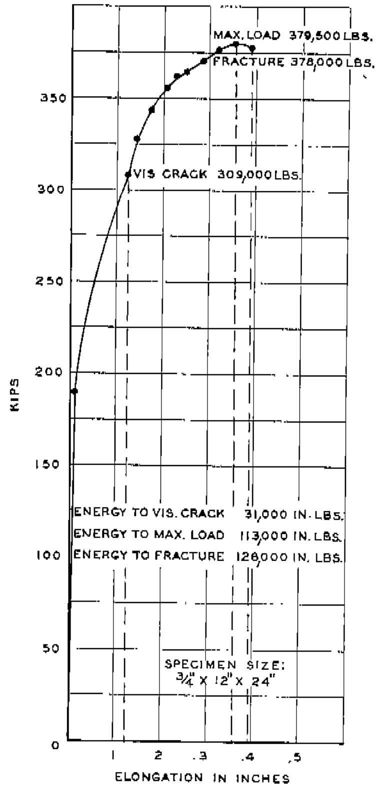

FIG. III-34 LOAD ELONGATION CURVE
SPECIMEN 3/4" XG-4, T-2
0°F, 10% SHEAR

SWARTHMORE COLLEGE
11-1-50

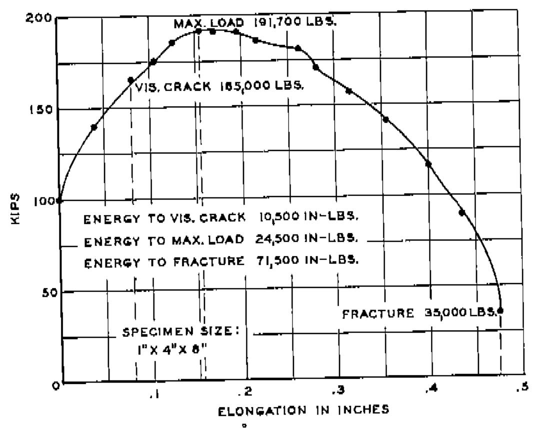

FIG. III-35
LOAD-ELONGATION CURVE
SPECIMEN XC-9
CODE T-2
0°F, 100% SHEAR

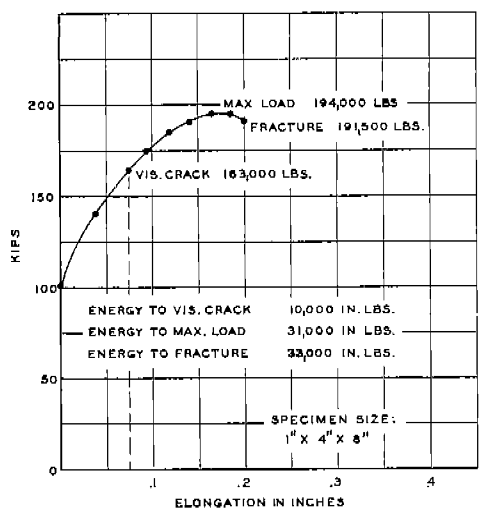

FIG. III-36
LOAD-ELONGATION CURVE
SPECIMEN XC-1
CODE T-2
-20°F, 0% SHEAR

SWARTHMORE COLLEGE
1-8-51

SWARTHMORE COLLEGE
11-20-50

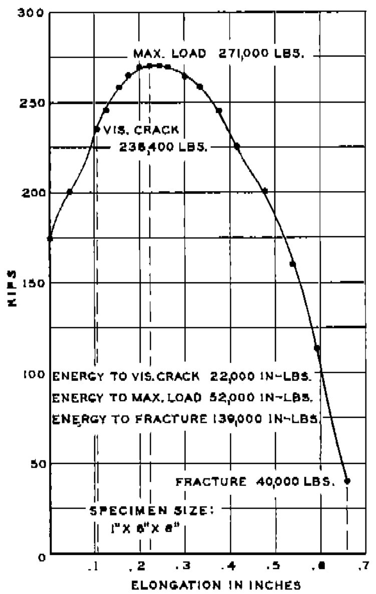

FIG. III-37
LOAD-ELONGATION CURVE
SPECIMEN XD-7
CODE T-2
10°F, 100 % SHEAR

SWARTHMORE COLLEGE
1-10-50

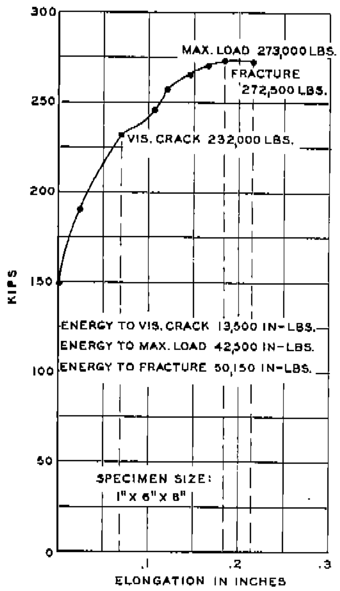

FIG. III-38
LOAD-ELONGATION CURVE
SPECIMEN XD-8
CODE T-2
0°F, 10% SHEAR

SWARTHMORE COLLEGE
1-8-51

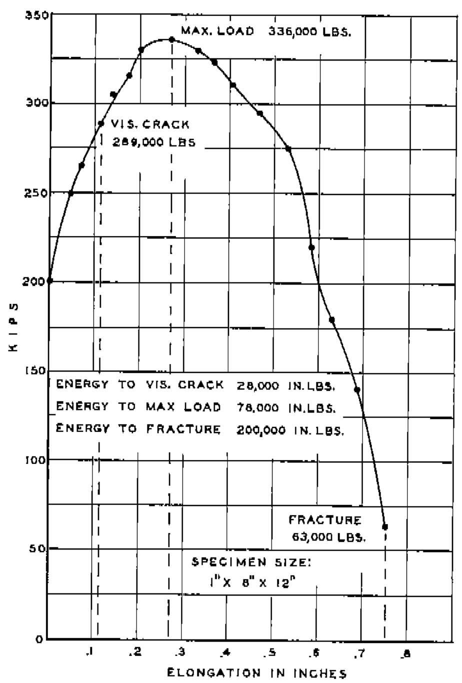

FIG. III-39
LOAD-ELONGATION CURVE
SPECIMEN XE - 6
CODE T - 2
50°F, 100 % SHEAR

SWARTHMORE COLLEGE
1-13-51

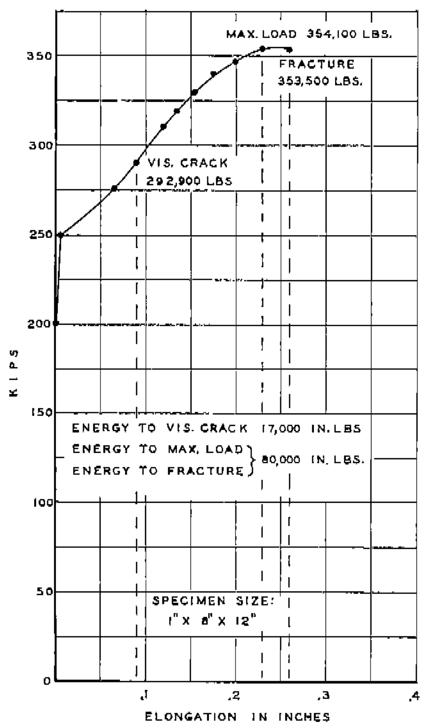

FIG. III-40
LOAD-ELONGATION CURVE
SPECIMEN XE - 5
CODE T - 2
-20°F 0 % SHEAR

SWARTHMORE COLLEGE
1-13-50

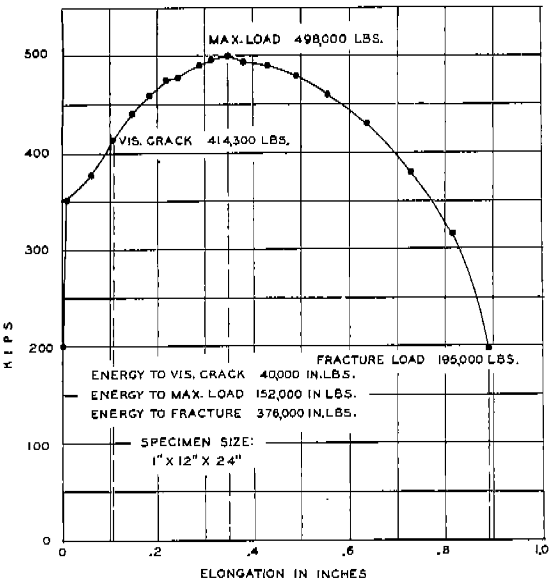

FIG. III-41

LOAD-ELONGATION CURVE
SPECIMEN XG-3
CODE T-2
20° F, 75% SHEAR

SWARTHMORE COLLEGE
1-25-51

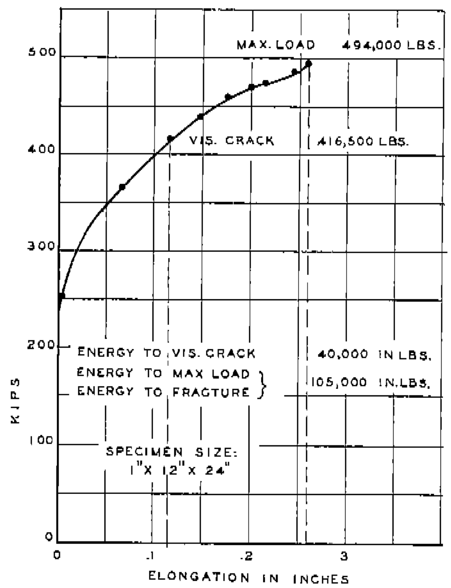

FIG. III-42

LOAD-ELONGATION CURVE
SPECIMEN XG-2
CODE T-2
0°F, 0% SHEAR

SWARTHMORE COLLEGE
1-24-51

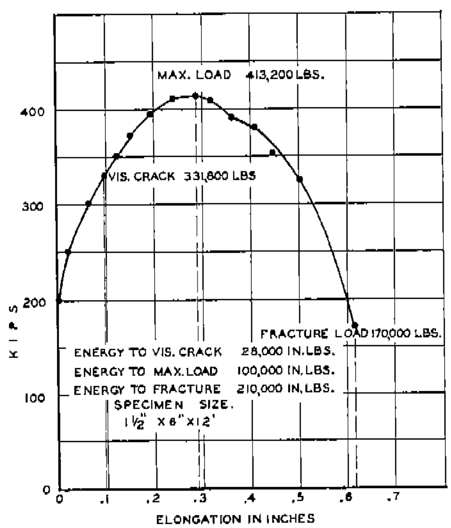

FIG. III -43

LOAD-ELONGATION CURVE
SPECIMEN XD-3
CODE T-2
40° F, 100% SHEAR

SWARTHMORE COLLEGE
1-25-51

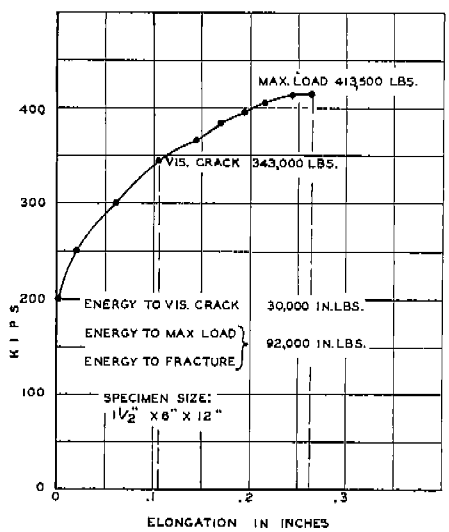

FIG. III - 44

LOAD-ELONGATION CURVE
SPECIMEN XD-1
CODE T-2
20° F, 0% SHEAR

SWARTHMORE COLLEGE
1-25-51

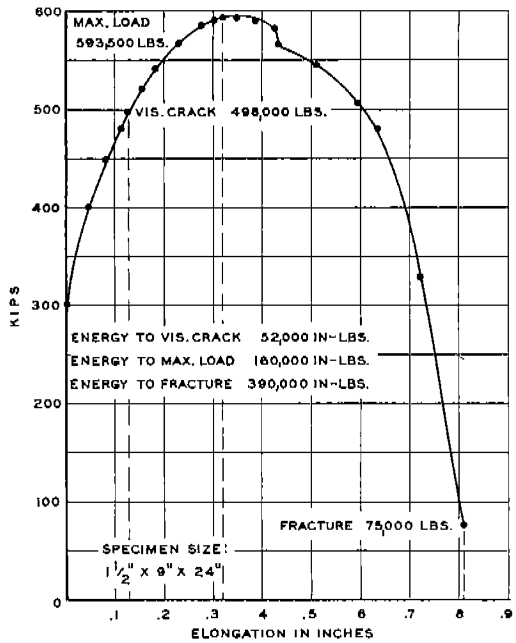

FIG. III-45
LOAD-ELONGATION CURVE
SPECIMEN XH-5
CODE T-2
40°F, 100% SHEAR

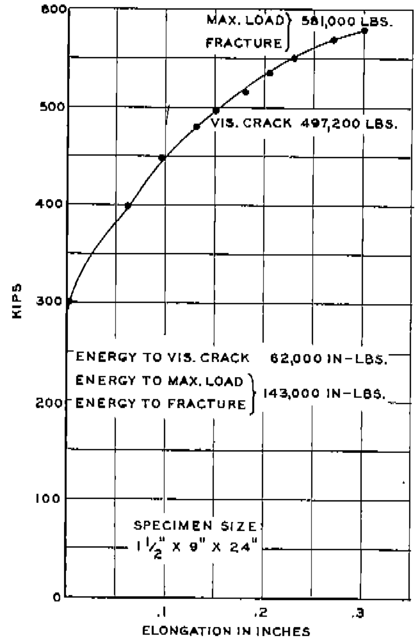

FIG. III-46
LOAD-ELONGATION CURVE
SPECIMEN XH-1
CODE T-2
60°F, 0% SHEAR

SWARTHMORE COLLEGE
1-16-51

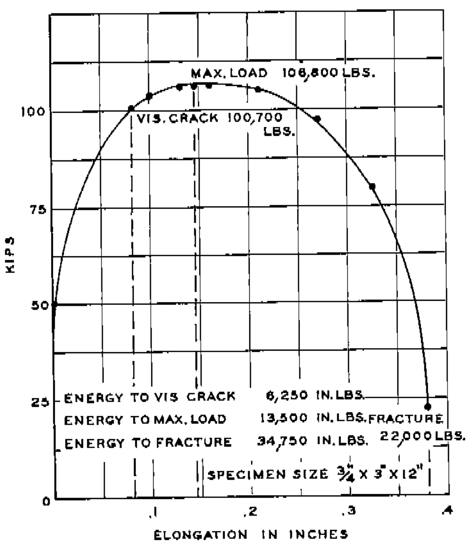

FIG. III-47 LOAD ELONGATION CURVE
SPECIMEN ¾" B-1, T-2R
75°F, 100% SHEAR

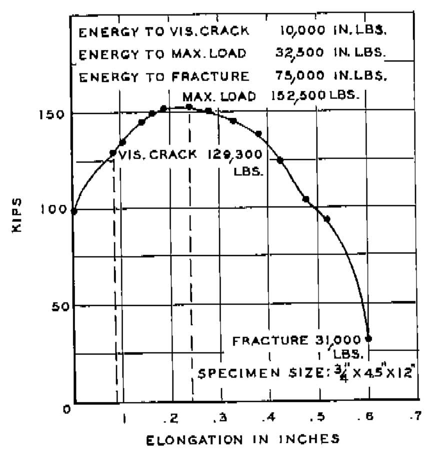

FIG. III-49 LOAD ELONGATION CURVE
SPECIMEN ¾" C-4, T-2R
73°F, 100% SHEAR

SWARTHMORE COLLEGE
11-1-50

SWARTHMORE COLLEGE
11-1-50

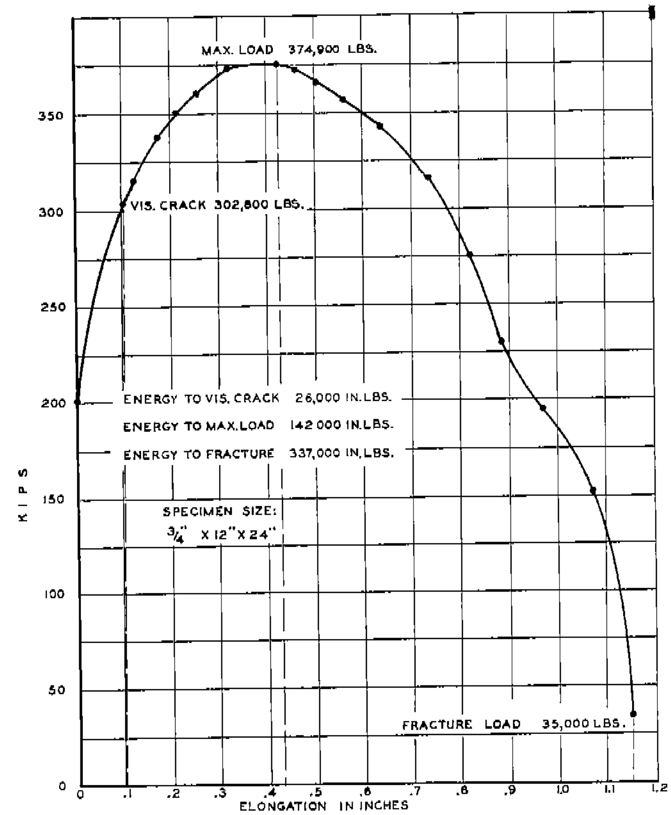

FIG.III-51 LOAD-ELONGATION CURVE
SPECIMEN GR-7
CODE T-2
50°F 100% SHEAR

SWARTHMORE COLLEGE
1-26-51

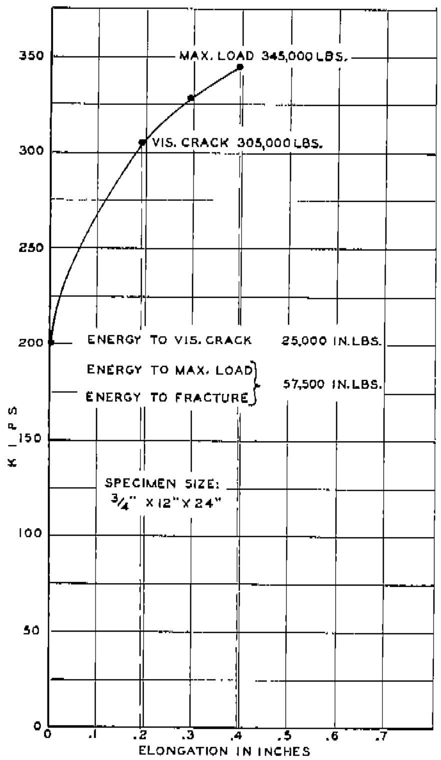

FIG.III-52 LOAD-ELONGATION CURVE
SPECIMEN G-1
CODE T 2-R
30°F 0% SHEAR

SWARTHMORE COLLEGE
1-26-51

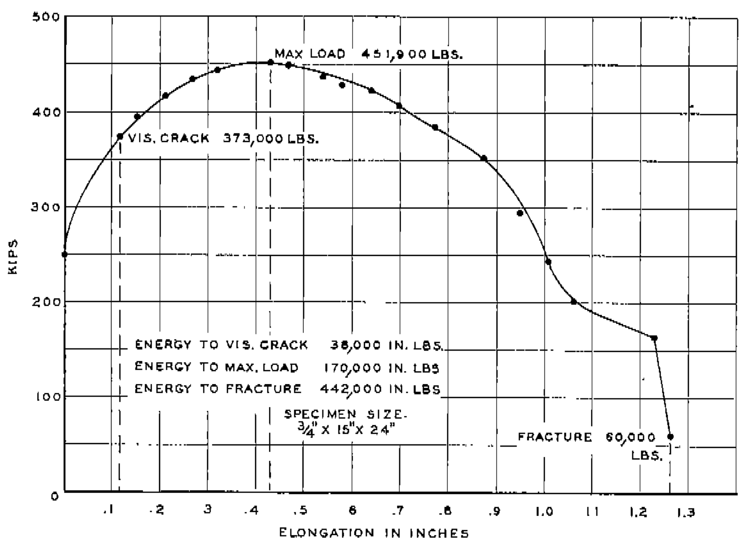

FIG. III-53 LOAD ELONGATION CURVE
SPECIMEN 3/4" I-1, T-2R
50°F, 100% SHEAR

SWARTHMORE COLLEGE
11-1-50

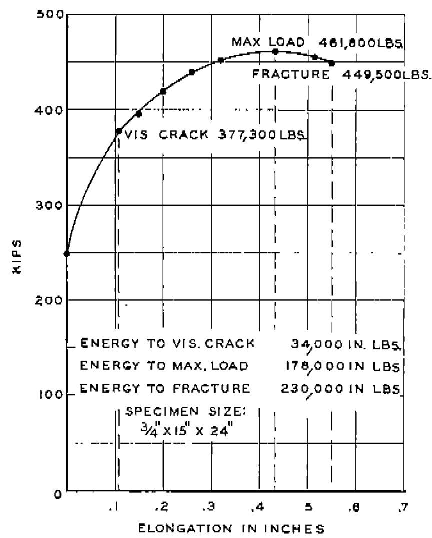

FIG. III-54 LOAD ELONGATION CURVE
SPECIMEN 3/4" I-3, T-2R
20°F, 20% SHEAR

SWARTHMORE COLLEGE
11-1-50